CLASSICAL AND ATYPICAL SCRAPIE: DETERMINANTS OF PRION PERMISSIBILITY, AND NEUROANATOMICAL PrP^{Sc} PROTEIN PATTERN AND LOCALIZATION

by

VALERIE MCELLIOTT

(Under the Direction of James Stanton)

ABSTRACT

Transmissible spongiform encephalopathies (TSEs) are a group of neurodegenerative diseases occurring in humans, cattle, and sheep. Conversion of the normal, host-encoded cellular prion protein (PrP^{C}) to a misfolded, disease-associated isoform (PrP^{D}) is the causative agent. Classical scrapie is the oldest described TSE, whereas atypical scrapie is more recent, but there are reported cases of both in Europe, US, and Canada. Globally, extensive eradication programs use passive and active surveillance in an effort to control and eliminate these diseases, as they are devastating economically and financially. Although surveillance has been effective in identification of affected animals, and the total number of scrapie cases has diminished, factors that contribute to prion permissibility and rate of prion accumulation remain unknown. Additionally, these factors could be extrapolated to human TSEs, providing the basis for development of a human cell culture system. Using immortalized ovine microglia clones, 6 genes with functions in apoptosis (survivin; follistatin-like 1), cell proliferation (osteonectin), efferocytosis (AXL tyrosine kinase inhibitor), cell-to-cell and cell-extracellular matrix adhesions (syndecan 4), and extracellular remodeling and repair (fibronectin 1) were studied for potential correlations with prion permissibility. Furthermore, expression of these genes relative to PRNP expression was evaluated. Transcript levels for matrix metalloproteinase 2 (MMP2) were also assessed to determine if expression was influenced by permissibility phenotype, or rate of prion

accumulation. To study an animal prion disease that mirrors the human condition in length of incubation period and slow rate of prion accumulation, PrP^{Sc} pattern and localization was characterized in 4 sheep experimentally infected with a natural North American atypical scrapie isolate.

Fibronectin 1 and survivin were strongly and negatively correlated with prion permissibility when evaluated relative to PRNP, and significant differential expression of survivin, osteonectin and follistatin-like 1 was between intermediately and poorly-permissive clones. Matrix metalloproteinase II transcript levels were significantly decreased in intermediately-permissive clones, and in cells with a fast rate of prion accumulation. In the atypical scrapie cases, PrP^{Sc} pattern and localization was similar to previously reported European pathotypes. These findings suggest potential determinants of prion permissibility exist, but further studies are needed to solidify these results.

INDEX WORDS: Classical scrapie, atypical scrapie, immortalized ovine microglia, genetic determinants, prion permissibility, PrP^{Sc} protein pattern, PrP^{Sc} protein neuroanatomical localization

CLASSICAL AND ATYPICAL SCRAPIE: DETERMINANTS OF PRION PERMISSIBILITY, AND NEUROANATOMICAL PrP^{Sc} PROTEIN PATTERN AND LOCALIZATION

by

VALERIE MCELLIOTT

BS, TEXAS A&M UNIVERSITY, 1999

DVM, TUSKEGEE UNIVERSITY, 2006

A Dissertation Submitted to the Graduate Faculty of The University of Georgia in Partial Fulfillment of the Requirements for the Degree

DOCTOR OF PHILOSOPHY

ATHENS, GEORGIA

2019

CLASSICAL AND ATYPICAL SCRAPIE: DETERMINANTS OF PRION PERMISSIBILITY, AND NEUROANATOMICAL PrP^{Sc} PROTEIN PATTERN AND LOCALIZATION

by

VALERIE MCELLIOTT

Major Professor:	JAMES STANTON
Committee:	KAORI SAKAMOTO
	ZHEN FU
	NICK FILIPOV

Electronic Version Approved:

Suzanne Barbour
Dean of the Graduate School
The University of Georgia
August 2019

DEDICATION

I dedicate this dissertation to my family, and with utmost gratitude, I thank them for their love, support, patience, and encouragement, during this time, and always. . .

TABLE OF CONTENTS

Page

LIST OF TABLES

Page

LIST OF FIGURES

Page

CHAPTER 1 INTRODUCTION

Transmissible Spongiform Encephalopathies (TSEs) are a group of progressive, permanent neurodegenerative diseases that affect multiple animal species, including: humans (Creutzfeldt-Jakob disease), sheep and goats (classical and atypical scrapie), cattle (bovine spongiform encephalopathy/BSE), cervids (chronic wasting disease/CWD), mink (mink spongiform encephalopathy/MSE), and a spectrum of other host species [1-4]. Conversion of the normal, host-encoded, cellular prion protein (PrP^{C}) to its abnormal, misfolded, disease-associated isoform (PrP^{Sc}; Sc for scrapie) is the mechanism for infection [3, 5]. In natural conditions, incubation periods are lengthy, and PrP^{Sc} deposition and accumulation ultimately occurs in the brain. Prion accumulation coupled with the host immune response (i.e., gliosis), typically precedes clinical signs of neurological impairment and derangement, as well as morphological evidence of neuronal and/or neuropil damage [6, 7].

Classical and atypical scrapie are variants of transmissible spongiform encephalopathy (TSE) affecting sheep and goats. Although both result in neurodegeneration and death, these diseases differ in clinical presentation, age of onset, genetic susceptibility, glycosylation features, rate of incubation period, and neuroanatomical distribution and pattern of PrP^{Sc}, indicating two separate pathophysiological processes [8-11]. Since 1952 in the US (i.e., USDA, APHIS) [12], and 2002 in Europe (EU) [13], eradication programs have been constructed and implemented in an effort to control and eliminate classical scrapie for a number of reasons. First, classical scrapie is highly infectious [14], and if a flock were found to be infected, the economic losses in culling, repopulation, trade embargos, enhanced testing, legal fees and financial compensation would be substantial. Second, the threat of an outbreak could be possible, and the scope of exposure may be gravely underestimated, with the onset of long

incubation periods [1] in subclinical carriers. Third, although there are no reports of zoonotic transmission of scrapie to humans, experimentally, BSE-infected brain homogenate is transmissible to sheep after oral inoculation [15, 16], and the clinical and pathogenetic profiles of BSE and scrapie are similar [17]. This could complicate diagnosis of scrapie from BSE, or introduce the possibility of a dual infection. Moreover, the first recorded cases of atypical scrapie in 1998 from Norway (Nor98) [9], exhibited different biochemical and molecular qualities from classical scrapie and BSE [8], so initial concerns were that this disease could represent a modified variant of BSE infection in sheep. However, subsequent evidence confirmed that this TSE was novel, and not associated with BSE or classical scrapie [8, 9], and thereafter, eradication efforts have been heightened at eliminating atypical scrapie as well.

Albeit, active and passive surveillance of classical and atypical scrapie worldwide has greatly diminished the number of total cases, and prevented potential disease outbreaks, as well as minimized economic losses; however, there have been some challenges. In an effort to eradicate classical scrapie in some countries, breeding programs are being engineered to select for resistant genotypes (i.e., ARR) [14], some of which promote susceptibility to atypical scrapie (i.e., ARR). Additionally, modifications to other genes apart from PRNP have not been addressed for the potential control and elimination of scrapie. Moreover, in atypical scrapie, detection methods such as ELISA and IHC are sensitive for identifying PrP^{Sc} in the central nervous system, but these methods are often not as sensitive for detecting lower titers of PrP^{Sc} in other tissues, such as lymph nodes, skeletal muscle, and peripheral nerves [18], and infectivity assays are needed for confirmation. Hence, the anatomic distribution of atypical PrP^{Sc} could be grossly underestimated, and this limits antemortem diagnosis. Further measures, such as analysis of transcript levels, and evaluation of correlations between these transcript levels and prion permissibility in classical and atypical scrapie, could be beneficial to the control and eradication of these diseases.

Many of the prion permissibility determinants are incompletely elucidated in natural and experimental disease of classical and atypical scrapie. Studies have identified that expression of PRNP is a known requirement for prion infection (i.e., presence of PrP^{C}) [14], and polymorphisms within the prion (PRNP) gene can enhance susceptibility to infection (i.e., VRQ in classical scrapie, ARR in atypical scrapie), but they are not sufficient for permissibility. Between animals, species, and prion isolates, there is great diversity in the phenotypic behavior, and this behavior is mimicked with varying cell culture systems derived from different species and different cell types [19-21]. Ultimately, however much of the cellular mechanisms that result in organismal and cultural diversity, are not fully known.

Recent studies have identified that some genes are differentially transcribed or expressed in the presence or absence of prion infection, in *ex vivo* and *in vivo* models of classical scrapie. Filali *et al.* performed transcriptomic analysis of the medulla oblongata from sheep chronically infected with a natural scrapie isolate, and identified the most significant gene ontology term involved in extracellular region proteins, and 11 of 24 genes involved in the extracellular matrix were deregulated [22]. For example, microarray and qRT-PCR analysis identified metallothionein 2A (MT2A; metal binding protein) and glutathione peroxidase 1 (GPX-1; oxidative stress) were significantly upregulated and positively associated with PrP^{Sc} (Sc for scrapie) deposition, whereas melatonin receptor 1B (MTNR1B; oxidative stress) and collagen alpha-2 chain (COL1A2; extracellular matrix) were significantly downregulated and negatively associated with PrP^{Sc} deposition [22]. The trend in expression of MTNR1B and GPX-1 have also been described in Alzheimer's and Parkinson's disease, respectively [22]. The silencing of genes such as fibronectin 1 (Fn1) and 3'-phosphoadenosine 5'-phosphosulphate synthase 2 (Papss2), which both function in extracellular matrix modeling and remodeling, promoted conversion of murine neuroblastoma cells (N2a) from a prion-resistant to prion-susceptible phenotype in another study [23]. In studies evaluating gene expression and prion permissibility,

Munoz-Gutierrez *et al.* discovered in prion highly-permissive immortalized ovine microglia, matrix metalloproteinase 14 (MMP14), which functions in extracellular matrix remodeling, and decorin (DCN) which contributes to extracellular matrix assembly, were both downregulated [24]. Also from Munoz-Gutierrez *et al.*, additional genes were discovered to be potentially upregulated or downregulated in mock and/or scrapie-inoculated, prion highly-permissive cells (i.e., 439) compared to poorly permissive cells (i.e., 438) [24].

For the current studies, we hypothesize that the expression of certain genes associated with apoptosis (survivin/BIRC5; follistatin-like 1/FSTL-1), cell proliferation (osteonectin/SPARC); cell-to-cell and cell-to-ECM adhesions (syndecan 4/SDC4), efferocytosis (AXL receptor tyrosine kinase/AXL), and extracellular matrix remodeling and repair (fibronectin 1/FN1; matrix metalloproteinase-2/MMP2), correlate with prion permissibility in ovine microglia cells, under *ex vivo* conditions. The aims of the first two studies are to: (1) determine if significant differential expression exists for AXL, BIRC5, FN1, FSTL1, SPARC, and SDC4, among inoculated, prion permissive clones independently and then relative to PRNP, (2) assess if correlations between expression of these genes and prion permissibility are present, and (3) validate significant differential expression of matrix metalloproteinase-2 (MMP2) in naïve ovine microglia sublines and clones of defined prion permissibility (i.e. highly or poorly), or prion accumulating (i.e. slow or fast) phenotype.

Human TSEs are characterized by long incubation periods and slow accumulation of prions [25], and currently, no human cell culture system exists in which to study these TSE variants. Ultimately, the creation of a stably-infected, human cell culture system would provide an opportunity to study the pathophysiology, molecular and cellular aspects of human prion disease. Once genetic determinants of prion permissibility have been validated for classical scrapie using *ex vivo* models, coupled with evaluation of *in vivo* models to identify potential determinants *in situ*, these determinants could potentially be extrapolated to the study of human prion disease in cell culture. Thus, the first step in analysis of the *in vivo/in situ* model is to

define the distribution of PrP^{Sc} in a slow, prion-accumulating isolate (i.e., US atypical scrapie), and assess if differential expression exists for any of the determinants. Our aim for the third study is focused on protein expression using an *in vivo* model of atypical scrapie. Although vastly different from classical scrapie and not reportable at this time [26, 27], the sporadic/low rate of infectivity, and paucity of information detailing the epidemiologic and pathophysiologic mechanisms of this disease, render additional investigation into atypical scrapie a necessity. The aims of this study are to: (1) characterize the localization and pattern of PrP^{Sc} deposition and accumulation in the brain of four, ARR sheep inoculated intracranially (i.e., intracerebrally) with a natural North American atypical scrapie isolate, and (2) determine if this atypical scrapie pathotype is the same as described in other countries, is the same as described in other countries, particularly in Europe [8, 9, 13, 16], but also Canada [28] and Australia [29].

Several goals can potentially be obtained from these projects to enrich the study of classical and atypical scrapie. First, recognizing novel or confirming predetermined genes as risk factors for prion permissibility, validates their utility as biomarkers of prion disease. These biomarkers could be used to identify at-risk animals and alter their genetic profile through breeding manipulation, thereby diminishing the impending spread of prion disease. Furthermore, at risk animals could be detected and culled before detection at slaughter or in fallen stock. Second, identifying abnormal intercellular and intracellular pathways coupled with the influence of the extracellular matrix provides more information on roles in prion disease pathogenesis. In this way, influential pathways could be targeted with inhibitors to impede propagation of prion disease. Third, knowledge of these determinants could be used to engineer a human cell culture system for the propagation of slowly-accumulating prions, which is the predominant manifestation of human prion disease. As it relates to atypical scrapie, identical or similar scrapie pathotypes of prion disease (i.e., US versus European) indicate some degree of conservation in the pathophysiological mechanism of disease, so it is possible that differentially-expressed genes and signaling pathways in these pathotypes are also preserved. Evaluation of

this atypical isolate that mirrors the rate of prion accumulation and incubation period in humans, could contribute to advancement of this culture system.

CHAPTER 2 LITERATURE REVIEW

Transmissible spongiform encephalopathies (TSEs) are a group of permanent, fatal, neurodegenerative disorders affecting a wide spectrum of hosts including humans (Creutzfeldt-Jakob disease [CJD], Kuru), ungulates (scrapie in sheep and goats; bovine spongiform encephalopathy [BSE] in cattle; chronic wasting disease [CWD] in cervids; camelids), mink (mink spongiform encephalopathy [MSE]), and felids (feline spongiform encephalopathy [FSE]) [1-4]. The term *prion* refers to “small, proteinaceous, infectious particles”, and the causative agent for TSEs involves accumulation of the misfolded, pathological isoform of normal cellular prion protein (PrP^C), referred to as disease-associated prion protein (PrP^D) [5]. PrP^D is partially to completely resistant to degradation by proteases, ultraviolet irradiation, heat, chemical solvents, detergents, and formalin [5, 62].

PrP^C is a protein encoded by the host gene PRNP, and is evolutionarily conserved amongst mammalian species [19, 63, 64]. Although the functions of PrP^C are not completely elucidated, studies have suggested roles in signal transduction, cell adhesion, anti-apoptosis, protection against oxidative stress, and in the regulation of synapses [65-70]. PrP^C is found predominately within lipid rafts and caveolae of the outer plasma membrane of cells, such as neurons, astrocytes, microglial cells, lymphocytes, follicular dendritic cells, choroid plexus epithelium, pericytes, and endothelial cells [19, 71-74]. This cellular protein has a secondary conformation consisting predominantly of α-helices with fewer β-pleated sheets [75]. According to the “protein-only” hypothesis introduced by Prusiner and Griffith, once PrP^C becomes misfolded through post-translational modifications into a majority of β-pleated helical sheets, infectious monomers and/or oligomers of PrP^D are formed that are self-perpetuating and act as

templates to autocatalytically convert other adjacent PrP^{C} proteins to polymerized PrP^{D} [19, 76-80]. In cultured scrapie-infected cells, the conversion of PrP^{C} to PrP^{Sc} (Sc for scrapie) is believed to take place not only on the cell surface but also within vesicles along the endolysosomal pathway [19, 81]. PrP^{C} and PrP^{Sc} have also been observed along the surface and within exosomes, which are believed to contribute to dissemination of prion disease in the CNS and lymphoreticular system [82]. Exosomes are membrane-bound vesicles secreted into the extracellular environment from multiple cells, including platelets [83], adipocytes, glial and stem cells [84], and are also found associated with cells used in cell culture, such as Rov and Mov cells (ovinized RK13 [rabbit kidney epithelial cells], and murine neuroglia cells, respectively) [85]. Extracellular PrP^{Sc} has also been discovered particularly in infected tissues [86], and *in vitro* studies have shown that a physiological environment containing excessive amounts of polysaccharides and collagen enhances the conversion of PrP^{C} to PrP^{Sc} [87]. Whether these various environments are solely sites of PrP^{Sc} conversion, PrP^{Sc} accumulation, or both remains incompletely elucidated, but it seems feasible that both processes are occurring to some extent.

PrP^{C} and PrP^{Sc} are bound to the plasma membrane by a glycosylphosphatidylinositol (GPI) glycoprotein anchor, embedded in lipid rafts at the C-terminal end, and this anchor has been proven necessary for the stable propagation of scrapie in infected cell culture models [65, 76, 77, 88, 89]. McNally *et al.* discovered that scrapie-infected, anchorless (GPI^{-}) PrP^{sen} (protease-sensitive prion protein) transiently produced anchorless PrP^{res} (protease-resistant prion protein) in cell culture, and it failed to transmit infection to mice [88]. However, in scrapie-infected cell-free systems or transgenic mice, anchorless PrP can be converted stably to PrP^{res} [90, 91], and in some studies, the CNS accumulation pattern of PrP^{res} is different from the pattern visualized in the presence of the GPI anchor (i.e., amyloid plaques with anchorless PrP conversion) [91]. PrP^{C} also has two N-linked glycosylation sites where glycans bind to asparagine (Asn) that is linked to N-acetylglucosamine (GlcNAc) residues, an event occurring

during post-translational modification [92, 93]. N-linked glycosylation can affect protein folding, oligomerization, stability, targeting, and recognition, and has been observed to influence the rate of fibril formation in PrP^{C} [92, 93]. PrP^{C} and PrP^{Sc} both exist as diglycosylated, monoglycosylated, and unglycosylated forms [94], and studies have shown differences in glycosylation patterns after proteinase K (PK) treatment between PrP^{C} and PrP^{Sc}, however, the implications in disease pathogenesis remain unknown. Russelakis-Carneiro *et al.* discovered that in uninfected mice and hamsters, diglycosylated and monoglycosylated PrP^{C} with slight traces of nonglycosylated PrP^{C} were identified in the brain and optic nerve, but only diglycosylated and monoglycosylated PrP^{C} were present in the retina [6]. However, upon stereotaxic injection of murine scrapie strains ME7 and 139A, the amount of unglycosylated PrP (PrP indicating total protein) increased with disease progression, becoming the predominant form in all 3 neuroanatomic regions [6].

Scrapie, which affects sheep, goats, and mouflons, is the first identified and oldest described prion disease [95]. There are two predominant variants of scrapie, classical and atypical. Although classical scrapie is an infectious disease, certain PRNP genotypes can either increase or decrease susceptibility to infection. The wild-type ovine PRNP gene encodes for the amino acids alanine (A) at codon 136, arginine (R) at codon 154, and glutamine (Q) at codon 171 [96, 97]. Polymorphisms in this gene at codons 136 (A/alanine or V/valine), 154 (R/arginine or H/ histidine), and/or 171 (Q/glutamine, R/arginine, or H/histidine) are primarily responsible for this variation in disease predisposition [1, 2]. Genotypes VRQ/VRQ, ARQ/VRQ, and ARQ/ARQ increase the potential for classical scrapie infection, whereas ARR/ARR diminishes the probability of infection [1, 98]. VRQ/VRQ and VRQ/ARQ have been associated with a shortened incubation period, different Western blot glycosylation pattern, and conformationally unstable PrP^{Sc} as compared to ARQ/ARQ [99]. Recently, Cassmann *et al.* revealed that Barbado sheep homozygous for lysine (KK) at codon 171 were resistant to classical scrapie experimentally after oronasal infection with a natural scrapie isolate [100]. In contrast to classical scrapie, in which

ARR/ARR normally confers resistance, homozygous ARR animals have increased susceptibility to atypical scrapie. Additional polymorphisms associated with increased susceptibility in atypical scrapie include phenylalanine (F) or leucine (L) at codon 141 (homozygous or heterozygous AFRQ and ALRQ), and histidine (H) at codon 154 (homozygous or heterozygous AHQ) [10, 14]. Atypical scrapie cases reported in Europe often were homozygous or heterozygous for ARQ or AHQ [13, 28, 52], whereas cases reported in the US were typically homozygous or heterozygous for AFRQ or ALRQ [12, 29]. In atypical scrapie, disease occurrence is believed to be spontaneous, or with a low rate of natural infectivity [8, 9].

Scrapie infection is naturally characterized by lengthy incubation periods ranging from 2 to 7 years for classical [1, 2, 9], and up to 20 years for atypical [8], so affected sheep and goats can be asymptomatic carriers initially, but ultimately all infected animals can succumb to active disease. At the onset of clinical signs in classical scrapie, prion infection is progressive, lasting approximately 2 weeks to 6 months before death occurs. These signs vary with the stage of infection and include: intense pruritus resulting in scraping and rubbing against objects with subsequent wool loss, dermal abrasions and excoriations (hence, the term “scrapie”), excitation, seizures, and paralysis [2]. In cases of atypical scrapie, the duration of asymptomatic illness is not definitively known, as many cases are only detected in fallen stock or slaughtered animals for human consumption [1], but the most common presenting clinical sign, when present, is ataxia. [9].

In classical scrapie, dissemination and propagation of prion infection, with deposition and accumulation of PrP^{Sc}, is dependent on multiple factors that can vary based on the mode of transmission, PRNP genotype, and the chronicity of infection. According to several studies of natural infection in sheep and experimental infection in rodents, it is proposed that infection begins with ingestion of exogenous PrP^{Sc} contaminants in feed or from the environment [1, 101]. PrP^{Sc} disseminates, replicates, and accumulates in the palatine tonsils and/or retropharyngeal lymph nodes [102, 103], before traveling to the intestines. From the intestines, PrP^{Sc} enters the

gut-associated lymphoid tissue (GALT), particularly ileal Peyer's patches via transcytosis by M cells [103] and/or an endocytosis/transcytosis process utilizing a ferritin-dependent mechanism [101], where it replicates in follicular dendritic cells within germinal centers of B-cell follicles [101, 104, 105]. PrP^{Sc} then travels by way of migrating intestinal dendritic cells from the intestines through the lymphatic system to reach the mesenteric lymph nodes [104, 106]. Once PrP^{Sc} enters the hematopoietic system, there is multicentric dissemination to other lymph nodes and the spleen by macrophages, migrating dendritic cells, and less commonly, lymphocytes [101, 104]. From enteric submucosal and myenteric plexuses [102-104], PrP^{Sc} travels along the length of the intestines via parasympathetic and sympathetic peripheral nerves [107], by retrograde axonal transport to the central nervous system (CNS), where it aggregates and accumulates first in the dorsal motor nucleus of the vagus nerve in the medulla oblongata [101, 102, 107], and then propagates in various groups of neurons within the grey matter of the brainstem (particularly the obex) and the thoracic spinal cord [102]. The mechanism of action for neurotoxicity remains under investigation, however, it has been suggested that either the deficiency of a critical biological PrP^{C} function and/or gain of PrP^{Sc} toxic properties result in neurodegeneration and disease [108]. From the CNS, PrP^{Sc} distributes to additional non-neuronal and non-lymphoid reticular system (LRS) tissues and organs such as adrenal glands, heart, skin, urinary bladder, mammary glands, pancreas, liver, lung, kidney, skeletal muscle, and placenta, through the peripheral nervous system (PNS) [104, 109, 110]. PrP^{Sc} is excreted into the environment from affected sheep, most commonly through contaminated placental tissue [110, 111], which can result in horizontal transmission of scrapie. Some studies have shown that PrP^{Sc} can be detected in the saliva [112], and milk or colostrum [113] of infected sheep, which could also be a factor for environmental transmission of scrapie, as the presence of infectious PrP^{CWD} has been identified in the salivary gland and urinary bladder of chronic wasting disease (CWD)-exposed deer [114]. Disease pathogenesis in atypical scrapie is not fully characterized, but based on the currently accepted theory of spontaneous origination, PrP^{Sc}

is believed to occur secondary to repetitive, physiological, chronic folding and metabolism of PrP^{C} in the brain [1, 8]. PrP^{Sc} deposition and accumulation typically affect the nucleus of the spinal nerve of the trigeminal tract, cerebellar and cerebral cortices, and with mixed frequency, substantia nigra for atypical scrapie [8, 28]. Of interest, Andreoletti *et al.* discovered that skeletal muscle, nerves, and lymphoid tissue from natural and experimental cases of atypical scrapie in sheep, were infectious in murine infectivity assays, but PrP^{Sc} was not detected in these tissues with Western blot, ELISA, or IHC [18]. This finding indicates that PrP^{Sc} in atypical scrapie may have a wider anatomic distribution than originally perceived, and other organs may play a role in disease pathogenesis, similar to classical scrapie. This result also reveals that for atypical scrapie, PrP^{Sc} content in tissues and organs with the exception of brain, is either much lower than observed in classical scrapie, or routine diagnostic tests, such as Western blot and ELISA, lack sufficient sensitivity to detect the prion protein.

Gross lesions are absent in classical and atypical scrapie. Characteristic CNS histopathologic lesions are consistent in cases of natural and experimental, classical and atypical, scrapie-infected sheep. They are usually bilaterally symmetrical and consist of intraneuronal and/or neuropil vacuolation (spongiform change), and gliosis [9, 115-117]. The morphology, quantity of vacuoles, and distribution can vary, but all are membrane-bound and often found within the neuronal perikarya, dendrites, and axonal terminals [116, 118, 119]. For classical scrapie, neurons within the brainstem (particularly the dorsal motor nucleus of the vagus nerve, and other nuclei in the obex) and spinal cord (dorsal horn and intermediate grey matter) are most commonly affected [102, 119]. Diseased neurons are infrequently degenerate or necrotic, characterized by chromatolytic changes or shrinkage, angulation, and hypereosinophilia. Neuronal loss is often inconspicuous or absent [115, 116, 118]. Perivascular amyloid plaques are more frequent with classical scrapie, and when present, they target vessels of the mesencephalon and rostral brain [120]. Plaque lesions are most likely a degenerative response induced by the presence of PrP^{Sc}, and are not specific to classical scrapie nor are

they a specific cause of PrP^{Sc}-induced neuropathology or clinical signs [116]. In experimental infection of mice with sheep scrapie strains, the pattern of vacuolation can vary and is specific to the type of strain inocula [115]. Neuropil vacuolation and spongiform change are common features of atypical scrapie, predominantly localized to the molecular layer (and less frequently, granular layer) of the cerebellum and the cerebral cortex [18, 28]. Non-perivascular plaques and plaque-like aggregates may also be present in atypical scrapie.

In classical and atypical scrapie, detection of PrP^{Sc} accumulation occurs in the central nervous system, but the predominant pattern varies between the two diseases. In classical scrapie, PrP^{Sc} patterns are most commonly intraneuronal and intraglial [121], whereas the pattern in atypical scrapie is in the neuropil of nuclei, white matter, or less frequently perineuronal [14, 28]. PrP^{Sc} accumulation, although becoming increasingly more severe as the infection progresses, can vary dramatically morphologically and topographically based on the scrapie strain and sheep breed [115].

Detection of PrP^{Sc} deposition in lymphoreticular tissues and organs is also a hallmark of classical scrapie, but PrP^{Sc} deposition has only been definitively observed in the brain of atypical scrapie cases, although infectivity assays suggest the presence of PrP^{Sc} deposition in other organs [18].

To differentiate classical and atypical scrapie, diagnostic techniques most often used include electron microscopy, immunohistochemistry, and immunocytochemistry (Western blot and ELISA) [115, 122]. Western blot remains the gold standard for confirmation of PrP^{Sc}, and after proteinase K (PK) treatment, a multiband pattern is apparent in atypical scrapie, whereas with classical scrapie, 3 distinct bands are visible [9].

In tissue sections, PrP^{Sc} can be found extracellularly in contact with the cell membrane of neurons, astrocytes, and other glial cells for both classical and atypical scrapie, as well as intracellularly in the CNS [115, 123, 124], and in myenteric and submucosal plexuses of the enteric nervous system in classical scrapie [103, 125]. Additionally, with classical scrapie, PrP^{Sc}

has been detected in follicular dendritic cells and macrophages of GALT and Peyer's patches [103]. In classical scrapie, PrP^{Sc} deposits and accumulation can also be found in other organs, such as pancreas, heart, kidney, skeletal muscle [109], placenta [110], and blood [126] of infected animals.

The most common electron microscopic findings in classical scrapie include the presence of "scrapie-associated fibrils" which are amyloid-positive plaques composed of PrP^{Sc} [127], glycogen granules and hypertrophic glial filaments within reactive astrocytes [128], vacuoles containing internal curled membrane fragments, dystrophic neurites, and membranous proliferation [129]. Limited details are within the literature characterizing electron microscopic findings in atypical scrapie.

Although polymorphisms in the ovine PRNP gene predispose affected sheep to the onset of prion disease and PrP^{C} is essential for conversion to PrP^{Sc}, the definitive mechanistic role and influence of other cellular products on prion disease pathogenesis remains unknown. However, growing numbers of studies are investigating the expression of various genes and proteins in both *ex vivo* and *in vivo* models of prion infection. Some of these studies have shown promise in identifying certain differentially- regulated or expressed genes in the presence and absence of scrapie infection, and it is plausible that with consistency and repetition of these results, these genes could be eventually classified as known risk factors and utilized as diagnostic biomarkers for prion infection. Additionally, identifying genes and proteins that affect prion permissibility of cells will provide more clarity in prion disease pathogenesis. This could lead to the development of activators and inhibitors that minimize the likelihood of prion infection, deposition, and accumulation. Gossner *et al*. discovered differential expression of genes in the lymph node and spleen of *VRQ/VRQ* classical scrapie-infected sheep. Genes associated with oxidative stress (i.e. SEPP1) were downregulated, whereas genes associated with apoptosis (i.e. DDX5) were upregulated, compared to mock-infected sheep [130]. The results of this study suggest programmed cell death is triggered by classical scrapie in

lymphoreticular organs and tissues, but antioxidant activity is diminished in homozygous VRQ scrapie-infected sheep. Filali *et al.* performed transcriptomic analysis of the medulla oblongata from ARQ/ARQ sheep chronically infected with a natural classical scrapie isolate, and identified metallothionein 2A (MT2A; metal binding protein) and glutathione peroxidase 1 (GPX-1; oxidative stress) were significantly upregulated and positively associated with PrP^{Sc} deposition, whereas melatonin receptor 1B (MTNR1B; oxidative stress) and collagen alpha-2 chain (COL1A2; extracellular matrix) were significantly downregulated [22]. These results suggest some antioxidants are variably expressed in classical scrapie infection, but upregulation coincides with the level of PrP^{Sc} deposition and could represent efforts at neuroprotection in homozygous ARQ scrapie infected sheep. Of interest, metal binding proteins may be upregulated secondary to increased inflammatory signaling, and/or increased recruitment of metals to the extracellular environment for reparative efforts.

Some studies have evaluated if genes are differentially expressed, based on susceptibility or resistance to prion infection in cell culture. Marbiah *et al*. isolated prion-resistant cell clones from highly-susceptible murine neuroblastoma cells (N2a), and after silencing nine genes that included fibronectin 1 (FN1) and 3'-phosphoadenosine 5'-phosphosulphate synthase 2 (Papss2), affected cells were converted to a prion-susceptible phenotype [23]. Furthermore, silencing of Papss2, FN1, and integrin subunit α8 (ITGA8) led directly to enhanced prion infection [23]. These genes encode key proteins in the extracellular matrix (ECM), and while FN1 and ITGA8 are critical for proper glycosylation, Papss2 is essential for proper sulphation [23]. These results suggest that resistance or susceptibility to prion infection in N2a cells is influenced by the differential expression of extracellular matrical genes.

Still, other studies have assessed if genes are differentially expressed in permissive and non-permissive cell culture systems, in the presence or absence of scrapie prions. Munoz-Gutierrez *et al.* discovered differentially-regulated or expressed genes between prion poorly-permissive and prion highly-permissive ovine, VRQ/VRQ microglia clones in RNAseq analysis

[24]. For example, in prion poorly-permissive clones compared to the highly-permissive counterpart, matrix metalloproteinase 14 (MMP14), which functions in extracellular matrix remodeling was upregulated, as well as decorin (DCN) which contributes to ECM assembly [24]. Furthermore, the most commonly modified biological pathways were genes involved in proteolysis, translation, and mitosis, but other genes of interest were associated with apoptosis, phagocytosis, extracellular matrix modeling and remodeling, and mitosis [24]. The results of Munoz-Gutierrez *et al.* suggest that differential expressed, or the upregulation and downregulation of genes could impact prion permissibility, and in this case, poorly- permissive ovine microglia may have increased remodeling and assembly of the extracellular matrix.

Although each of these studies identified differentially-regulated or expressed genes, and activation of physiological processes that may support prion replication and accumulation, some limitations exist. Gossner *et al.* were unable to validate half of the differentially-expressed genes that were conserved in both tissues, and the evaluation of other lymph nodes peripheral to the inoculation site may have identified if gene expression variations are consistent as disease progresses in similar tissues. Filali *et al.* evaluated the transcriptomic profile of chronically, prion-infected sheep, but some genes could be expressed differently in acute stages of infection. Marbiah *et al.* used clones derived from parental N2a mouse-derived cells but inoculated with a sheep scrapie strain (RML), and since prion strains may behave differently depending on the cell culture line utilized, there is some uncertainty as to whether the scrapie strain or the murine host exerts the most influence to the differentially-regulated gene profile. Furthermore, in Marbiah *et al.*, the mechanism by which the ECM acts on prion susceptibility is undetermined, and it is unknown if this mechanism extends to other species and cell types. For Munoz *et al.*, the gene expression profile of only two clones were assessed, but the expression in other clones from the same subline and correlations with prion permissibility remained unknown.

In the proposed studies, certain differentially-expressed genes, or genes with a possible link to prion permissibility identified in the investigation of Munoz *et al*., will be further validated in additional, inoculated microglia clones to: (1) determine if clone and/or treatment status are significant to gene expression, (2) assess if any significant correlations exist between gene expression and prion permissibility, and (3) evaluate the role of PRNP in the expression of these target genes (target gene/PRNP expression). These genes include: AXL receptor tyrosine kinase (AXL), fibronectin 1 (FN1), survivin (BIRC5), syndecan 4 (SDC4), osteonectin (SPARC), and follistatin-like 1 (FSTL1). These genes encode extracellular matrical proteins that aid in tissue remodeling and repair of the microenvironment, cell-to-cell and cell-to-ECM adhesions, apoptosis, cell proliferation (i.e., mitosis), and efferocytosis. Differential regulation or expression of matrix metalloproteinase II (MMP2), which functions in extracellular matrix remodeling and repair, will also be assessed in naïve clones and sublines of either a defined prion permissibility (i.e., highly or poorly) or prion accumulating (i.e., slow or fast) phenotype.

AXL receptor tyrosine kinase (AXL) is a member of the TAM family that includes Tyro3 and Mertk, and is expressed in phagocytic cells of the nervous, immune, and reproductive systems, in addition to sentinel immune cells, neurons, microglia, and endothelial cells [131, 132]. In the presence of ligand, growth arrest specific protein 6 (Gas6), AXL binds not only to Gas6 but also to phosphatidylserine receptors on the surface of apoptotic cells, activating phagocytosis in a process known as efferocytosis [131-134]. This binding activates several signaling pathways to include MAPK/ERK kinases and PI3K/AKT that result in efferocytosis, and also cell proliferation, migration, and adhesion [135-137]. In mouse models, a double knockout of Mertk and AXL in microglia has resulted in the accumulation of apoptotic cells within the CNS, and affected microglia exhibited decreased motility and delayed response to injury [138]. Inhibitors of tyrosine kinase enzymatic activity have been shown in some studies to promote degradation of PrP^{Sc} in prion-infected cells. Ertmer *et al.* noted that not only was PrP^{Sc} digested by lysosomes in 3 different cell lines (murine neuroblastoma cells, murine

hypothalamic cells, and murine non-neuronal cells) exposed to a commercial tyrosine kinase inhibiting agent ST1571, but additionally, the localization, expression, and biogenesis of PrP^C remained consistent and was not affected by ST1571 [139]. In Munoz-Gutierrez *et al.*, AXL had upregulated expression of a 1.5 to 1.8-fold change in highly-permissive inoculated ovine microglia clones compared to the poorly-permissive counterpart [140], so the influence of AXL on prion permissibility was assessed, since the process of efferocytosis could potentially contribute to propagation of prion disease in the CNS.

Fibronectin 1 (FN1) is a large molecular weight, structural glycoprotein that functions in ECM collagen assembly, cell adhesion and motility, and actin cytoskeletal organization [141]. Other functions include inhibition of apoptosis, phagocytosis, and microglial activation [142, 143]. Fibronectin 1 is synthesized by macrophages [144], epithelial and mesenchymal cells, and has multiple binding domains for collagen, other molecules of fibronectin, heparin, and integrins [141]. Assembly of fibronectin dimers into an insoluble fibrillar network is crucial to its activation, and is dependent on binding with integrin (particularly α5β1), arginyl-glycyl-aspartic acid (RGD), and synergy motifs [141]. Takahasi *et al.* has shown that FN assembly can still occur in the absence of RGD [144]. Microglial morphology and adhesion capability can vary based on the composition of extracellular matrix substrates such as fibronectin. Milner *et al*. discovered that in the presence of plastic, vitronectin, and fibronectin, microglia had strong avidity for fibronectin and adopted an amoeboid, activated morphology, whereas with laminin, small, individualized microglia were poorly adhered to the substrate [142]. As previously mentioned, Marbiah *et al.* observed that silencing of ITGA8 and FN1 in prion-resistant N2a cells inhibited MMP2/9 secretion, leading to increased prion susceptibility [23]. In Munoz et al., FN1 was downregulated by a 1.5-fold change in inoculated, highly- permissive ovine microglia clones compared to poorly-permissive clones [140]. Based on these studies, diminished transcript levels of FN1 could enhance prion susceptibility and permissibility; therefore, the role of FN1 with prion permissibility was evaluated. Additionally, some extracellular matrical proteins (i.e., growth

factors) can become concealed within the fibronectin matrix and elude degradation by proteases [143]; it is plausible then that PrP^{C} and PrP^{Sc} could also utilize a similar mechanism to promote increased expression and accumulation, respectively.

BIRC5 (also known as Baculoviral IAP Repeat containing 5 and survivin) is a protein that inhibits apoptosis, promotes cell division [145], and is overexpressed in cancer [146]. BIRC5 is the smallest member of the inhibitor of apoptosis (IAP) family at 142 amino acids in length [147], and is intricately involved at the G2:M transition of the cell cycle [148]. Survivin binds to hepatitis B X-interacting protein (HBXIP), which when coupled to procaspase-9 directly inhibits apoptosis [146]. Jiang *et al.* revealed that BIRC5 expression occurs during embryogenesis, and is essential for neuronal development [149]. BIRC5 was downregulated by a 5.7 to 6.7-fold change in inoculated, highly-permissive ovine microglia clones, in contrast to poorly-permissive clones ovine microglia clones [140]. Rare reports discuss expression of BIRC5 as it relates to prion disease, so the influence of this gene with prion permissibility was further characterized. As an inhibitor of apoptosis, this function could contribute to accumulation and dissemination of scrapie prions.

Syndecan 4 (SDC4) is a transmembrane heparin sulfate proteoglycan that is suggested to contribute cell-to-cell-adhesion, and the assembly of scaffolding and signaling ECM proteins at the interior of the plasma membrane [150]. These scaffolding proteins bind to and determine the membranous location of cell surface receptors, connect with the cytoskeleton, assist in signal transduction [150], and also inhibit apoptosis [151]. SDC4 also functions in degradation of the ECM. Cellular heparin sulfate receptors, such as SDC4, have been reported to contribute to the formation of PrP^{Sc}. Horonchik *et al.* exposed N2a, CHO, and GT1–1 cells inoculated with purified prion rods to sulfation inhibitors (bacterial heparinase III or chlorate), which significantly reduced the binding and uptake of prion protein rods for some of the inhibitors [152]. Based on reports of SDC4 enhancing formation of PrP^{Sc}, and the downregulation by 2.0 in inoculated, highly-permissive ovine microglia clones compared to poorly-permissive clones [140], this gene

was also included in the analysis to determine if any correlations with prion permissibility existed.

Osteonectin, also known as Secreted Protein Acidic and Rich in Cysteine (SPARC), BM-40, and 43K protein, is a matricellular protein composed of an extracellular calcium-binding domain and a follistatin-like domain [153]. SPARC has a variety of functions, including inhibiting cell proliferation by arresting the cell cycle, modulating cell-ECM interactions, cell migration, and survival [153, 154]. SPARC also regulates growth factors PDGF, VEGF, and FGF-2 [153]. Vincent *et al.* discovered SPARC is expressed by radial glia, microglia, brainstem astrocytes, and brain barriers in embryogenesis, remaining in specialized radial glia, microglia and brainstem astrocytes into adulthood [154]. SPARC expression in specialized glia suggests a role in neurogenesis, synaptic plasticity, angiogenesis, and cell migration [154]. Booth *et al.* identified differential expression of SPARC between non-infected and scrapie-infected brain tissue from C57BL/6 mice experimentally inoculated (i.e., intracerebral) with one of two mouse-adapted prion strains (i.e., ME7, 79a) [155]. SPARC was downregulated by a 2.0-fold change in highly-permissive ovine microglia clones in contrast to poorly- permissive clones [24]. Enhanced PrP^{Sc} accumulation has been reported in non-dividing cells in cell culture [156], and as an inhibitor of cell proliferation, this gene was further assessed.

Follistatin-like 1 (FSTL1), also known as transforming growth factor β1 stimulated clone 36 (TSC-36) or follistatin-related protein (FRP), was originally identified in the mouse osteoblastic cell line MC3T3-E1 [157, 158]. FSTL1 is a secreted glycoprotein produced predominately by mesenchymal cells [158] as well as endothelial cells and neurons [159]. FSTL-1 is also a member of the SPARC family [160]. Although the specific function of FSTL-1 has not been elucidated, various studies have recognized a role in different signaling pathways of cell survival or anti-apoptosis [159, 161], cell proliferation, differentiation and organ development [160, 162], metastatic neoplasia [163] , and recently, inflammation [158]. Genes that upregulate FSTL1 include IL-1β, TNFα, FOS, ERK1/2, TGFβ, and AKT, and some of these

genes are also regulated by FSTL1 [160]. Scarce reports in the literature evaluate the role of FSTL-1 in prion disease, so this gene was further characterized in the study, since it was also downregulated by a 1.67-fold change in inoculated, highly-permissive ovine microglia clones compared to poorly-permissive clones [24]. With a role in inhibition of apoptosis, this gene may also contribute to prion accumulation and dissemination in the CNS.

Matrix metalloproteinases (MMPs) are a group of zinc-dependent, endopeptidases that degrade various substrates in the extracellular matrix (ECM) during remodeling and repair [31]. MMPs are ubiquitous in the central nervous system, and in humans, they are reported to be secreted by neurons, oligodendrocytes, microglia, reactive astrocytes, and endothelial cells [34, 35]. Matrix metalloproteinase-2 (MMP-2 or Gelatinase A), degrades fibrillar collagens I, II, III, V, VII, and X, collagen IV, denatured collagen or gelatins, laminin, elastin, fibronectin, cell adhesion molecules, proteoglycans, growth factors, and cytokines [31, 36, 165]. Activators of MMP2 include MMP-14 (a.k.a. MT1-MMP) in conjunction with Tissue Inhibitor of Metalloproteinase II (TIMP-2) [31, 165], serine proteases, reactive oxygen species, and other additional MMPs, such as MMP-16 and MMP-2 [31, 165]. Inhibitors of MMP-2 include TIMP-2, TIMP-3, and TIMP-4 [31]. MMP2 is ubiquitously distributed and is one of the major enzymatic proteins responsible for ECM remodeling, cell survival, angiogenesis, inflammation, and signaling [31]. Lewis *et al.* discovered that MMP-2 degrades PrP^C at the amino terminus, and when inhibited by a pan-MMP inhibitor, there was an increase in C1 fragments [167]. In Marbiah *et al*., when MMP2 transcript levels were decreased subsequent to silencing of FN1, prion revertant, murine neuroblastoma cells became susceptible to infection with scrapie prions [23]. Additionally, MMP2 transcript levels were decreased by a fold change of 1.5 in inoculated, highly-permissive ovine microglia clones in contrast to poorly-permissive clones [24]. These findings suggest that decreased MMP2 transcript levels influence prion susceptibility and permissibility, so this gene was also further characterized.

In another study, prion protein expression will be further assessed in four ARR/ARR sheep intracranially inoculated with a natural North American atypical scrapie isolate. The aims of this study are to: (1) characterize the neuroanatomical localization and pattern of PrP^{Sc}, and (2) determine if this pathotype compares to other atypical pathotypes reported in the literature. Identical or similar pathotypes of European atypical and US atypical prion disease indicate some degree of conservation in the pathophysiological mechanism of disease, so it is possible that differentially-expressed genes and signaling pathways in these pathotypes are also preserved. Hence, since atypical scrapie has similarities to human prion disease (i.e., long incubation period, slow accumulation of PrP^{Sc}), this disease can be studied accordingly and potentially extrapolated to human prion disease, encouraging the development of a human cell culture model system.

CHAPTER 3 EXPRESSION AND CORRELATION OF EXTRACELLULAR MATRICAL AND NON-EXTRACELLULAR MATRICAL PROTEINS WITH PRION (PrP^{Sc}) PERMISSIBILITY IN AN OVINE MODEL OF CLASSICAL SCRAPIE

Transmissible spongiform encephalopathies (TSEs) are a group of progressive, fatal neurodegenerative diseases that affect cattle (bovine spongiform encephalopathy), small ruminants (scrapie), cervids (chronic wasting disease), felids (feline spongiform encephalopathy), humans (Creutzfeldt-Jakob disease and Kuru) [2,19] and now camelids [30]. Classical scrapie is the oldest described prion disease, dating back to over 250 years ago [31]. Due to the public concern for all prion diseases, and the economic and financial devastation associated with this disease, eradication efforts have been implemented in various countries for the control and elimination of classical scrapie.

Originally coined as “proteinaceous infectious particle or prion” [32], TSEs are caused by a misfolded, pathogenic isoform (PrP^{D}; D for disease-associated) of the normal, host-encoded, cellular prion protein (PrP^{C}; C for cellular) [32 – 37]In this disease, PrP^{D} can promote autocatalytic conversion of normal PrP^{C} to PrP^{D} in a perpetuating, positive feedback cycle [5, 33 –36]. While most TSEs are initiated after exposure to PrP^{D} from an infected animal, PrP^{C} has also been reported to spontaneously convert to PrP^{D} [37-39]. Although there are variations in several of the key components contributing to prion infection in hosts, including heterogeneity of PrP^{D} strains [40], neuroanatomical distribution of lesions and PrP^{D} deposits [2, 40], and post-translational PrP^{C} modifications [36], the common denominator is the conversion of PrP^{C} to its pathological isoform, PrP^{D}.

PrP^{C} is a protein encoded by the host gene PRNP which is evolutionarily conserved amongst mammals [19, 41, 42]and is constitutively expressed in several cell types, but notably

in adult neurons [43], glial cells [44], lymphocytes, and monocytes [45]. In sheep, PrP^C is 256 amino acids long [42, 46]. Polymorphisms in PrP^C have been reported in codons 136 (A/alanine or V/valine), 154 (R/arginine or H/ histidine) and/or 171 (Q/glutamine, R/arginine, or H/histidine) that increase susceptibility (i.e. VRQ/VRQ, ARQ/VRQ, ARQ/ARQ) or confer resistance (ARR/ARR) to classical scrapie in sheep [42, 47, 48].

Currently, many of the functions of PrP^C are suggested, and internalization of PrP^C through certain cellular receptors is only hypothesized [19, 49, 50]. Additionally, receptors for internalization, and sites of conversion and/or accumulation of PrP^D are also only hypothesized or suggested [19, 51]. This generalized paucity of knowledge in prion disease pathogenesis hinders the development of diagnostic aids, and of most importance, treatments in prion disease.

Various experimental model systems have been used to study and further characterize classical scrapie. In vivo models provide excellent systems to study the clinical aspects of the disease, and serve as the final test for potential therapies [52 – 54]. However, with in vivo models, assessment of cellular and extracellular factors that may influence disease onset or progression could be challenging to identify. Cell culture models serve as practical and informative ex-vivo systems, providing an avenue to study and dissect the role of cellular and extracellular constituents in prion disease pathogenesis, that cannot be dissected at the tissue or animal level. Furthermore, these models allow for the development and testing of treatments prior to animal testing. While transgenic cell culture models, such as ovinized rabbit kidney epithelial cells (Rov) [55], and ovinized mouse cerebellar astrocytes [19] allow for the expression of PrP^C from a normal prion host (e.g., sheep) and have provided useful information in prion research, these models cannot account for species-to-species variation in all of the other proteins. To circumvent potential complications with species-to-species variation in protein expression, non-transgenic cell culture lines can be used. For this study, immortalized ovine microglia cells [56, 57] were utilized. Microglia are innate, myeloid immune cells of the brain that

have similar functions to macrophages [58, 59]. These resident phagocytic cells have also been localized to the neuroanatomical vicinity of PrP^D deposits and contain intracellular PrP^D, which contributes to prion protein degradation but also potential dissemination [59]. Additionally, the use of non-transgenic expression of PrP^C increases the chances that PrP-non-PrP protein interactions are appropriate.

Using N2a cells inoculated with a mouse-adapted scrapie isolate (ScN2a), Marbiah *et al.* demonstrated that the downregulation of 9 extracellular matrix genes through silencing increased susceptibility to prion infection, and when fibronectin 1 was inhibited from binding to integrin α8, prion propagation was enhanced [23]. Some of the genes silenced include Chga and Lrrn4, which both function in remodeling and homeostasis of the extracellular matrix environment [23]. Munoz-Gutierrez *et al.* evaluated the transcriptomic profile in immortalized ovine microglial clones derived from the same subline, between one permissive and one relatively resistant to scrapie prions, and twenty-two genes were differentially expressed [24]. Additionally, several other genes were potentially differentially expressed or regulated (i.e., AXL, BIRC5, SPARC) [24]. Due to the limited nature of a single pairwise analysis, the relevance of these findings is unknown. Based on the demonstrated significance of the FN1-related ECM in N2a cells, and the potential, but inconclusive results from the previous pairwise microglial analysis, this paper studied these genes. Some of these variably-expressed or regulated genes contribute to remodeling, repair, and collagen assembly in the extracellular matrix (fibronectin1 [FN1]), adhesions between cells and the extracellular matrix (syndecan 4 [SDC4]), cellular proliferation (osteonectin [SPARC]), efferocytosis (AXL tyrosine kinase receptor [AXL]), and apoptosis (survivin [BIRC5]; follistatin-like 1 [FSTL1]) [24]. Dinkel *et al.* identified significant correlations between prion permissibility and genes implicated in cell growth (i.e. RARRES1), protein degradation (SQSTM1), and heparin binding (SEPP1) amongst 6 ovine microglia clones derived from the same subline and with varying degrees of prion permissibility [60]. All three of these studies depict the upregulation or downregulation of genes that either directly, indirectly,

or potentially contribute to prion susceptibility or permissibility, and the functional diversity of these genes indicate that susceptibility and permissibility are multifactorial.

While FN1 and its role in the ECM has been investigated in ScN2a cells, this has not been investigated in myeloid cells or in sheep scrapie. Furthermore, AXL, BIRC5, FSTL1, SPARC, and SDC4 have not been investigated in sheep scrapie nor myeloid cells. Based on statistically significant fold changes, Munoz-Gutierrez *et al*. discovered in a highly permissive microglia clone inoculated with a natural scrapie isolate, an upregulated fold change expression of 1.5 for AXL, but downregulated fold change expression of -1.5 for FN1, -1.7 for FSTL1, -3.0 for SPARC, -2.0 for SDC4 and -6.7 for BIRC5 [24], as compared to the relatively non-permissive clone. Only for BIRC5, SPARC and SDC4 were these changes two-fold or greater. Additionally, BIRC5 and SPARC also had significant downregulated fold changes in highly permissive Mock-inoculated microglia clones (-5.8 and -3.3 respectively) [24]. For this study, we expanded the analysis of AXL, BIRC5, FSTL1, FN1, SPARC and SDC4 into three additional immortalized, ovine microglia clones of varying prion permissibility, and one clone that reverted from highly to intermediately permissive to determine if any correlations existed.

Methods

A previously established immortalized (hTERT) ovine microglia cell subline (Subline H) was utilized [57, 61], which was approved by the Institutional Animal Care and Use Committee of Washington State University (ASAF04575). Six clones within the subline were further evaluated in the experimental study (438, 440, 434, 439Late, 441, and 439Early), arranged in order of diminishing permissibility to scrapie prion infection [60]. Clone 438 was least permissive; clones 440, 434, and 439Late of intermediate permissiveness, and clones 441 and 439Early as highly permissive [24, 60, 61]. 439Late and 439Early refer to a single clone whose permissibility changed after continual passage [62], and are treated as two separate clones in the study. These clones were previously inoculated with either a natural, sheep-derived scrapie

isolate (Utah) (derived from Animal Disease Research Unit; USDA Agricultural Research Service, Pullman, WA from a natural infected sheep in Utah, USA), or uninfected ovine brain homogenate (Mock) [56, 60]. Cells were cultured under standard conditions of Opti-MEM media (Gibco), supplemented with 10% complement-inactivated fetal bovine serum (Atlanta Biologicals), 10,000 units/mL penicillin (Hyclone), 10,000 µg/mL streptomycin (Hyclone), and 200 mM L-Glutamine (Hyclone). Cells were passaged every 3 to 4 days at a 1/5 dilution.

Cell suspensions for use with five experiments were previously collected at passage 5 (P-5) for Mock-inoculated clones, and for Utah-inoculated clones at passages P-2 (experiment 2.3Redo), P-4 (experiment 2.2), P-5 (experiment 1), P-6 (experiment 2.3), and P-7 (experiment 2.7) [60]. Over the course of all experiments, a total of at least 3 independent replicates of each clone, per inoculation status, were tallied. Cell suspensions were homogenized with QIAshredders (Qiagen) according to manufacturer's instructions. RNA was extracted from lysates using RNeasy Mini Kit (Qiagen), per manufacturer's directions. Eluted RNA was collected into DNA LoBind microcentrifuge tubes (Eppendorf) and stored at -80 °C until further use. When ready to use, RNA purity and concentration was measured using NanoDrop 2000 spectrophotometer (Thermo Scientific).

RNA was standardized at 10 µg/50 µL, and residual DNA was removed using Invitrogen DNA-free DNase Treatment and Removal kit (Fisher Scientific). A total volume of 50 µL was prepared per sample using 5 µL of 10x DNase I buffer, 1 µL of rDNase I, eluted RNA, and nuclease-free water. Each sample was incubated at 37 °C for 30 minutes before adding 5 µL of DNase Inactivation reagent. After addition of the inactivation reagent, the sample was mixed frequently and incubated at room temperature (~25 °C) for 2 minutes. Subsequent to centrifugation of the sample at 10,000 x g for 1.5 minutes, RNA was collected and transferred to a new, 0.5 mL DNA LoBind microcentrifuge tube (Eppendorf). RNA was either immediately stored at -80 °C, or purity and concentration were measured using NanoDrop 2000 spectrophotometer (Thermo Scientific), before storage for later use.

DNase-treated RNA was standardized to 1 µg/20 µL and first strand cDNA synthesis was performed using SuperScript III First-Strand Synthesis Supermix for qRT-PCR (ThermoFisher Scientific). Each sample consisted of 10 µL of 2x RT reaction mix, 2 µL of RT enzyme mix, 1 µg of DNase- treated RNA, and DEPC-treated water for a total volume of 20 µL. Samples were gently mixed, then incubated at 25 °C for 10 minutes, 50 °C for 30 minutes, and 85 °C for 5 minutes. After incubation, samples were chilled on ice for 5 minutes, and then 1 µL of *E. coli* RNase H was added before an additional incubation at 37°C for 20 minutes. After the last incubation, samples were chilled on ice for 5 minutes, and immediately stored at -80 °C.

Genes identified from previous RNAseq data in two clones of varying prion permissibility [24] were further assessed (**Table 3.1**). These annotated genes include fibronectin 1 (FN1), follistatin-like 1 (FSTL-1), osteonectin (SPARC), survivin (BIRC5), syndecan 4 (SDC4), AXL receptor tyrosine kinase (AXL), and prion protein (PRNP). 18s rRNA ribosomal RNA (18s rRNA) and hypoxanthine phosphoribosyltransferase 1 (hPRT1) are both reference genes that have shown stable expression as internal controls in quantitative PCR analyses [66-68] and were hence utilized as reference genes in this study. With the exception of PRNP [64] and FN1 [65], which were previously published, primers were designed for each gene according to a reference sequence listed for the gene using the database program from the National Center of Biotechnology Information [63]. Standard curves for each primer set were performed to determine efficiency, confirm predictability across dilutions ($r^2 > 0.85$), and establish a single, repeatable product melting temperature. The resulting products were also evaluated by standard agarose gel electrophoresis to confirm the product size.

Table 3.1. Primers for qRT-PCR and RT-PCR.

Genes	Gene name	Accession number for sequence	Forward primer sequence (5' – 3')	Reverse primer sequence (5' – 3')	Amplicon size (bp)
AXL[a]	AXL receptor tyrosine kinase	XM_004015278.4	AAGGACAGCCAATCCACCAG	ACACCTCTCCATAACGGGTCT	165
BIRC5[a]	Baculoviral IAP repeat-containing protein 5/Survivin	XM_004013098.3	CCCGACTTGGCTCAGTGTTT	AGCACAACCAGATGAATGCTT	102
hPRT1[a]	Hypoxanthine phosphoribosyltransferase	XM_015105023.1	GGCTCCGTTATGGCGGC	TTCGGTCCTGTCCATAATTAGTCC	150
18srRNA[a]	18s ribosomal RNA	XR_003587981.1	GAGGCCCTGTAATTGGAATGA	GCAGCAACTTTAATATACGCTATTGG	120
FN1[c]	Fibronectin 1	XM_004004911.4	TCTCGTGCCAGTGCTTAG	CTGACGATCCCACTTCTCTCC	110
FSTL1[a]	Follistatin-like 1	XM_027980274.1	TCATTCCAGACGGCTGGTTC	CTGGAGTCCAAGCGAGAGTC	100
PRNP[b]	Prion protein	NM_001009481.1	CCGTTACCCCAACCAAGTGT	CGCTCCATTATCTTGATGTCAGT	159
SPARC[a]	Osteonectin	XM_012177565.3	CTGTGACCTGGACAACGACA	GGAGGCGTGGCTTTAGATCA	109
SDC4[a]	Syndecan 4	XM_027977234.1	CTGATGACGAGGACATCGGG	ATAGGGACCAAGGGGTGCAT	127

[a] Primers were designed using either presumed or curated mRNA from selected genes in the database program of NIH, US National Library of Medicine, National Center for Biotechnology Information (NCBI) [63].

[b] PRNP primer sequences were derived from a previous publication [64].

[c] FN1 primer sequences were designed using PriFi [65].

All PCR products were cloned and sequenced to confirm amplification of the correct gene target. Superscript IV first strand cDNA synthesis system kit for RT-PCR (ThermoFisher Scientific) was used, according to manufacturer's instructions. Each reaction contained 50 ng of RNA, derived from naïve ovine microglia clone 439. First strand cDNA samples were then immediately used or stored at -20 °C. Conventional PCR was implemented using Advantage II PCR Enzyme System (Clontech) according to manufacturer's directions. Each reaction was composed of 40 µL of nuclease-free water, 5 µL of 10X PCR buffer, 1 µL of 50x dNTPs, 1 µL forward primer, 1 µL reverse primer, either 1 µL of Taq polymerase or nuclease free water, and 1 µL of cDNA. The PCR protocol was as follows: 95 °C for 5 minutes; 30 cycles of 95 °C for 30 seconds, 55 °C for 30 seconds, and 72°C for 30 seconds; and 72 °C for 7 minutes. Gel electrophoresis was used to assess the size and solitary nature of the products. Bands not exposed to ultraviolet imaging were cut from the gel, and the DNA was purified using QIAEX II Agarose Gel Extraction Kit (QIAGEN) according to manufacturer's instructions. Eluted, purified DNA was ligated into a pGEM-T easy vector system (Promega) per manufacturer's directions. Two microliters of each ligation reaction were transformed into 50 µL of JM109 high efficiency competent cells and plated, according to manufacturer's instructions with few modifications. Cells were heat shocked at 43°- 45 °C, transformation cultures were incubated for 2 hours at 37 °C with a shaking speed of 420 rpm, and approximately 200 µL of transformation cultures were plated onto LB/Ampicillin plates. After an overnight incubation at 37 °C, up to 9 clones were selected per plate, and evaluated for the presence of the correct gene product using conventional PCR and gel electrophoresis. Selected clones were isolated on an additional LB/Ampicillin agar plate, and placed in a 37 °C incubator for 8 – 12 hours. For each gene, a single clone of the correct size was further isolated in 3 µL of ampicillin, 3 mL of sterile LB medium, and a pipette tip containing the colony, in an overnight 37 °C incubation with a shaking speed of 420rpm. After incubation, DNA was eluted (QIAprep Spin Miniprep Kit, QIAGEN), per manufacturer's directions, and measured for concentration and purity using NanoDrop 2000

spectrophotometer (Thermo Scientific). Eluted DNA was submitted for commercial Sanger sequencing using GENEWIZ (www.genewiz.com) or MCLAB (www.mclab.com). Forward and reverse sequences were aligned using software programs Mega 6 (Molecular Evolutionary Genetics Analysis; www.megasoftware.net) and Geneious Prime (www.geneious.com), and the resulting consensus sequences were aligned to the National Center of Biotechnology Information (www.ncbi.nlm.nih.gov) nt database, using megablast.

Each reaction contained 10 µL SsoAdvanced Universal SYBR Green Supermix, 0.4 µL forward primer, 0.4 µL reverse primer, and 7.2 µL nuclease-free water. Either 2.5 µL of appropriately diluted cDNA or nuclease-free water for negative control was added to each reaction, and a single non-reverse transcriptase (NRT) control was run for each clone and gene. Reactions were then run with CFX96 Touch Real-Time PCR Detection System (Bio-Rad) with the following protocol for all primers: 95 °C for 30 minutes; 35 times of 95 °C for 15 seconds then 60 °C for 30 seconds, followed by 95 °C for 10 minutes, 60 °C for 5 minutes, and an increase in temperature in 0.5 °C increments from 60 °C to 95 °C.

Gene expression data normalized to reference genes 18s rRNA and hPRT1 was retrieved and evaluated from at least 3 independent replicates using the software program CFX Manager 3.1 (www.bio-rad.com: Bio-Rad, Hercules, CA). Statistical analyses were performed using JMP version 14 (www.jmp.com; SAS Institute, Cary, NC.). However, for Utah-inoculated clone 439Early, only 2 of the 3 independent replicates had the acquisition of data for BIRC5 (i.e., low, undetectable levels of transcript in one replicate). Relative prion permissibility was previously determined [60]. Normality of the data distribution was assessed per inoculation status, using histograms and Goodness-of-fit test. For data that was not normally distributed, Box-Cox transformation was used for approximation to normality, and this newly configured data was assessed for normality using histograms and Goodness of Fit test. Fold changes were computed manually using raw normalized expression (Mode in CFX Manager: Normalized expression (ΔΔ Cq)) collectively, and then relative to the previously identified least permissive

clone, 438 [60], for each gene by treatment group. Statistical significance of fold change (i.e., clone) was assessed using One-way ANOVA and *post hoc* Tukey-Kramer HSD for multiple pairwise comparisons ($p < 0.05$). Correlation of mean normalized gene expression with prion permissibility per treatment group was calculated using multivariate analysis with Pearson's correlation coefficient (Pearson's r). The effect of inoculation status, and the interaction of clone and inoculation status on gene expression were analyzed using pooled, raw expression data by gene in Two-way ANOVA and *post-hoc* Tukey HSD for multiple pairwise comparisons ($p < 0.05$). For genes in which inoculation status was not influential to expression, mean normalized gene expression data were pooled by gene and clone, and correlations between genes, as well as with prion permissibility were calculated using Pearson's r and Benjamini-Hochberg multiple comparison correction. qRT-PCR analyses and statistical calculations as previously described were also performed for relative density expression (Mode in CFX Manager: Relative quantity (ΔCq)) of target genes relative to PRNP (target gene/PRNP ratios) using at least 3 independent replicates.

Results

Seven genes with a potential role in prion permissibility were assessed with RT-qPCR, and normalized to 18s rRNA and hPRT1b. Gene expression data from Mock-inoculated clones showed a normal distribution (Goodness-of-Fit; $p > 0.05$). Utah-inoculated clones were not normally distributed for SDC4 (Goodness-of-Fit; $p < 0.001$) and SPARC (Goodness-of-Fit; $p < 0.01$) but were normally distributed for the remaining genes. For SDC4 and SPARC, raw expression values from Utah-inoculated clones were transformed with Box-Cox Y transformation test, and these values were deemed as normally distributed after assessment with histograms and Goodness of Fit test ($p > 0.05$) and subsequently utilized in parametric statistical analyses as such.

To determine if the RNA levels of the targeted genes significantly differed between clones, fold changes in normalized gene expression were statistically compared amongst all of the clones from at least 3 independent replicates collectively using one-way ANOVA and *post hoc* Tukey-Kramer HSD for multiple pairwise comparisons. Correlations to prion permissibility were assessed using Pearson's correlation coefficient test with corrections by Benjamini-Hochburg procedure (www.biostathandbook.com/multiplecomparisons.html). Statistically significant differences in expression were observed for BIRC5 ($p < 0.001$), SPARC ($p < 0.001$) and FSTL1 ($p < 0.01$) (**Figure 3.1**). For BIRC5, differential gene expression was significantly decreased for both 439Late and 439Early compared to all other clones ($p < 0.05$), and this decreased expression was a four-to-eight-fold change compared to clone 438. Expression of FSTL1 in clones 439Late ($p < 0.05$) and 439Early ($p < 0.05$) was significantly decreased compared to clone 434, and clone 439Late was also significantly decreased compared to clone 438 ($p < 0.05$), but these changes were less than two-fold compared to clone 438. Additionally, clone 440 had significantly decreased expression of FSTL1 compared to clones 438 ($p < 0.05$) and 434 ($p < 0.05$), but these changes were also less than two-fold compared to clone 438. With SPARC, clones 439Late and 439Early had significantly diminished expression compared to clones 438 ($p < 0.0001$ and $p < 0.01$) and 434 ($p < 0.001$ and $p < 0.05$), and these changes were two-to-three-fold compared to clone 438. Additionally, 439Late SPARC expression was significantly decreased compared to clone 441 ($p = 0.0378$). Furthermore, clone 438 had significantly increased SPARC expression compared to clones 441 ($p < 0.05$) and 440 ($p < 0.01$), and clone 434 was also significantly increased compared to 440 ($p < 0.05$), but these changes were less than two-fold compared to clone 438. Significant differential gene expression was lacking for AXL, FN1, PRNP and SDC4 in all pairwise comparisons.

Since clone 439 exhibited variation in permissibility over time, differences in gene expression were also assessed for 439Late relative to the most permissive clone, 439Early [60] in all evaluated genes. Only in BIRC5 was there a two-fold change expression in 439Late

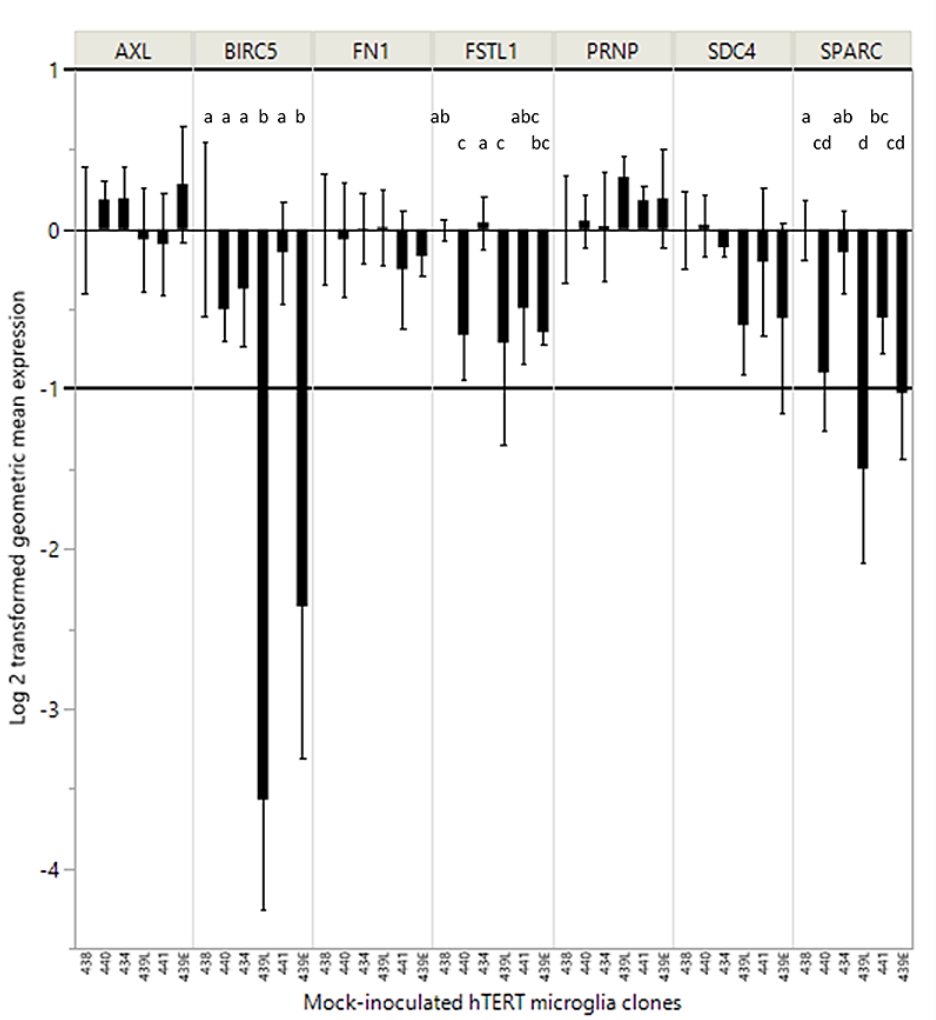

Figure 3.1. Fold change in gene expression for Mock-inoculated clones. Fold changes were assessed using normalized gene expression relative to the least permissive clone (438) for Mock-inoculated clones. Expression data was normalized to 18s rRNA and hPRT1, scaled to 438, and then the geometric mean and geometric standard deviation factor were calculated for graphical representation. Solid, black horizontal lines (i.e., 2^{1} or 2^{-1}) demarcate the two-fold change threshold. The x-axis is ordered by increasing prion permissibility phenotype (left to right). The horizontal axes are partitioned into panels by gene (AXL, BIRC5, FN1, FSTL1, PRNP, SDC4, SPARC). Error bars indicate 1 geometric standard deviation factor from the geometric mean. In differentially expressed genes, clones that do not share the same letter had significant differential mean expression ($p < 0.05$). E = Early Mock, L = Late Mock

relative to 439Early, but this change was not statistically significant ($p > 0.05$).

There were no statistically significant correlations between mean normalized gene expression of Mock-inoculated clones and prion permissibility ($p > 0.05$).

As described in section 3.2, analysis of fold changes in gene expression and correlations with prion permissibility were also performed for Utah-inoculated clones for at least 3 independent replicates, with the exception of clone 439Early for BIRC5 in which data from only 2 out of 3 independent replicates was available to assess (i.e., low, undetectable transcript levels in one replicate). Individual, significant variations in gene expression were present for PRNP ($p < 0.05$) and SPARC ($p < 0.01$) (**Figure 3.2**).

A single, significant increase in PRNP expression was observed for clone 439Late as compared to clone 438 ($p < 0.05$); however, this change was less than two-fold compared to clone 438. With SPARC, expression levels were significantly increased for clone 439Late as opposed to clone 438 ($p < 0.01$), and clone 434 ($p < 0.01$), but this variation was also less than two-fold compared to clone 438. Although a two-fold change in BIRC5 expression was present for 439Late and 439Early relative to clone 438, these differences were not statistically significant ($p > 0.05$) due to the low expression levels in these clones. BIRC5 tended to amplify late in RT-qPCR with Utah-inoculated clones. Significant differential gene expression was also lacking for AXL, FN1, FSTL1, and SDC4 in all pairwise comparisons. No significant differential expression existed for clones 439Late versus 439Early in any of the examined genes.

As also described for the Mock-inoculated clones, significant correlations were not observed between mean normalized gene expression and prion permissibility ($p > 0.05$).

The data for the Mock and Utah-inoculated clones were combined to increase the sample sizes. A two-way ANOVA, *post hoc* Tukey-Kramer HSD for multiple pairwise comparison, and Pearson's correlation coefficient test were used for assessing gene-to-gene correlations, as well as correlations between gene expression levels and prion permissibility. Corrections to Pearson's test were performed using Benjamini-Hochburg procedure

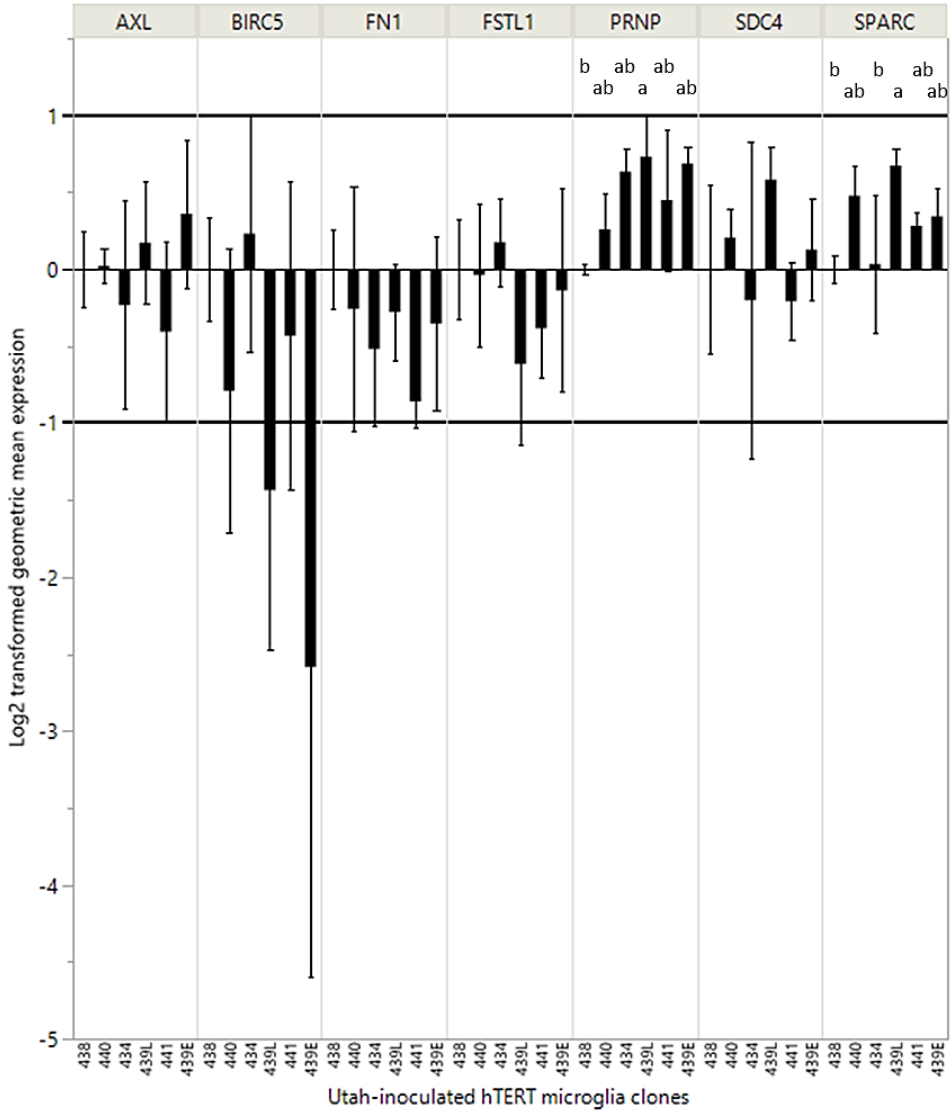

Figure 3.2. Fold change in gene expression for Utah-inoculated clones. Fold changes were assessed using normalized gene expression, relative to the least permissive clone (438) for Utah-inoculated clones. Expression data was normalized to 18s rRNA and hPRT1, scaled to 438, and then the geometric mean and geometric standard deviation factor were calculated for graphical representation. Solid, black, horizontal lines (i.e., 2^{1} or 2^{-1}) demarcate the two-fold change threshold. The x-axis is ordered by increasing prion permissibility phenotype (left to right). The horizontal axes are partitioned into panels by gene (AXL, BIRC5, FN1, FSTL1, PRNP, SDC4, SPARC). Error bars indicate 1 geometric standard deviation factor from the geometric mean. In differentially expressed genes, clones that do not share the same letter had significant differential mean expression ($p < 0.05$). E = Early Utah, L = Late Utah

(www.biostathandbook.com/multiplecomparisons.html). For FSTL1, SPARC, and SDC4, the effect of inoculation was significant ($p < 0.05$), and the interaction of inoculation status and clone were also significant for SDC4 and SPARC ($p < 0.05$), so these genes were not included in this aspect of the study. However, data could be combined for AXL, FN1, BIRC5, and PRNP. For BIRC5 ($p < 0.001$) and PRNP ($p < 0.01$), the effect of clone remained statistically significant with two-way ANOVA, frequently involving the same original clones as described in sections 3.2 and 3.3, but with some modifications to be addressed. When data was combined for BIRC5, the significant variation in gene expression of clones 439Early and 439Late, compared to clone 440 were no longer significant ($p > 0.05$). In PRNP, although clone 439Early lacked a two-fold change to other clones, collective data indicated that 439Early is weakly but significantly ($p < 0.05$) increased relative to 438. Pearson's correlation coefficient test, with Benjamini-Hochburg correction, was used to determine if the gene expression levels from the combined Mock and Utah-treated clones correlated with other expressed genes or with prion permissibility. No significant correlations were identified between genes ($p > 0.05$) or with prion permissibility ($p > 0.05$).

Since inoculation status was influential to gene expression for FSTL1, SPARC, and SDC4 with two-way ANOVA, the ratio of normalized mean expression derived from both treatment groups (i.e., Mock-inoculated/Utah-inoculated) was constructed to evaluate if inoculation with scrapie prions influenced transcript levels of these three genes (**Figure 3.3**). For SPARC, transcript levels were approximately three-fold higher for clones 438 and 434 ($p < 0.05$) as compared to clone 439Late subsequent to inoculation with scrapie prions.

Although normalized PRNP expression was determined to lack two-fold changes in expression and displayed absent to minimal, significant variation amongst the clones in this, as well as another study [60], the influence of target genes relative to PRNP expression of other genes were evaluated to determine if target gene/PRNP ratios were significant relative to prion permissibility. Raw target gene/PRNP ratios were calculated using the relative quantity of

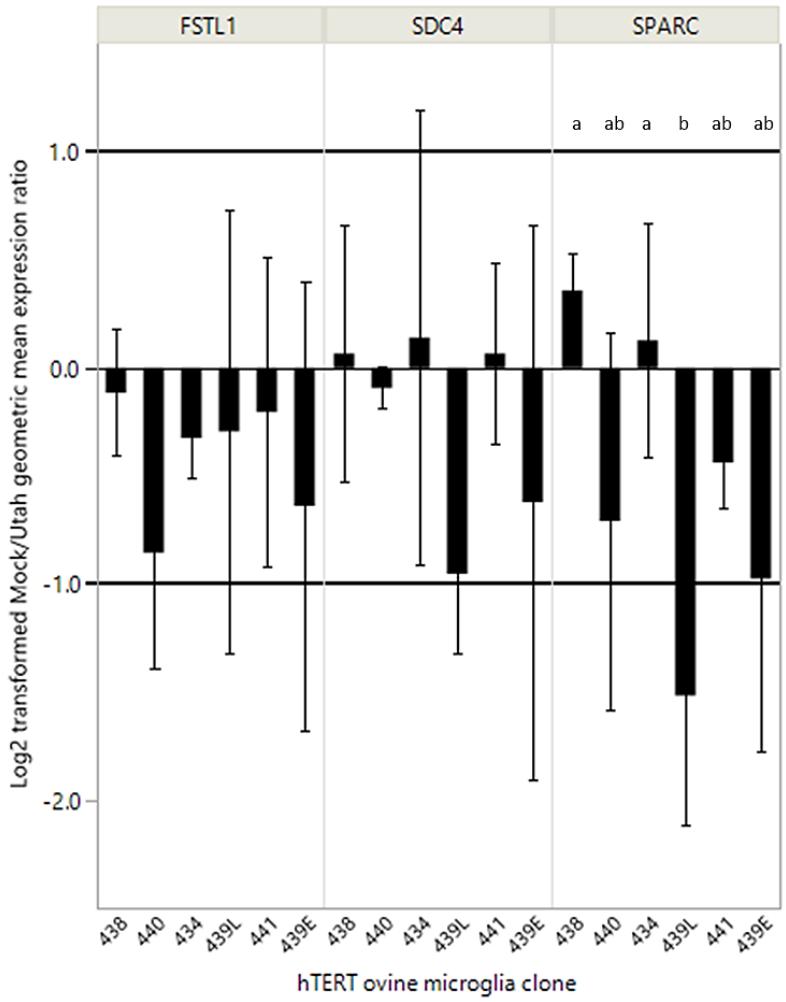

Figure 3.3. Effect of inoculation on transcript levels of FSTL1, SDC4, and SPARC. The effect of inoculation on transcript levels was calculated by dividing the Mock-inoculated value by the Utah-inoculated value. Geometric mean and geometric standard deviation were calculated for graphical representation. Solid, black horizontal lines (i.e., 2^{1} or 2^{-1}) demarcate the two-fold change threshold. The x-axis is ordered by increasing prion permissibility phenotype (left to right). The horizontal axis is partitioned into panels by gene (FSTL1, SDC4, SPARC). Error bars indicate 1 geometric standard deviation factor from the geometric mean. In differentially-expressed genes, clones that do not share the same letter had significant differential mean expression ($p < 0.05$). E = Early, L = Late

expression (i.e., non-normalized) for target genes and PRNP, per clone. Fold changes in expression and correlations with prion permissibility were statistically evaluated as previously described in section 3.2. Statistically significant differences in expression were observed for BIRC5/PRNP ($p < 0.001$), SPARC/PRNP ($p < 0.001$), FSTL1/PRNP ($p < 0.01$) and SDC4/PRNP ($p < 0.01$) (**Figure 3.4**). In BIRC5/PRNP, differential gene expression of 439Late and 439Early were significantly decreased compared to clones 438 ($p < 0.001$ and $p < 0.01$), and 441 ($p < 0.01$ and $p < 0.05$), and this decreased expression was a five-to-eight-fold change for 439Late and 439Early compared to clone 438. Earlier in the study, significant fold changes with BIRC5 in 439Early and 439Late were also described for both treatment groups, independent of PRNP expression. Moreover, for BIRC5/PRNP, clone 439Late had significantly diminished expression compared to clones 434 ($p < 0.01$) and 440 ($p < 0.05$). SPARC/PRNP had significant decreased expression for clones 439Late and 439Early compared to clones 438 ($p < 0.001$ and $p < 0.01$) and 434 ($p < 0.001$ and $p < 0.05$), and a two-to-three-fold change in expression existed in clones 439Late and 439Early compared to clone 438. Also, for SPARC/PRNP, clones 440 and 441 had significantly diminished expression compared to 438 ($p < 0.01$ and $p < 0.05$), and clone 440 was significantly decreased from 434 ($p < 0.05$), but these changes were slightly less than two-fold relative to clone 438. In FSTL1, clone 439Late had significantly diminished expression from clones 438 ($p < 0.05$) and 434 ($p < 0.05$), but these differences were less than two-fold. For SDC4/PRNP expression, 439Late was significantly decreased compared to clones 438 ($p < 0.01$), 440 ($p < 0.05$), and 434 ($p < 0.05$), but these differences were also less than two-fold relative to clone 438. Relative to PRNP expression, significant differential gene expression remained absent for AXL and FN1.

Although an approximately three-fold change in BIRC5/PRNP expression was present in clone 439Late compared to 439Early, this difference was not significant ($p > 0.05$). No significant differences in expression of clones 439Early versus 439Late were present for any of

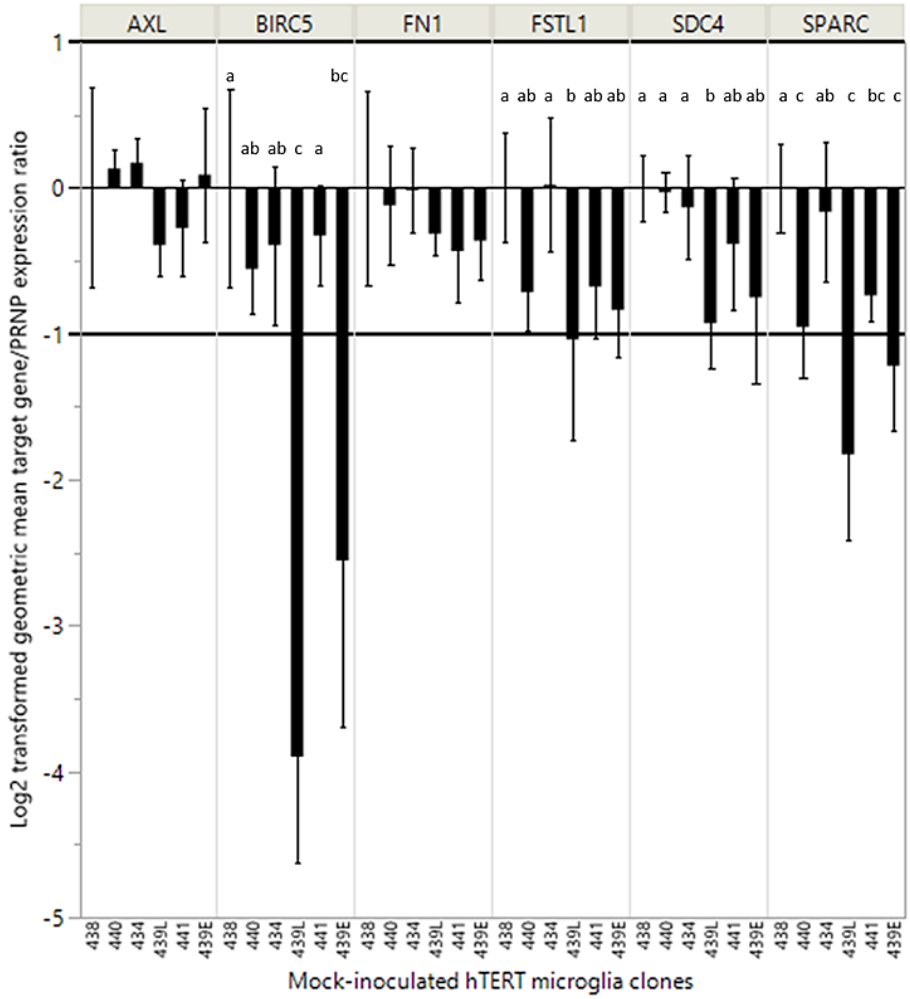

Figure 3.4. Fold change in target gene/PRNP expression in Mock-inoculated clones. Fold changes were assessed using relative expression data, scaled to the least permissive clone (438) for Mock-inoculated clones. Relative expression ratios were constructed (i.e., target gene/PRNP expression), and then the geometric mean and geometric standard deviation were calculated for graphical representation. Solid, black horizontal lines (i.e., 2^{1} or 2^{-1}) demarcate the two-fold change threshold. The x-axis is ordered by increasing prion permissibility phenotype (left to right). The horizontal axes are partitioned into panels by gene (AXL, BIRC5, FN1, FSTL1, SDC4, SPARC). Error bars indicate 1 geometric standard deviation factor from the geometric mean. In differentially-expressed genes, clones that do not share the same letter had significant differential mean expression ($p < 0.05$). E = Early Mock, L = Late Mock

the remaining gene ratios. No significant correlations to prion permissibility were identified amongst all gene ratios.

Fold change data and correlations to prion permissibility were constructed and statistically assessed as previously described in section 3.5. Statistically significant differences in expression were observed for AXL/PRNP ($p < 0.05$) (**Figure 3.5**). For AXL/PRNP, clone 441 had significantly diminished expression compared to clone 438 ($p < 0.05$), but this change was less than two-fold. Clones of BIRC5/PRNP lacked significant differential expression, but an approximately three-to-six-fold change in expression was noted in clones 439Late and 439Early relative to clone 438. In FN1/PRNP, there was also an absence of significant differential expression amongst the clones, but two-fold changes in expression were present in clones 439Late, 439Early, 434, and 441, relative to clone 438, and mean expression was highest in the least permissive clone (i.e., 438). In FSTL/PRNP, no significant differential expression was observed amongst the clones, but a two-fold change was present in clone 439Late relative to clone 438. Significant differential gene expression was lacking for SDC4/PRNP and SPARC/PRNP.

For BIRC5/PRNP, clone 439Late had a two-fold higher transcript level relative to 439Early, but this change lacked statistical significance. No additional significant differences in expression were present in clone 439Early versus 439Late for any of the remaining gene ratios.

No significant correlations with prion permissibility were detected amongst the gene ratios.

Target gene/PRNP expression ratios were pooled from Mock and Utah-inoculated clones for AXL/PRNP, BIRC5/PRNP and FN1/PRNP, and the impact of clone and inoculation status with expression, as well as correlations to prion permissibility were evaluated using similar procedures as described in section 3.4 (**Figure 3.6**). Neither inoculation status, nor the interaction of clone with inoculation status were influential to expression of genes selected for this portion of the study, so treatment groups were pooled to increase sample sizes. For

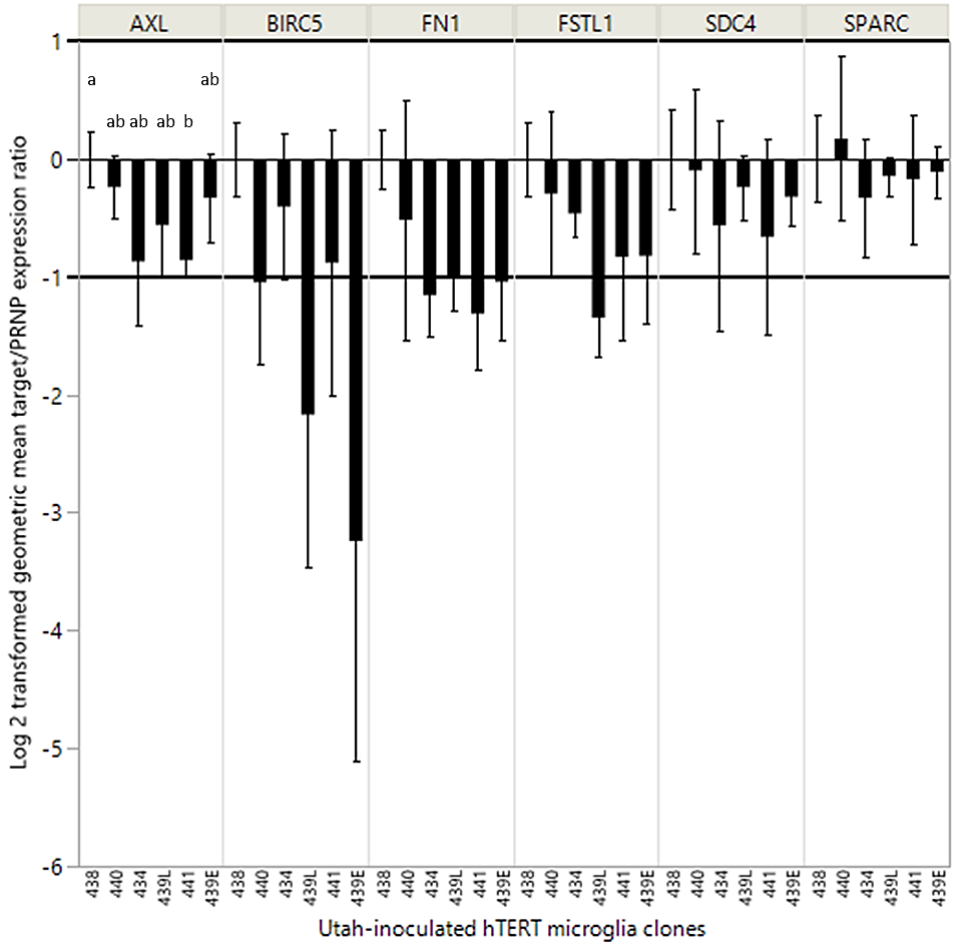

Figure 3.5. Fold change in target gene/PRNP expression in Utah-inoculated clones. Fold changes were assessed using relative expression data, scaled to the least permissive clone (438) for Utah-inoculated clones. Relative expression ratios were constructed (i.e., target gene/PRNP expression), and then the geometric mean and geometric standard deviation factor were calculated for graphical representation. Solid, black, horizontal lines (i.e., 2^{1} or 2^{-1}) demarcate the two-fold change threshold. The x-axis is ordered by increasing prion permissibility phenotype (left to right). The horizontal axes are partitioned into panels by gene (AXL, BIRC5, FN1, FSTL1, SDC4, SPARC). Error bars depict 1 geometric standard deviation factor from the geometric mean. In differentially-expressed genes, clones that do not share the same letter had significant differential mean expression ($p < 0.05$). E = Early Utah, L = Late Utah

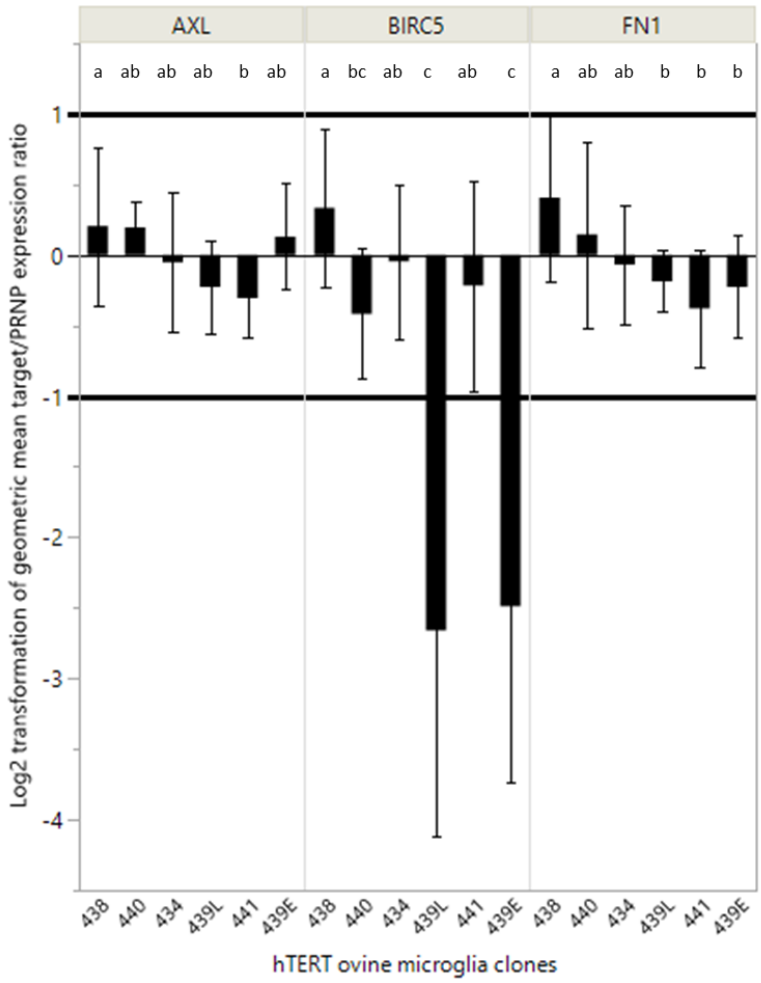

Figure 3.6. Comparison of target gene/PRNP expression for Mock and Utah-inoculated clones. Expression ratios were pooled from Mock and Utah-inoculated clones, relative to PRNP expression, for genes in which inoculation was insignificant. Geometric mean and geometric standard deviation factor were calculated per ratio for graphical representation. Solid, black, horizontal lines (i.e., 2^{1} or 2^{-1}) demarcate the two-fold change threshold. The x-axis is ordered by increasing prion permissibility phenotype (left to right). The horizontal axis is partitioned into panels by gene (AXL, BIRC5, FN1). Error bars depict 1 geometric standard deviation factor from the geometric mean. In differentially-expressed genes, clones that do not share the same letter had significant differential mean expression ($p < 0.05$). E = Early, L = Late

AXL/PRNP, the effect of clone was significant ($p < 0.01$) for clones 438 and 441. In BIRC5/PRNP, although the effect of clone remained significant to gene expression ($p < 0.001$) with many of the same clone comparisons depicted in section 3.5, further significant differential comparisons included clones 439Early and 434 ($p < 0.01$), clones 441 and 439Late ($p < 0.01$), and clones 440 and 438 ($p < 0.05$). Furthermore, BIRC5/PRNP differential expression became insignificant between clones 440 and 439Late ($p > 0.05$). Of interest, when FN1/PRNP was assessed jointly for both treatment groups, the effect of clone became significant ($p < 0.01$), and expression of clone 438 was significantly increased compared to 439Late ($p < 0.05$), 441 ($p < 0.01$) and 439Early ($p < 0.05$), with clones 441 and 439Early previously characterized as highly permissive to scrapie prion infection.

Additionally, BIRC5/PRNP (r = -0.7187, adjusted *p*-value < 0.05), and FN1/PRNP (r = -0.7841, adjusted *p*-value < 0.01) were strongly and negatively correlated with prion permissibility (**Table 3.2**).

Discussion and Conclusions

Identifying definitive determinants of prion permissibility is key in unraveling prion disease pathogenesis, and it also acts as a catalyst in the development of preventative measures and effective treatment protocols. Multiple studies of classical scrapie have implemented the use of cell culture models, and from these studies, potential determinants of prion permissibility have been identified [23, 24, 60]. In this study, 6 genes (AXL, BIRC5, FN1, FSTL1, SPARC, SDC4) that previously demonstrated either differential gene expression or the potential to affect prion permissibility between two clones (i.e., 438 and 439) of contrasting prion permissibility [24], were further characterized. The previous results were expanded into a set of six sheep microglia clones of varying prion permissibility. Raw gene expression levels were were evaluated, as were gene expression values relative to PRNP (i.e., target gene/PRNP).

Table 3.2. Significant correlations between target gene/PRNP and prion permissibility.

Gene-Gene interaction[a]	Pearson's Correlation	Adjusted p-value[b]
FN1/PRNP	-0.7841	0.0076
BIRC5/PRNP	-0.7187	0.0127

[a] Data was derived from at least 3 independent replicates. A *p*-value < 0.05 was considered significant. Ratio expression was scaled to 438.

[b] Adjusted *p*-value were derived from the formula (Pearson's *p*-value x (total number of *p*-values/*p*-value rank)). The value obtained from this calculation was compared to the previous adjusted *p*-value, and the smaller of the two was recorded. This value is also referred to as the Benjamini-Hochburg *p*-value (www.biostathandbook.com/multiplecomparisons.html).

Overall, there were no significant differences in gene expression observed between clones 439Late and 439Early. Significant correlations with prion permissibility were identified in expression ratios only (i.e., target gene/PRNP), and no significant correlations were detected between genes. Clone was the most common, influential factor to gene expression.

As previously stated, clone 439 was originally determined to have high permissibility to infection with naturally-derived classical scrapie isolates [56], but over time and subsequent subpassage, a shift to a more intermediate permissibility phenotype manifested [60]. Thus, this provided an opportunity to temporally compare a clone to itself. Clone 439Late was consistently decreased by a two-to-three-fold change from 439Early with BIRC5 raw expression and BIRC5/PRNP ratios, but these changes were not statistically significant. Unlike clone 439Early, clone 439Late was significantly decreased in FSTL1 raw expression, FSTL1/PRNP and SDC4/PRNP expression ratios, but these variations were also less than two-fold. Similar to a previous study including 439Late and 439 Early [60], these limited transcriptional analysis studies failed to find significant difference. A transcriptome-wide approach could be used in future studies to determine the differences between the 439Late and 439Early that result in the change of permissibility phenotype, as well as the rest of the clones, which have not been evaluated on a transcriptomic level (i.e., 434, 440, 441).

FN1/PRNP expression was strongly and negatively correlated with prion permissibility in ovine microglia. Furthermore, with pooled, Mock and Utah-inoculated FN1/PRNP expression, the effect of clone became significant with decreased expression in clones 439Late, 439Early, and 441 compared to clone 438. These findings suggest that the expression profile of FN1, relative to PRNP may contribute to prion permissibility. Marbiah *et al.* observed that FN1 silencing enhanced the levels of PrP^{D} accumulation in prion-susceptible murine neuroblastoma cells (i.e., R7 cells) [23]. The influence of clone parallels findings reported by Munoz-Gutierrez *et al.* in which FN1 expression was downregulated in highly-permissive clone 439 compared to poorly-permissive clone 438, both infected with scrapie prion [24]. Collectively, these findings

suggest that transcript levels of FN1 influence prion permissibility, and that this applies across different prion isolates and types of cell culture model systems. While the mechanism of fibronectin's influence on permissibility is unknown, possible causes include prion protein binding or extracellular matrix remodeling. Growth factors have been reported to bind to FN1, becoming concealed and able to evade proteolytic degradation, with subsequent accumulation in the FN1 fibrillar matrix [69]. Potentially, prion protein could have a similar interaction with FN1. Additional studies of FN1 are warranted to determine if similar correlations with prion permissibility exist in other cell culture systems (i.e., Rov or 1D4 cells) and prion strains (i.e., natural scrapie isolates X124 or SSBP-1, Nor98, human prion isolates). Furthermore, future studies to silence FN1 or deletion of FN1 from culture media in order to create cell culture models for human prions may be warranted. With these subsequent studies, further knowledge may be provided to strengthen the classification of FN1 as a biomarker of prion permissibility.

BIRC5 had consistently low expression in clones 439Late and 439Early. This is consistent with previous results [24]. However, BIRC5 expression was very low (nearly undetectable). While BIRC5/PRNP expression was strongly and negatively correlated with prion permissibility, this correlation was likely skewed by the results of the related 439Early and 439Late clones. Thus, the significance of these comparisons, involving such a poorly expressed gene is questionable. Since BIRC5 has a role in apoptosis (i.e., it directly inhibits activation of caspase-9, and formation of the apoptosome, suppressing the intrinsic signaling pathway of apoptosis) [70], future studies may be best targeted toward apoptosis, rather than BIRC5 specifically.

SPARC and SPARC/PRNP expression were significantly different in multiple pairwise comparisons, but lacked a correlation with prion permissibility. While likely not important to prion permissibility amongst the clones, it is possible that the permissibility of different clones have different genetic determinants. With specialized functions in cellular adhesion, proliferation, migration [71, 72], and matrix metalloproteinase activity [72], it is possible that decreased

expression of SPARC may result in pathological abnormalities in these functions that enhance prion infectivity. Booth *et al.* identified differential expression of SPARC between non-infected and scrapie-infected brain tissue from C57BL/6 mice experimentally inoculated (i.e., intracerebral) with one of two mouse-adapted prion strains (i.e., ME7, 79a) [73]. Interestingly, SPARC was also significantly affected by the inoculation status of the microglia clones. These findings indicate that for some genes, inoculation influences transcript levels, which may potentially contribute to prion permissibility, in contrast to other genes studied in ovine microglia [24, 60]. It is also possible that the pre-inoculation state of the cell is critical for initial prion replication. To the authors' knowledge, this report depicts the first characterization of SPARC in prion permissive ovine microglia clones.

PRNP expression was significantly increased in inoculated clone 439Late compared to 438, and collectively in Mock and Utah-inoculated clones 439Late and 439Early compared to clone 438, but these variations in expression were less than two-fold. Previous studies using these clones also identified some variation in expression that was of a similar magnitude in one study [60], but in the remaining study, the results were not statistically significant [24]. Additionally, in this study, many significant differential comparisons were present in target gene/PRNP expression ratios (i.e., FN1/PRNP, BIRC5/PRNP, FSTL1/PRNP). These findings suggest that transcript level ratios of certain target genes and PRNP may also influence prion permissibility. Future gene expression studies of prion diseases are suggested to evaluate gene transcript levels relative to PRNP, to account for the potential of PRNP levels interacting with the target gene levels.

FSTL1, AXL and SDC4 results demonstrated sporadic pairwise comparisons that were significant, but these genes lacked patterns or correlations. Based on these results, it is unlikely that FSTL1, AXL, or SDC4 affect prion permissibility.

Some limitations were present in this study. First, only 2 out of 3 replicates of Utah-inoculated 439Early could be assessed for BIRC5, which hindered full assessment of BIRC5 for

this clone; however, this could also be due primarily to low transcript levels. Second, only a single scrapie isolate was used (i.e., Utah), and assessed for differential gene expression amongst the clones. Currently, only clone 439Early from the subline has been assessed for permissiveness to other natural scrapie isolates (i.e., Pullman 1, Pullman 3, X124, 13-7) [61]. If the remaining clones are also discovered to be permissive to these isolates, evaluation and comparison of the transcriptomic profiles between clones and scrapie isolates would be beneficial. This would allow the identification of similar or disparate genes that could be differentially expressed, providing more insight on prion disease pathogenesis in ovine microglia. Thirdly, assessment of gene expression and correlations with prion permissibility were only performed for ovine microglia of VRQ/VRQ genotype, which is characterized by a rapid incubation period and fast accumulation of PrP^{Sc}. Extrapolation of the results from this study towards the development of an ARQ/ARQ sheep prion culture system could aid in the development of the first cell culture system for slowly accumulating PrP^{Sc}, which is more characteristic of most human prion diseases.

In conclusion, definitive determinants of prion permissibility are currently limited, but one extracellular matrix gene identified in this study (FN1), shows considerable promise in becoming an acknowledged determinant of prion permissibility. The studies previously performed by Marbiah *et al.*, Munoz-Gutierrez *et al.*, and this current study suggest that alterations in FN1 expression levels consistently correlate with prion permissibility across two distinct cell culture model systems. For this study, FN1/PRNP expression was strongly and negatively correlated with prion permissibility. These findings suggest prion permissibility is not dependent on individualized gene expression in ovine microglia cells, but other factors may be involved to include cell of origin, type of scrapie isolate or strain, post-transcriptional or post-translational factors, and possibly additive effects of gene expression (e.g., target gene levels relative to PRNP levels).

Future studies are needed to fully characterize the functionality of these genes and their role in prion permissibility in different cell culture model systems, with various prion isolates or strains, and transcriptomic analysis.

CHAPTER 4 MATRIX METALLOPROTEINASE 2 IN DEFINED PRION-PERMISSIVE AND PRION-ACCUMULATING CULTURED NAÏVE OVINE MICROGLIA

Matrix metalloproteinases (MMPs) are a group of zinc-dependent, proteolytic enzymes that are known for degrading various substrates in the extracellular matrix (ECM) during remodeling and repair [74], and embryonic development and reproduction [75], but additional functions include angiogenesis, cell survival, signaling, and inflammation [74]. These proteins are secreted as zymogens or inactive proenzymes, and become activated when the pro-domain undergoes a conformational change, which disrupts binding to the catalytic domain [76], and exposes the active site cleft.

MMPs are ubiquitous in the central nervous system, and in humans, they are reported to be secreted by neurons, oligodendrocytes, microglia, reactive astrocytes, and endothelial cells [77, 78].

Inducers of MMPs include: growth factors, cytokines, chemical agents, physical stress, and cancer [75]. MMPs can also promote the release of substances like cytokines and growth factors by cleaving soluble binding proteins [79]. Tissue inhibitors of metalloproteinases (TIMPs) also regulate the activities of MMPs through inactivation by binding to the catalytic site. A single TIMP can also inhibit multiple MMPs, and in some cases, can activate other pro-MMPs [74].

Matrix metalloproteinase 2 (MMP2) is classified with MMP9 as gelatinases, which are soluble matrix metalloproteinases. This enzyme has three fibronectin type II modules in the gelatin-binding domain of the catalytic site, that can bind to the alpha-1 chain of collagen 1 with a high affinity, and cause subsequent cleavage [76, 79]. Multiple known substrates can activate MMP2, which include the complex interaction of TIMP-2 and MMP-14 (membrane bound membrane type-1 MMP) coupled with other active MMP2 molecules [80], thrombin and

activated Protein C [81], and some studies have identified other potential substrates, such as osteopontin, galectin-1, and heat shock protein 90α (HSP90α) [82]. However, if TIMP2 levels are higher than MMP-14 and active MMP2, activation of additional MMP2 will not occur [83]. MMP2 cleaves various substances such as gelatin (denatured collagen), collagens I, IV, and V, fibronectin, elastin, and vitronectin [84]. MMP2 has a plethora of functions that include extracellular matrix remodeling, but also advancement of inflammatory cell migration through disrupted basement membranes, lysis of chemoattractants, and promotion as well as inhibition of inflammation [83]. TIMP-2 and TIMP-3 are effective at inhibiting the action of MMP2 [79].

The role of MMP2 expression and activity in neurodegenerative diseases has been studied extensively. Overexpression of MMP2 has been reported early in Alzheimer's disease, and MMP2 is capable of degrading soluble amyloid A plaques and physiologically normal tau, but cannot digest hyperphosphorylated or dephosphorylated tau, which are pathological variants [85]. MMP2 has also been shown through confocal microscopy to be localized to the same areas as neurofibrillary tangles and dystrophic neurites in the entorhinal and transentorhinal cortex [85]. These findings suggest that secreted MMP2 is a protective response to the presence of amyloid and tau, but the inability to clear neurofibrillary tangles leads to their accumulation and the onset of a positive, repetitive, feedback cycle recruiting more MMP2. Both of these events likely contribute to progressive neural damage and neurodegeneration. Lorenzl *et al.* discovered decreased MMP2 levels in the substantia nigra, largely within microglia and astrocytes in brain tissue from patients with Parkinson's disease, and hypothesize that these modifications may contribute to disease progression [86]. In Amyotrophic Lateral Sclerosis (ALS) patients, increased MMP2 levels have been shown in astrocytes in the neocortex and spinal cord, but are decreased in the motor cortex; however, MMP9 expression was significantly increased in the motor cortex and segments of the spinal cord (thoracic and lumbar), and the latter may contribute more extensively to the pathogenesis of ALS.

Aberrant protein misfolding and accumulation is a feature not only present in Alzheimer's disease and Parkinson's disease, but also in other neurodegenerative disorders such as prion disease, suggesting some similarities in disease pathogenesis. It is plausible then that these disorders may share certain molecular and mechanistic pathophysiology. MMP2 could be one of these elements, as it has also been recently implicated as a contributing factor to prion susceptibility and permissibility in cell culture models. Marbiah *et al.* determined that when prion-resistant murine neuroblastoma cells previously susceptible to infection with RML, a mouse adapted prion scrapie strain (i.e. revertants), were exposed to an agent (i.e., RGD) that interfered with signal transmission between fibronectin 1 (FN1) and integrins, secretion of MMP2 was arrested [23]. Additionally, these revertants became more susceptible to infection with RML prions [23]. Munoz *et al.* discovered significantly higher levels of MMP2 transcripts by RNAseq in poorly-permissive immortalized ovine microglia (i.e., 438 clone), when inoculated with scrapie prions, compared to highly-permissive microglia (i.e., 439 clone) in RNAseq [24]. Moreover, Munoz *et al.* revealed sublines of ovine microglia that phenotypically accumulate prions rapidly (i.e., subline A/286 cells), or through a slower, prolonged process (i.e., subline H/308 cells) [56]. In the current study, we expanded upon this premise by evaluating if MMP2 levels are differentially expressed in clones that are highly, intermediately, or poorly permissive to scrapie prion infection (clones 441 and 439Early – **high**; clones 440, 439Late and 434 – **intermediate**; clone 438 – **poor**), or in ovine microglia sublines with a defined prion accumulating phenotype (i.e., slow versus fast accumulation). We also evaluated if switching of supernatant between the sublines influenced expression of MMP2.

Ovine microglia were previously extracted from the brain of a VRQ/VRQ fetus, acquired from a near-term Suffolk-cross sheep [64]. These microglia were immortalized (hTERT) and several sublines created, with the subsequent origination of 5 clones from one scrapie prion permissive subline (i.e., subline H) through cloning by limiting dilution [56]. Over time and subsequent passages, one clone became less permissive to prion infection; however this clone

was also included in the study (i.e., 439Late) [60]. Two sublines (subline *H*/308 cells and subline *A*/286 cells) [56], arranged from slow-to-fast accumulation rate, and six clones (438, 440, 434, 439Late, 441, 439Early) [60], ordered by increasing prion permissibility phenotype, were used. Naïve, subline cells and clones were rapidly thawed from cryogenic stasis, and cultured under standard conditions of Opti-MEM media (Gibco), supplemented with 10% complement-inactivated fetal bovine serum (Atlanta Biologicals), 10,000 units/mL penicillin (Hyclone), 10,000 µg/mL streptomycin (Hyclone), and 200 mM L-Glutamine (Hyclone). Cells and clones were passaged every 3 to 4 days at a 1/5 dilution, and maintained in T-25 culture flasks at 37 °C.

After growth of clones to at least 90% confluency, approximately 150 µLs of supernatant was collected for 3 independent replicate assays. In one independent assay at 90% confluency, approximately 150 µLs of supernatant was collected from the sublines at four consecutive time points (i.e., 1 – 4 days post supernatant switch (dps)), which also included supernatant from control samples. After collection, supernatant was centrifuged at 500 x g (JA50.5 rotor) for 10 minutes at 4 °C, and then transferred to 2 mL microcentrifuge tubes and stored at -20 °C until used. Supernatant was standardized using Pierce BCA Protein Assay Standardization kit (ThermoFisher Scientific) according to manufacturer's instructions, and protein concentration was measured using Epoch Microplate Spectrophotometer (Biotek) by manufacturer's instructions. Samples were standardized to 3000 µg/mL in a total volume of 100 µL. MMP2 was denatured using Novex Zymogram Gels (ThermoFisher Scientific, Invitrogen) according to manufacturer's directions with few modifications. 12.5 µL of each diluted standardized sample was added to 12.5 µL of 2X Tris-Glycine SDS Sample Loading buffer, and a total of 20 µL of this mixture was added to a well and run at 125 volts for 1.5 hours. Ten microliters of Precision Plus Protein Dual Color Standards ladder (BIORAD) was also run for size reference. Next, gels were renatured, developed, and incubated overnight at 37°C before staining with SimplyBlue Safestain (ThermoFisher Scientific, Invitrogen) by manufacturer's instructions with few modifications. Twenty-five milliliters of ultrapure water were added first for rinsing the gel, and

30 to 50 mL of ultrapure water was added twice after staining. Protein bands on zymogram gels were visualized using VersaDoc 4000 Imaging Systems (BIORAD), and the density of the bands were quantified with Fiji-Image J software program [87, 88]. Each clone was assessed from at least 3 independent replicate assays, and each subline from 1 independent assay. Fold changes in MMP2 expression, when used, were scaled to the slow, prion-accumulating subline (308), or least permissive clone (438). MMP2 data for clones was $\log_{10}$ transformed, averaged, and statistically compared with One-way ANOVA, *post-hoc* Tukey-Kramer for multiple comparisons, and nonparametric parameters (Wilcoxon test) using JMP version 14 (www.jmp.com; SAS Institute, Cary, NC). MMP2 levels for sublines were assessed at 1 day-post-supernatant switch [dps] and at 4 dps, then combined, and statistically evaluated with One-way ANOVA, and Pooled T test. For supernatant switching, raw MMP2 levels remained separate, and were compared to control supernatant MMP2 values at 1 and 4 dps.

MMP2 densities of the clones were determined to be normally distributed with histograms and Goodness of fit test, for all except clone 434 ($p > 0.05$). MMP2 levels were notably different between naïve ovine microglia ($F = 10.2239$, $p < 0.001$). Compared to clone 438, MMP2 expression was significantly decreased in intermediately permissive clones 434 (ChiSquare = 13.1871, ChiSquare *p*-value < 0.05) and 439Late ($p < 0.001$) (**Figure 4.1.**). Additionally, MMP2 levels were significantly increased in clones 440 ($p < 0.01$) and 441 ($p < 0.01$) compared to clone 439Late. Furthermore, MMP2 expression was significantly different between 439 clones ($p < 0.01$) with increased expression in clone 439Early. Data was pooled from 1 and 4 dps for the control and experimental subline groups (i.e., supernatant switching samples) in assessment of MMP2 levels. When evaluated relative to the slow prion-accumulating subline (308), subline 286 had significantly downregulated MMP2 expression, however, only one independent assay was assessed ($p < 0.05$) (**Figure 4.2.**). Additionally, when data was not pooled, MMP2 levels in samples 308cells/286supernatant and

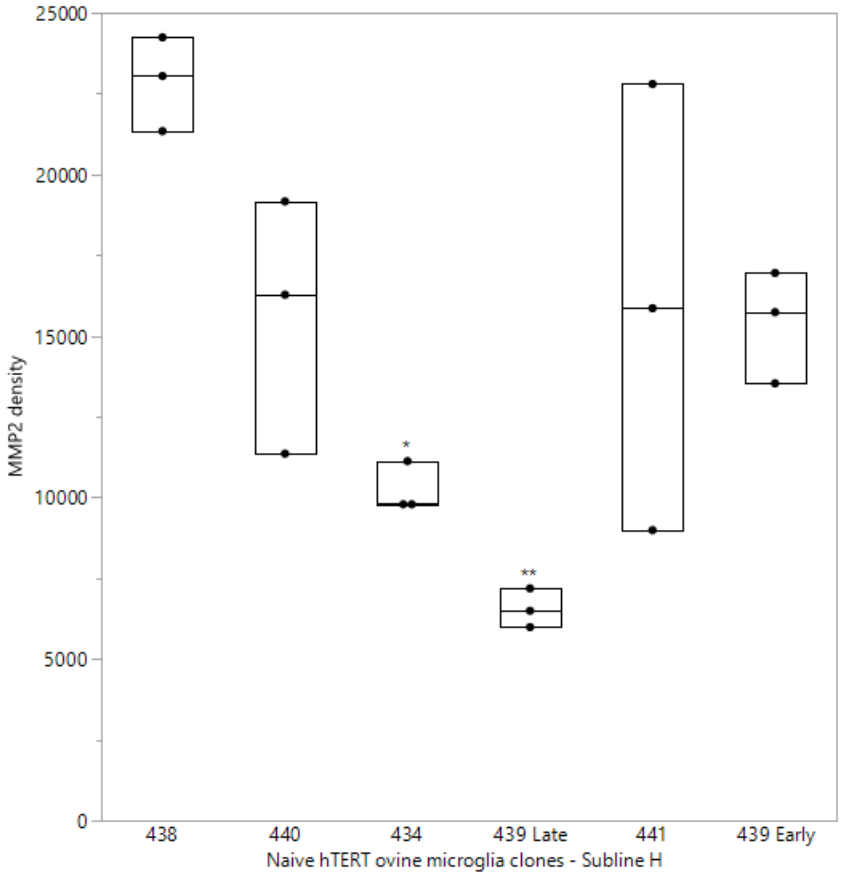

Figure 4.1. Density of MMP2 in naïve ovine microglia clones. MMP2 transcript levels were compared between naïve immortalized ovine microglia clones from at least 3 independent replicate assays. Along the y-axis is the raw MMP2 density plotted as points for each replicate, superimposed on a box plot configuration that includes horizontal lines to indicate upper, middle or median, and lower quartiles (top to bottom). The x-axis lists the microglia clones arranged in order of least to most permissive to scrapie prions (left to right). * - $p < 0.05$; ** - $p < 0.01$

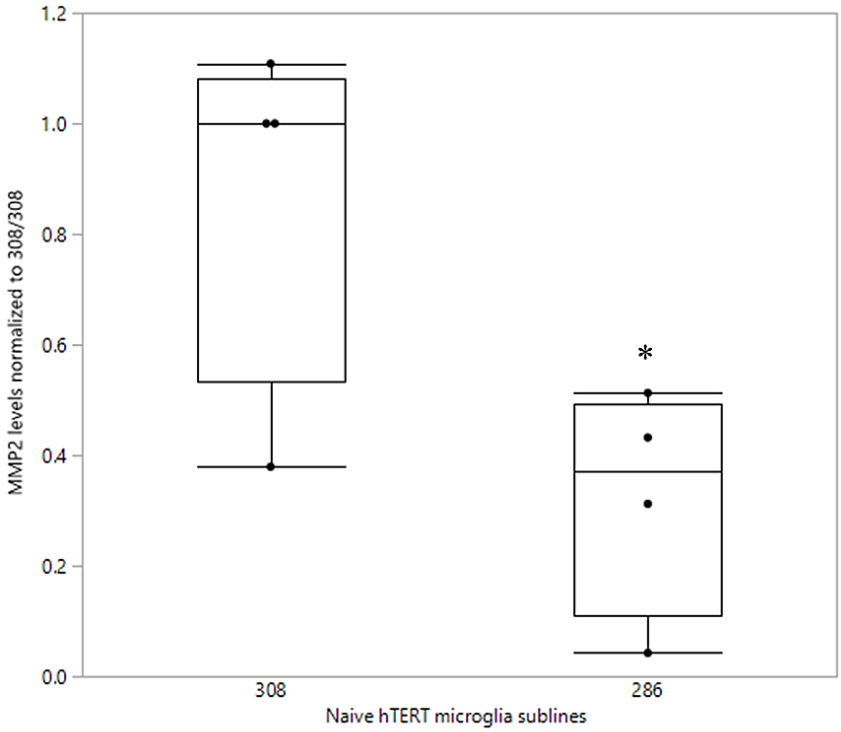

Figure 4.2. Density of MMP2 in naïve ovine microglia sublines. MMP2 transcript levels were pooled from control and experimental groups of naïve, immortalized, ovine microglia sublines, then scaled to 308cells/308supernatant from one independent assay. Along the y-axis is the MMP2 density normalized to 308/308 (slow prion accumulating subline) plotted as individual data points, and superimposed on a box plot configuration that includes horizontal lines to indicate upper, middle or median, and lower quartiles (top to bottom). The x-axis lists the microglia sublines arranged in order of slow to fast scrapie prion accumulation (left to right). * - $p < 0.05$

286cells/308 supernatant tended to resemble levels depicted in the control samples at 4 dps, respectively (i.e., 308cells/308supernatant and 286cells/286supernatant) (**Figure 4.3**). Although only one independent assay was performed, preliminary results of supernatant switching suggest switching is non-influential to expression of MMP2 transcript levels between the sublines.

These results indicate that MMP2 expression in clone 438 is significantly increased compared to intermediately-permissive clones (434 and 439Late), and MMP2 expression is not significantly different between highly-permissive (439Early) and poorly- permissive (438) ovine microglia clones. These results are in contrast to those depicted by Munoz *et al.* in which naïve and scrapie-inoculated poorly-permissive ovine microglia (438) had significantly increased MMP2 levels, compared to the highly-permissive clone, 439Early. These findings also suggest expression and transcription of MMP2 are not solely responsible for prion permissibility phenotype in ovine microglia. With subsequent passaging of clone 439, this clone adopted an intermediately-permissive phenotype (439Late), and with that, MMP2 expression levels significantly decreased. In the naïve microglia sublines, results suggest that MMP2 levels are significantly decreased in the fast prion-accumulating subline (i.e., 286), compared to a slower rate of accumulation in the other subline (i.e., 308). Preliminary results of the sublines also suggest that supernatant switching is not influential to MMP2 transcript levels. In conclusion, MMP2 is not directly related to prion permissibility in naïve ovine microglia clones, and any effect of MMP2 activity on prion permissibility would be multifactorial. MMP2 transcript levels were differentially expressed between the fast and slow, prion-accumulating sublines, and supernatant switching did not appear to effect levels of MMP2, but these results are from only one independent assay, so additional replicates are needed for validation of these findings.

In a couple of follow-up experiments, Dinkel *et al.* observed that MMP2 expression amongst microglia clones was not significantly different based on inoculation status (i.e., Mock versus Scrapie), and Munoz-Gutierrez *et al*., discovered a similar trend of MMP2 transcript

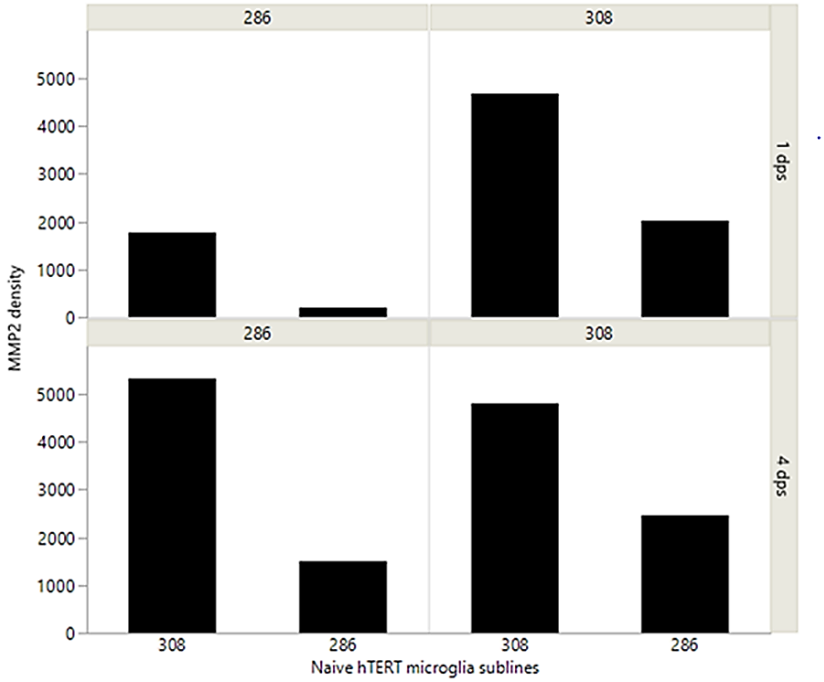

Figure 4.3. Density of MMP2 in supernatant switched samples. MMP2 levels were compared between controls (i.e., 308cells/308supernatant and 286cells/286supernatant) and experimental samples (i.e., 308cells/286supernatant and 286cells/308supernatant) at 1 and 4 dps, for one independent assay. Along the y-axis are microglia sublines arranged from slow to fast rate of prion accumulation (left to right). Raw MMP2 density is plotted on the x-axis. The two horizontal axes in the graph depict the origin of supernatant present for the sublines, and the right, opposing y-axis indicates the day supernatant was collected (i.e., 1 versus 4).

levels between the sublines in the presence of scrapie prions (data not shown). Both of these studies suggest inoculation status does not impact MMP2 expression in permissive clones, or in slow and fast prion-accumulating sublines. Future studies geared towards evaluating MMP2 expression, relative to the expression of other genes (i.e., prion protein [PRNP], fibronectin 1 [FN1], survivin [BIRC5]) could be beneficial in deciphering other factors that may contribute to prion permissibility and accumulation. Assessment of MMP2 in other cell culture lines permissive to scrapie prions (i.e., ID4, Rov) would also be advantageous, to determine if similar trends exists as observed in murine neuroblastoma cells and ovine microglia

CHAPTER 5 HISTOLOGIC AND IMMUNOHISTOCHEMICAL NEUROPATHOLOGICAL CHARACTERIZATION OF ATYPICAL SCRAPIE IN EXPERIMENTALLY-INFECTED SHEEP

Atypical scrapie is a progressive, fatal, neurodegenerative disease that affects sheep and goats, and is classified as a transmissible spongiform encephalopathy (TSE). This scrapie variant was originally identified in 1998, from 5 field cases in 5 different flocks localized to Norway [8, 9], and has striking dissimilarities to classical scrapie in signalment, clinical signs, biochemical profile, and pathophysiological mechanism. Compared to classical scrapie, atypical scrapie tends to occur in older animals [8] with a presenting complaint of ataxia, and although infectious experimentally, natural cases are typically spontaneous, or with a low rate of infectivity [89]. Additionally, susceptibility to atypical scrapie is influenced by a genotype that confers resistance to classical scrapie (e.g., $A_{136}R_{154}R_{171}$) [90]. On Western blot after proteinase K (PK) treatment, atypical scrapie produces a multiband pattern, whereas with classical scrapie, 3 distinct bands are visible [9]. Neuroanatomical deposition and accumulation of PrP^{Sc} (Sc for scrapie) in atypical scrapie is highest at the level of the cerebellar and cerebral cortices [91], whereas in classical scrapie, brainstem nuclei in the obex are preferentially affected. Since the initial discovery of atypical scrapie in Norway [9], eradication programs have detected occasional cases through either passive surveillance of clinical suspects, or active surveillance at slaughter and in fallen stock, within various countries throughout Europe, Australia, Canada, Japan, New Zealand, and the United States [12, 13, 15, 28, 29, 91-95]. In these reported cases, the timeline of discovery through ancillary testing varied from 1999 – 2016. The majority of atypical scrapie cases in Great Britain, Belgium, Portugal, Germany, and France were reported in the early 2000s, including one case in Great Britain from 1989 that was retrospectively

identified, but cases in the United States, Canada, New Zealand, and some in Australia were reported later in time (i.e., 2008 - 2016). This evidence indicates that although several of the initial cases were detected in Europe, since that time, the prevalence of atypical scrapie has become more widespread.

While European atypical scrapie has been widely and extensively studied, the discovery of atypical scrapie in the United States is relatively new. When known, European atypical scrapie has been reported to affect various breeds (i.e., Merino, Rambouillet), but in the US, the majority of initial cases have been in “black-faced sheep” such as Suffolk [12], and the reason for this is unknown. Additionally, homozygous and heterozygous genotypes $A_{136}R_{154}Q_{171}$ and $A_{136}H_{154}Q_{171}$ were reported in Europe, but in the US and Canada, a genotypic polymorphism homozygous for either leucine (L) or heterozygous for phenylamine (F) at codon 141 was initially reported (i.e. $A_{136}L_{141}R_{154}\,Q_{171}$; $A_{136}F_{141}R_{154}\,Q_{171}$). This evidence suggests that in US atypical scrapie cases, different breeds of sheep are more susceptible to disease, and the genetic profile is also variable, compared to cases in Europe. Currently, it is unknown if the European variant of atypical scrapie is analogous to the United States variant.

The aim of this project was to characterize the pathology and pattern of PrP^{Sc} deposition and accumulation in four, ARR/ARR sheep intracranially (i.e., intracerebrally) inoculated with brain homogenate from a natural, North American, atypical scrapie isolate, depicted in the study from Loiacono *et al*. [12]. These findings were then compared to other reported pathotypes, particularly from Europe but also from Canada, Australia, New Zealand, and Japan, to determine if this isolate was similar or disparate, suggesting the introduction of a novel isolate. Also, of interest, was comparing the pathologic lesions observed, to those described in classical scrapie.

Multiple sections of brain were assessed for PrP^{Sc} localization and accumulation using previously established protocols [96, 97], with minor modifications. Nine areas of gray matter and two areas of white matter were evaluated: G1 (caudal medulla at the obex), G2 (cerebellar

cortex), G3 (superior colliculus), G4/5 (hypothalamus and medial thalamus), G6 (hippocampus), G7 (septum), G8 (cerebral cortex at level of G4/5), G9 (forebrain cortex at level of G7), W1 (cerebellar white matter), and W2 (mesencephalic tegmentum). An additional section of more caudal medulla at the level of the central canal was also evaluated. Approximately 4-µm sections were routinely cut and used for routine histopathology (hematoxylin and eosin stained) and immunohistochemistry. Brains from two sheep with classical scrapie were used for comparison of histopathologic lesions and immunohistochemical staining patterns.

All hematoxylin and eosin (H&E) prepared slides of the various brain sections were evaluated independently by two board-certified veterinary pathologists, as a single blind trial. Defined lesions previously diagnosed in atypical scrapie disease [8, 9] (i.e., plaque-like aggregates, gliosis, neuronal necrosis, and neuronal vacuolation) were evaluated, and if present, severity (i.e., mild, moderate, severe) was recorded subjectively. A consensus was derived for any interpretations in which there was an initial discrepancy. The presence of frequent neuropil vacuolation was noted (data not shown); however, the lack of age-matched controls precluded the ability to definitively score or interpret the validity of this particular change.

A dual combination of primary, anti-prion protein antibodies was used in this study (i.e., 89/160 at a concentration of 10 µg/mL, and 99/97 at a concentration of 10 µg/mL). PrP^{Sc} immunolabeling was evaluated in all brain sections, and the character of the immunolabeling was recorded utilizing the nomenclature previously implemented [91]. PrP^{Sc} accumulation was graded on a subjective scale of 0–3 (0 = absence of immunolabeling; 1 = mild immunolabeling; 2 = moderate immunolabeling; 3 = intense immunolabeling) based on the localization and severity for each brain section. For any given level of sectioning, IHC was performed on all experimental animals in the same run.

The four experimental sheep are hereafter referred to as: “3913, 3914, 3916, and 3917” when not described as a single unit of four. Additionally, brain sections from two sheep (4124 and 4130) infected with classical scrapie were used for comparison.

Results

In addition to **G1**, caudal sections of medulla were also evaluated in all four animals, and these results were pooled together. In all four animals, there was minimal to moderate, globular and punctate immunolabeling of the dorsal, lateral, and ventral nerve tracts (cuneate fasciculus, spinocerebellar tract, spinal trigeminal tract, pyramids), as well as the medial lemniscus and medial longitudinal fasciculus **(Figure 5.1a)**. In three animals (3914, 3916, 3917), the neuropil of several nuclei and the reticular formation were similarly stained, but with decreased frequency and a more limited distribution than the nerve fiber tracts. In the classical scrapie cases, the neuropil of the nuclei had extraneuronal, punctate to globular immunolabeling. Nerve fiber tracts had rare punctate to absent immunolabeling **(Figure 5.1b)**. Affected nuclei in the atypical scrapie animals include external cuneate, spinal trigeminal, spinal vestibular, lateral reticular, hypoglossal, raphe, and rarely, dorsal motor nucleus of the vagus nerve, cuneate, gracilis and inferior olive (dorsal and medial). Intraneuronal immunolabeling was notably absent **(Figure 5.2a)**. Overall, 3913 had the least amount of PrP^{Sc} immunolabeling, as compared to the other animals. In the classical scrapie animals, the dorsal motor nucleus of the vagus nerve had abundant, frequent, intraneuronal, finely granular to punctate immunolabeling **(Figure 5.2b)**. All other nuclei were similarly, but less severely affected. Less commonly, finely granular to punctate immunolabeling was in or adjacent to glial cells. In all four atypical scrapie animals, there was a mild to moderate increase in microglia and astrocytes (gliosis), particularly of the dorsal motor nucleus of the vagus nerve, with less involvement of the nucleus of the solitary tract. Rare, shrunken, hypereosinophilic neurons and/or rounded, hypereosinophilic spheroids

a) b)

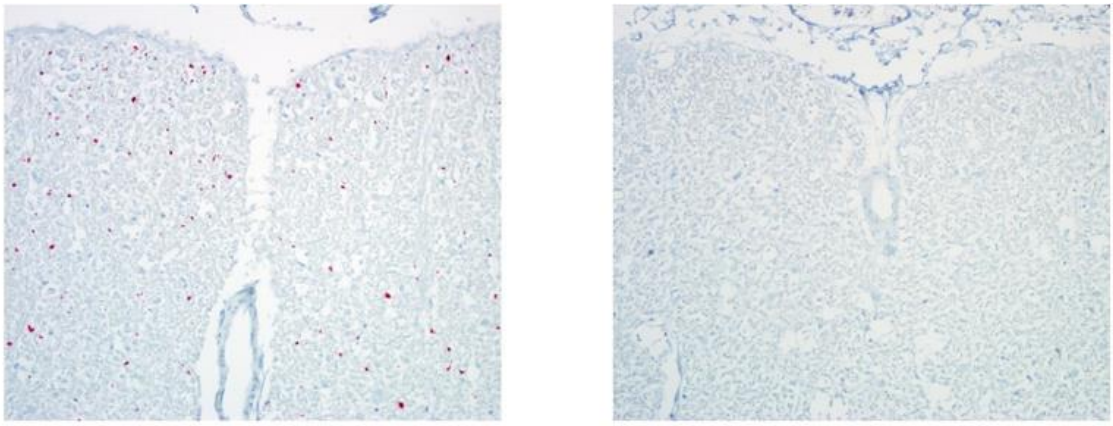

Figure 5.1. Immunolabeling of the spinocerebellar tract in atypical and classical scrapie. (a) Punctate to globular extracellular PrP^{Sc} immunolabeling in spinocerebellar nerve fiber tract. Animal 3917, caudal medulla, 20X, IHC. (b) Absence of PrP^{Sc} immunolabeling in spinocerebellar nerve fiber tract. Animal 4130, caudal medulla, 20X, IHC.

a) b)

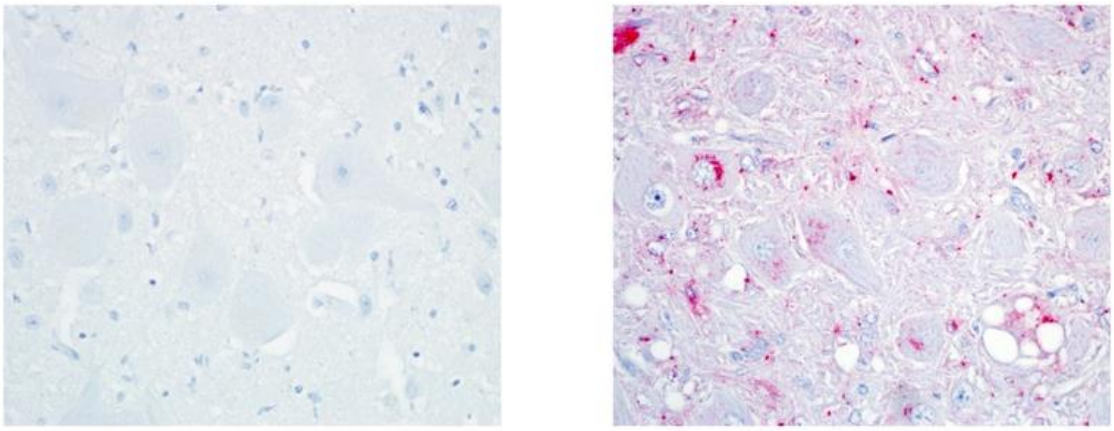

Figure 5.2. Immunolabeling of the dorsal motor nucleus of the vagus nerve in atypical and classical scrapie. (a) Absent PrP^{Sc} immunolabeling in the dorsal motor nucleus of the vagus nerve. Animal 3917, caudal medulla, 40X, IHC. (b) Diffuse finely granular to aggregated intraneuronal, intraglial, and neuropil immunolabeling. Note there is vacuolation of the neuropil and occasional neurons are expanded by well-circumscribed, discrete vacuoles. Animal 4124, caudal medulla, 40X, IHC.

were also in a few of the nuclei (i.e., external cuneate, spinal vestibular, spinal trigeminal, lateral reticular nucleus).

Sections of cerebellar cortex (**G2**) were evaluated in all four animals. The cerebellar folia were nearly diffusely affected by segmental to patchy immunostaining. The immunostaining was predominantly coalescing to discrete, finely granular in the molecular layer of all four animals, which often tapered in severity at the interface of the molecular and Purkinje layers **(Figure 5.3a).** The immunolabeling was more prominent in the dorsal vermis as compared to the ventral vermis and lateral hemispheres. Three animals (3914, 3916, 3917) had mild punctate immunolabeling of the granular layer. In all four animals, the neuropil of the deep cerebellar nuclei had rare, widely-spaced, punctate and globular immunolabeling. Overall, 3913 had the least amount of PrP^{Sc} immunolabeling, as compared to the other animals. Mild to moderate gliosis (astrocytes and/or microglia) diffusely affected the folia of the vermis and hemispheres in all four animals. Glial cells often extended to the interface of the molecular and Purkinje cell layers. Additionally, there was mild segmental spongiosis of the Purkinje cell layer in all four animals, with loss of Purkinje cells. In the classical scrapie animals, punctate to globular immunolabeling was most prominent in the granular layer of cerebellar folia, with less frequent, finely granular and linear patterns. Rare punctate immunolabeling was in the molecular layer **(Figure 5.3b)**. Deep cerebellar nuclei had finely granular to punctate, intraneuronal immunolabeling, with similar but less severe accumulation in the neuropil.

In the four animals inoculated with atypical scrapie, there was an absence of PrP^{Sc} immunolabeling in the caudal midbrain, including the superior colliculus (**G3**). Additionally, only minimal gliosis, as well as neuronal and axonal changes were observed on H&E in the superior colliculus. In the classical scrapie animals, the superior colliculi had mild to moderate, patchy, finely granular to punctate immunolabeling in neurons, in glia, around glia, and free in the neuropil.

a) b)

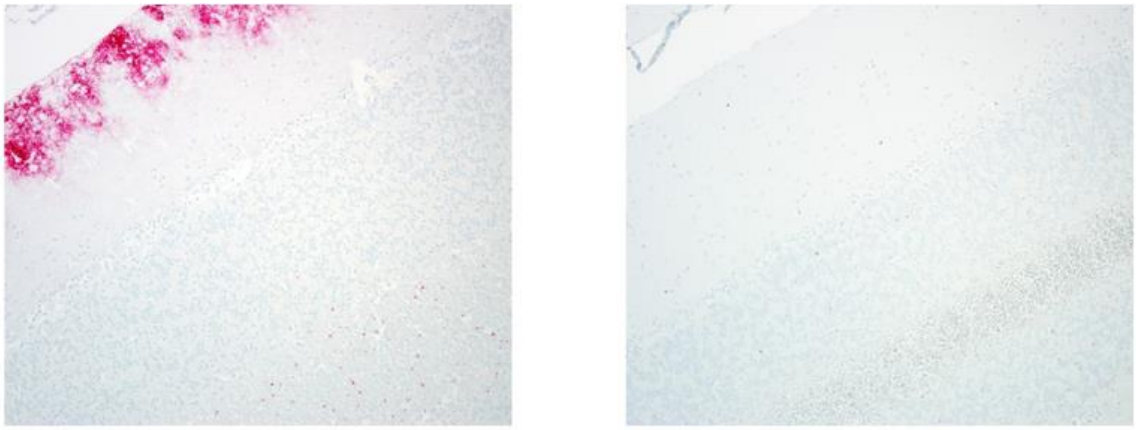

Figure 5.3. Immunolabeling of cerebellum in atypical and classical scrapie.

(a) There is patchy but diffuse, coalescing, finely granular PrP^{Sc} immunolabeling in the molecular layer of the cerebellum, and punctate PrP^{Sc} immunolabeling in the white matter of the folia. Note that there is rare PrP^{Sc} immunolabeling in the granular layer. Animal 3917, cerebellum, 10X, IHC. (b) PrP^{Sc} immunolabeling is absent from the molecular layer, but there is punctate to finely granular PrP^{Sc} immunolabeling in the granular layer. Animal 4124, cerebellum, 10X, IHC.

Sections of hypothalamus and medial thalamus (**G4/5**) were evaluated in all four animals. The hypothalamic sections from all four animals lacked immunolabeling. In the thalamus, there were frequent multicentric aggregates and fewer areas of punctate staining in several nuclei (i.e., ventral posteriolateral thalamic, ventral posteriomedial thalamic, ventrolateral, ventral anterior thalamic) with less common immunolabeling in the external medullary lamina, and rare involvement of the internal capsule in all four animals. This staining consistently resulted in a curvilinear pattern of deposition that extended from the ventral-median to the dorso-lateral thalamus, and less frequently the dorsal thalamus. Amorphous, lightly eosinophilic, moderately circumscribed, aggregates were more frequent on H&E in 3916 and 3917 as compared to 3913 and 3914, which almost always coincided with the localization of aggregate forms on IHC*.* On H&E, these aggregates were sometimes surrounded by hypereosinophilic degenerate nerve fibers, few microglia, and occasional lipofuscin-laden microglia or macrophages. There was mild aggregate and punctate immunolabeling of the intralaminar and mediodorsal thalamic nuclei in two animals (3916, 3917), with moderate microgliosis in 3917. Mild microgliosis was in the periventricular and reuniens thalamic nuclei of 3914. Overall, 3913 had the least amount of PrP^{Sc} immunolabeling as compared to the other animals. Multifocal to diffuse, periventricular punctate immunolabeling was in the medial amygdaloid region in two animals (3916, 3917). Punctate immunolabeling was also at the angle of the amygdalohippocampus-internal capsule-tail of the caudate nucleus, and had a more scattered distribution in the cerebral peduncle of the same animals. In the classical scrapie animals, the arcuate nucleus of the hypothalamus had diffusely, finely granular to less frequent punctate, intraneuronal immunolabeling. A similar immunolabeling pattern was in some thalamic and amygdaloid nuclei, but the distribution was variable between the two animals (4124 – few neurons, 4130 – numerous neurons). Some nuclei lacked PrP^{Sc} immunolabeling (i.e., ventral posteriolateral, ventral posteriomedial, mediodorsal). Punctate immunolabeling was in and

surrounded several glial cells. Vascular aggregates and finely granular perivascular immunolabeling were more frequent in the thalamus of 4124.

Sections of hippocampus (**G6**) were evaluated in all four animals. Multicentric aggregates, with less frequent, finely granular immunolabeling predominated in the dorsal hippocampal commissure at the interface of white and gray matter, and at the medial most extent of the commissure (adjacent to entorhinal cortex) in 3914, 3916, and 3917. These aggregates disrupted the ventral, medial, and dorsal aspects of the hippocampal commissure. Similar, but less common aggregates were in the dorsal hippocampus between the dentate gyrus and CA1 for the same animals. In 3916, regionally extensive punctate immunolabeling was at the junction of CA3 with the dentate gyrus, and rare punctate foci were in the neuropil superior to CA1. Mild to moderate gliosis (mixture of astrocytes and microglia) partially to circumferentially surrounded these aggregates. In 3914, 3916, and 3917, there was mild to moderate microgliosis in multiple neuroanatomic locations (i.e., CA3, the junction of the dentate gyrus with CA3, the dentate gyrus, the area between CA1 and the dentate gyrus) with minimal involvement of CA1. The posterior thalamic nuclear group had aggregated and less frequent, finely granular immunolabeling. These areas coincided with aggregates on H&E. Immunolabeling extended slightly into the midbrain from the posterior thalamic nuclear group in 3914, 3916, and 3917. Widely scattered, punctate, immunolabeled foci were in the subcallosal bundle and corpus callosum in animals 3916 and 3917, which were infrequent in 3914 and rare in 3913. Focal, globular, intraependymal immunolabeling was restricted to one animal (3914). With the exception of the subcallosal bundle and corpus callosum, additional PrP^{Sc} immunolabeling was absent in the hippocampus and other neuroanatomic regions of the forebrain in one animal (3913). In the classical scrapie animals, occasional pyramidal neurons in the hippocampus had intraneuronal, finely granular immunolabeling, with rare, punctate, intraglial accumulation. Rare neurons in the lateral geniculate nucleus also had similar immunolabeling. In 4130, there was regionally extensive, finely granular immunolabeling in the

neuropil of the dorsal hippocampal commissure and subjacent to ependymal cells. Occasional perivascular aggregates surrounded small-caliber vessels.

Comparisons of PrP^{Sc} patterns in the basal nucleus of atypical and classical scrapie cases are depicted in **Figure 5.4** (**G7**). Mild, punctate immunolabeling was in the neuropil of the lateral and medial septal nuclei of 3914, 3916 and 3917, with a complete absence of immunolabeling in 3913. In all 4 subjects, multiple neurons in the lateral septal nucleus were enlarged, rounded, and prominent, with a vesicular nucleus and clumped Nissl substance. The distribution of these atypical neurons was diffuse in 3913 and 3914, and multifocal in 3916 and 3917. Additionally, scant to few, type II Alzheimer-like astrocytes were often adjacent to these aforementioned neurons. The lateral septal nucleus was infiltrated by mild to moderate gliosis (mixture of astrocytes and microglia). In 3916 and 3917 only, the medial septal nucleus exhibited similar, but milder neuronal and inflammatory changes. Amongst all animals, there was variation in the type and distribution of neuropil immunolabeling in the gray matter of the internal capsule. This included finely granular and regionally extensive (3913), punctate and multifocal (3917), aggregated to finely granular (3914), and widespread punctate to globular (3916). In all four animals, there was immunolabeling in the internal capsule white matter that varied from mild and punctate (3913, 3914), to moderate, punctate, and globular (3916, 3917). Immunolabeling was more widespread in 3914 as compared to 3913. Rare, punctate immunolabeling was in the corpus callosum (3917), globus pallidus, and putamen (3916). Tissue sections of putamen from 3913 and 3914, as well as the globus pallidus from 3914, were absent from examined histologic and immunohistochemical slides. The lateral olfactory tract had punctate to globular immunolabeling, which extended into the olfactory tubercle in 3913, 3916, and 3917. Although the lateral olfactory tract was absent from the tissue section for 3914, two punctate foci were in the olfactory tubercle. There was an absence of immunolabeling in the caudate nucleus; however, occasional type II Alzheimer-like astrocytes were in the caudate nucleus of one animal (3917). In the animals with classical scrapie, few to multiple neurons

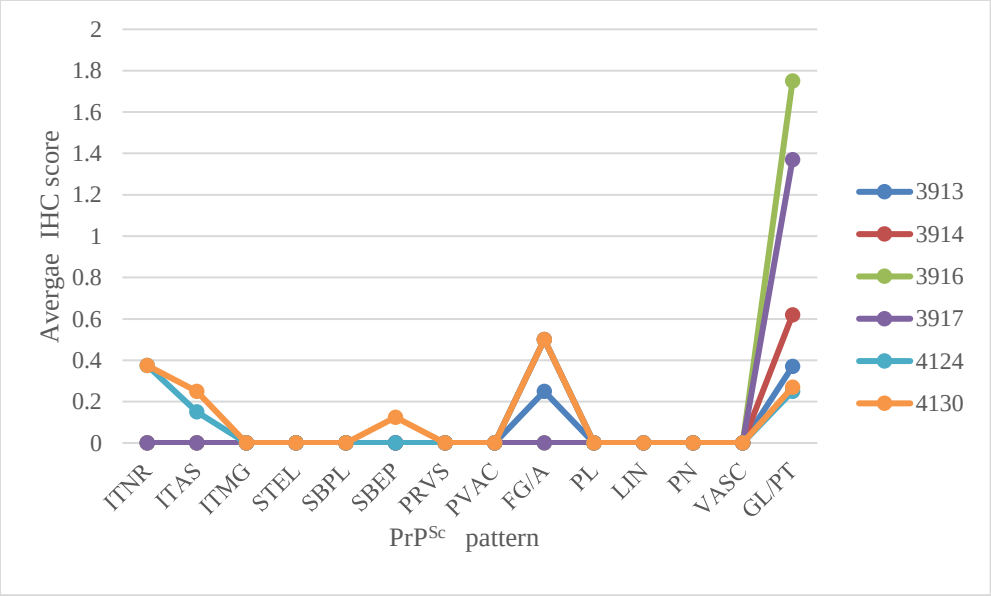

Figure 5.4. Comparison of PrP^{Sc} immunolabeling at the level of the basal nuclei (G7) in atypical and classical scrapie. Categories for immunolabeling PrP^{Sc} patterns implemented by Moore *et al*. were utilized, and these patterns were recorded, averaged, and plotted per subject. Atypical scrapie subjects are depicted in blue, red, lime green, and purple; classical scrapie animals are depicted in aqua and orange. The y axis lists average immunolabeling scores, and types of PrP^{Sc} patterns are situated along the x axis. The predominant pattern in atypical scrapie cases was globular to punctate (GL/PL), whereas in classical scrapie, intraneuronal (ITNR), intra-astrocytic (ITAS), subependymal (SBEP), and finely granular to aggregate (FG/A) were most frequently observed. Immunolabeling patterns: ITNR - intraneuronal, ITAS - intra-astrocytic, ITMG - intra-microglial, STEL - stellate, SBPL - subpial, SBEP - subependymal, PRVS - perivascular, PVAC - perivacuolar, FG/A - fine granular and aggregates, PL - plaque-like aggregates, LIN - linear, PN - perineuronal, VASC - vascular, GL/PT - globular and punctate. Note: Neuroanatomical areas included in the assessment at G7 were: lateral and medial septal nuclei, internal capsule (white and gray matter), and ventrolateral to ventral olfactory tract.

in various neuroanatomic locations of the tissue section (i.e., stria terminalis, caudate nucleus, lateral and medial septal nuclei, internal capsule – gray matter, piriform cortex, globus pallidus, putamen) had a predominance of finely granular, intraneuronal immunolabeling. Punctate to finely granular, intraglial and periglial immunolabeling was also less frequently and variably distributed in the aforementioned tissue sections. Finely granular perivascular and vascular aggregates, as well as finely granular ependymal and subependymal foci were rare.

Immunolabeling of the cerebral cortex (**G8 depicting the cerebral cortex at the level of G4/5**) was confined to the interface between the cortex and the corona radiata in 3914, 3917, and 3916, and was often punctate to globular. Mild, segmental microgliosis was also present at this interface, with slight extension into the cortex in 3916 and 3917. In the corona radiata, there was variation in the character of PrP^{Sc} immunolabeling amongst some of the animals. The immunolabeling was more widespread in two animals (3916, 3917), comprised of multicentric aggregates largely localized to the gyral tips, and punctate to globular accumulation in the inferior corona radiata. In these same animals, the lateral gyri were most frequently and prominently involved with diminished immunolabeling of the medial/middle gyri. The locale of aggregates in the lateral gyri often coincided with similar, aforementioned aggregates on H&E in 3916 **(Figures 5.5a and 5.5b)**, but these aggregates were less overt on H&E in 3917. There was also mild microgliosis in the inferior aspect of the corona radiata of some gyri. Animal 3916 also had mild, scattered perivascular edema. In animal 3914, the immunolabeling in the corona radiata was punctate to globular in the gyral tips with rare punctate accumulation in the inferior corona radiata. Lastly, animal 3913 had only rare punctate immunolabeling that was confined to the periventricular white matter, and a focal, intraventricular aggregate adhered to the apical surface of a single ependymal cell.

There was an absence of immunolabeling in G8 from classical scrapie animal 4124. Animal 4130 had abundant, finely granular and less frequent, punctate intraneuronal immunolabeling that was confined to few segments of laminar cortical neurons, and a regionally

a) b)

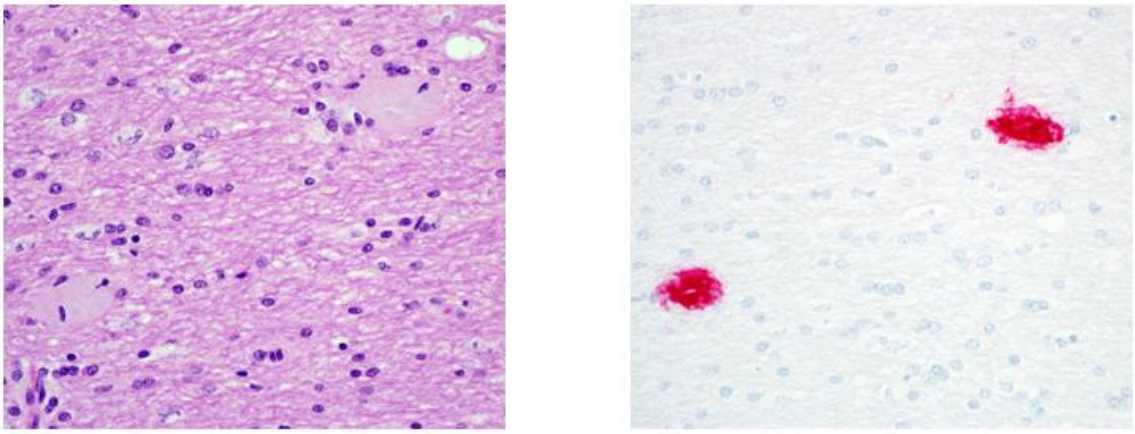

Figure 5.5. Histopathology and immunolabeling of PrP^{Sc} aggregates in the cerebrum. (a) Aggregates in the corona radiata with displacement of nerve fibers and mild gliosis, H&E, 40X. (b) Immunolabeling of PrP^{Sc} multicentric aggregates coinciding with the localization of plaques on H&E, IHC. Animal 3916, forebrain, 40X

extensive area of intertwined white and gray matter. Occasional perivascular aggregates, and rare, finely granular immunolabeling in the ependyma were additional features.

Immunolabeling of the gray matter in the forebrain cortex (**G9 at the level of the forebrain cortex at G7**) was rare, but when present, was often punctate, occurring at the interface of the cerebrocortex and corona radiata in two animals (3916, 3917) with slight extension into the cortex. No significant histopathologic lesions were in the cortex of any animal. PrP^{Sc} immunolabeling of the corona radiata in two animals (3916, 3917) was most pronounced in gyral tips, tapering in severity at the inferior base (adjacent to the lateral ventricle). The pattern varied from mainly multicentric aggregates to less common, globular and punctate immunolabeling. There were aggregates on H&E in the corona radiata of gyral tips that occasionally coincided with aggregates on IHC.

Variable numbers of astrocytes and microglia surrounded these aggregates. Rare, punctate immunolabeling was widely scattered in the corona radiata of 3914, and there was an absence of immunolabeling in 3913. Additionally, there was moderate, widespread, punctate, periventricular immunolabeling (3916, 3917), and focal, globular immunolabeling of intraventricular debris (3913).

For the classical scrapie animals, the dorsal aspect of G9 was unable to be evaluated for 4130; however, few neurons in 4124 had finely granular, intraneuronal immunolabeling, with a similar intracellular pattern in rare glial cells. Additionally, few meningeal and corona radiata vessels had vascular to perivascular, aggregated to punctate immunolabeling. Finely granular ependymal and subependymal PrP^{Sc} accumulation was rare. In 4130, a focal, plaque-like, extraneuronal aggregate was in the cerebrocortex.

In all four animals, the white matter of the cerebellum (**W1**) was assessed. The white matter of the folia had globular and punctate immunolabeling, with extension into but tapering of severity at the level of the ventral vermis **(refer to Figure 5.3a)**. Occasional globular, periventricular immunolabeling was also in the same animals. No significant histopathologic

lesions were in the cerebellar white matter in any of the four animals. In the classical scrapie animals, mild, finely granular to punctate immunolabeling of glial cells and the neuroparenchyma was widely scattered in the cerebellar white matter.

The mesencephalic tegmentum (**W2**) had an absence of immunolabeling, as well as significant histopathologic lesions in all four animals. However, the superior cerebellar peduncle possessed rare, globular immunolabeling in two animals (3913, 3914). In the classical scrapie animals, the dorsal tegmental bundle and medial forebrain bundle had rare punctate immunolabeling. However, the gray matter dissecting through the bundles had finely granular to punctate immunolabeling that was intraneuronal, intraglial, adjacent to glia, and free in the neuropil. The gray matter PrP^{Sc} accumulation in the medial forebrain bundle was more severe than in the dorsal tegmental bundle.

Discussion and Conclusions

Overall, the PrP^{Sc} localization and patterns of PrP^{Sc} accumulation are similar to those previously described for atypical scrapie [12, 13, 15, 28, 29, 91-94,98], indicating this atypical scrapie pathotype is not specific to the US and has a worldwide distribution. Gray matter PrP^{Sc} immunolabeling in the animals inoculated with atypical scrapie was of the greatest magnitude and diffusely distributed in the molecular layer of the cerebellar cortex. In various nuclei with PrP^{Sc} immunolabeling, accumulations were in the neuropil of those nuclei. Intraneuronal PrP^{Sc} deposits were absent in brain sections from all atypical scrapie-inoculated animals. Nerve fiber tracts in the various brain sections had more widespread PrP^{Sc} accumulation. The most frequent immunolabeling patterns in the current study included punctate, globular, and multicentric aggregates, which were all extracellular and also previously reported in the literature.

In contrast, the sheep infected with classical scrapie most commonly had intraneuronal, glial (peri- and intra-), perivascular to vascular, and subependymal immunolabeling (in order of decreasing prevalence). These immunolabeling types have been previously acknowledged and

described in other classical scrapie cases [99-101]. Additionally, the regions with the most pronounced PrP^{Sc} immunolabeling in the classical scrapie-infected sheep of the current study include the dorsal motor nucleus of the vagus nerve, granular layer of the cerebellum, superior colliculus, and hypothalamus. However, the atypical scrapie-infected sheep had absent to minimal immunolabeling in these areas, with a predominance of PrP^{Sc} immunolabeling in the lateral nerve tracts of the medulla, molecular layer of the cerebellum, corona radiata, thalamic nuclei, and hippocampal commissure.

Amongst the atypical scrapie-inoculated animals, animal 3913 had the least widespread amount of PrP^{Sc} accumulation. This animal succumbed to disease unassociated with prion infection during the experiment (abomasal empyting defect), so the relative paucity of PrP^{Sc} accumulation as compared to the other animals is likely due to the shorter incubation period. The remaining three sheep in the current study (3914, 3916, 3917) had longer post-inoculation intervals but still had only minimal to mild clinical signs. The lack of denser PrP^{Sc} accumulation as compared to previously published studies [29, 91] is likely due to the fact that these animals represent an earlier stage of disease progression, as previous studies investigated PrP^{Sc} deposition patterns in animals with more severe clinical signs.

Furthermore, there were some subtle differences in localization that were not noted in previous publications, to the best of the authors' knowledge [12, 13, 28, 29, 91-93, 98]. For example, the hippocampal commissure and the dorsal hippocampus had aggregated and finely granular immunolabeling compared to previous reports of finely granular to nondisclosed type of immunolabeling in the hippocampus (the hippocampal commissure was not specifically mentioned in previous studies) [91, 98]. Additionally, finely granular immunolabeling was diffusely observed in up to three laminar layers of the neocortex in 3 separate brain lobe sections in a previous study [91], whereas in the current study, punctate to globular immunolabeling was largely restricted to the interface of the gray and white matter with rare involvement of the cortex in only 2 brain lobe sections. In other studies [91, 98], finely granular

to punctate to nondisclosed type of immunolabeling was in the caudate nucleus, whereas there was a complete absence of immunolabeling in the caudate nucleus in the current study. Also, punctate immunolabeling has been noted in the olfactory tract [98], but in the current study, punctate immunolabeling was also in the olfactory tubercle (olfactory tubercle not specifically mentioned in previous studies). In the current study, cerebellar cortical PrP^{Sc} immunolabeling was largely confined to the molecular layer, but in previous reports [12, 28, 29, 91], there was also greater involvement of the granular layer.

This diversity in localization of PrP^{Sc} deposition could be due to several possible reasons. First, as it is well-established, genotypic polymorphisms in PRNP can influence susceptibility to atypical scrapie infection [8, 102]. The sheep in the current study were homozygous ARR, but in other previously described studies [12, 91, 98], homozygous and heterozygous AHQ, ARQ, AFRQ, ALRQ, and ARR sheep were used, for example. However, as was previously reported, phenotypic expression is variable even within the same genotype, suggesting other molecular and cellular factors may contribute to this expression [91]. Second, the sheep in the current study were intracranially/intracerebrally inoculated with a natural atypical scrapie isolate, whereas sheep in other studies were spontaneously infected [12, 91] or orally inoculated [98]. This could have also contributed to variation in PrP^{Sc} localization due to alterations in disease pathogenesis. Lastly, the difference in immunolabeling localization could be due to differences in incubation time between the studies. In this study, the average incubation period was approximately 5 – 7 years of age, whereas in other studies it was 1 year, or the incubation interval was not specifically defined as atypical scrapie was detected during passive or active surveillance. The longer the incubation period, the greater propensity for PrP^{Sc} localization and accumulation in multiple areas.

Future directions include: a) an assessment of the transcriptomic profile in atypical scrapie, to identify if differential expression of genes exists relative to classical scrapie, and determination of correlations with prion permissibility, and b) comparison of the transcriptomic

profile between ARR and AFRQ sheep to identify if similar gene transcripts are also differentially-expressed in atypical scrapie. Additionally, the long incubation period, slow prion-accumulating phenotype, and spontaneous origin of atypical scrapie is similar to human prion disease, so the identification of differentially-expressed genes and cellular processes in atypical scrapie could be extrapolated to human prion disease, validating the development of a human cell culture system.

CHAPTER 6 CONCLUSIONS

Classical and atypical scrapie are relevant, economically and devastating TSE diseases, in which control and elimination are imperative. Although eradication programs have greatly diminished the number of scrapie cases, additional efforts could be implemented that target antemortem detection from a genetic perspective, including evaluating genes in addition to PRNP. Currently, definitive determinants of prion permissibility are not specifically known; however, several studies have highlighted genes that could potentially contribute to prion permissibility. Being able to identify determinants from *in vivo* models of atypical scrapie, coupled with determinants discovered in *ex vivo* models of classical scrapie, provides a plethora of genes that could not only be targeted and manipulated for the eradication of classical and atypical scrapie, but also extrapolated to human TSEs inspiring the development of a human cell culture model system. At this time, there is no human cell culture line in existence for further characterizing human TSEs at the molecular, cellular, or subcellular levels, in a species-specific model system.

In classical scrapie, when evaluated relative to PRNP, fibronectin 1 (FN1) showed promise as a potential determinant in ovine microglia, exhibiting a strong, negative correlation with prion permissibility. Marbiah *et al.* also observed that silencing of FN1 led to increased prion susceptibility in murine neuroblastoma cells. Although additional studies are needed, the results of both studies highly suggest that expression of FN1 is linked to prion permissibility and susceptibility, in at least two, distinct cell culture systems. Thus, development of future cell culture models of prion disease may want to target inhibition of FN1 expression. Survivin (BIRC5) was also strongly and negatively correlated with prion permissibility in ovine microglia. However, the low transcript levels of survivin in ovine microglia, preclude its use as a suitable

determinant in these cells, and with a role in anti-apoptosis, evaluation of the apoptotic pathway may prove more enlightening. Matrix metalloproteinase II (MMP2) was not observed to significantly affect prion permissibility in ovine microglia clones, but in a preliminary study involving ovine microglia sublines, significantly decreased MMP2 expression was present in cells with a fast rate of prion accumulation. Even though MMP2 levels were not influential to prion permissibility independently, the multifactorial interaction of MMP2 with other genes could contribute to prion permissibility. As observed with Marbiah *et al.*, when the interaction of FN1 with integrin α8 was impeded, this led to decreased secretion of MMP2 and subsequently increase prion susceptibility. Further analysis of MMP2 expression, coupled with the expression of other genes such as PRNP, is essential for detecting potential synergistic and non-synergistic links with prion permissibility or susceptibility.

Lastly, histologic lesions and PrP^{Sc} pattern and localization of atypical scrapie in the North American cases was similar to previous reports of atypical scrapie in Europe (particularly Great Britain), as well as Canada, Australia, and Japan. This indicates that although the prevalence of atypical scrapie has increased worldwide, the pathophysiology remains largely conserved. Since the appearance of atypical scrapie in North America is relatively new as compared to Europe, known factors contributing to the onset of disease in this location are few. Furthermore, there remains a limited understanding of disease pathogenesis, breed predisposition, and signalment of atypical scrapie, and the absence of a well-established, stable, atypical scrapie isolate or strain. Characterizing PrP^{Sc} protein neuroanatomical pattern and localization of atypical scrapie, with subsequent gene expression analysis could lead to the development of a suitable, experimental model of study, with retained emphasis on control and eradication.

BIBILIOGRAPHY

1. Beringue, V., Andreoletti, O., *Classical and atypical TSE in small ruminants.* Animal Frontiers, 2014. **4**(1): p. 33 - 43.

2. Imran, M., Mahmood, S., *An overview of animal prion diseases.* Virology Journal 2011. **8**: p. 493-500.

3. Prusiner, S.B., *Molecular biology of prion diseases.* Science, 1991. **252**(5012): p. 1515 - 1522.

4. Babelhadj, B., Di Bari, M.A., Pirisinu, L., Chiappini, B., Gaouar, S.B.S., Riccardi, G., Marcon, S., Agrimi, U., Nonno, R., Vaccari, G., *Prion Disease in Dromedary Camels.* Emerging Infectious Diseases, 2018. **24**(6).

5. Prusiner, S., *Novel Proteinaceous Infectious Particles Cause Scrapie.* Science 1982. **216**(4542): p. 136-144.

6. Russelakis-Carneiro, M., Saborio, G.P., Anderes, L., Soto, C., *Changes in the Glycosylation Pattern of Prion Protein in Murine Scrapie.* The Journal of Biological Chemistry, 2002. **277**(39): p. 36872-36877.

7. Soto, C., Satani, N., *The intricate mechanisms of neurodegeneration in prion diseases.* Trends in Molecular Medicine, 2011. **17**(1): p. 14 - 24.

8. Benestad, S.L., Arsac, J.N., Goldmann, W., Noremark, M., *Atypical/Nor98 scrapie: properties of the agent, genetics, and epidemiology.* Veterinary Research, 2008. **39**(19): p. 14.

9. Benestad, S.L., Sarradin, P., Thu, B., Schonheit, J., Tranulis, M.A., *Cases of scrapie with unusual features in Norway and designation of a new type, Nor 98.* The Veterinary Record, 2003. **153**: p. 202 - 208.

10. Moum, T., Olsaker, I., Hopp, P., Moldal, T., Valheim, M., Moum, T., Benestad, S.L., *Polymorphisms at codons 141 and 154 in the ovine prion protein gene are associated with scrapie Nor98 cases.* Journal of General Virology, 2005. **86**: p. 231 - 235.

11. Luhken, G., Buschmann, A. Brandt, H., Eiden, M., Groschup, M.H., Erhardt, G., *Epidemiological and genetical differences between classical and atypical scrapie cases.* Veterinary Research, 2007. **38**: p. 65 - 80.

12. Loiacono, C.M., Thomsen, B.V., Hall, S.M., Kiupel, M., Sutton, D., O'Rourke, K., Barr, B., Anthenill, L., Keane, D. , *Nor98 scrapie identified in the United States.* Journal of Veterinary Diagnostic Investigation, 2009. **21**(4): p. 454 - 463.

13. Orge, L., Galo, A., Machado, C., Lima, C., Ochoa, C., Silva, J., Ramos, M., Simas, J.P., *Identification of putative atypical scrapie in sheep in Portugal.* Journal of General Virology, 2004. **85**: p. 3487 - 3491.

14. Greenlee, J.J., *Review: Update on Classical and Atypical Scrapie in Sheep and Goats.* Veterinary Pathology, 2019. **56**(1): p. 6 - 16.

15. Kittelberger, R., Chaplin, M.J., Simmons, M.M., Ramirez-Villaescusa, A., McIntyre, L., MacDiarmid, S.C., Hannah, M.J., Jenner, J., Bueno, R., Bayliss, D., Black, H., Pigott, C.J., O'Keefe, J.S., *Atypical scrapie/Nor98 in a sheep from New Zealand.* Journal of Veterinary Diagnostic Investigation, 2010. **22**(6): p. 863-875.

16. Hunter, N., *Scrapie and experimental BSE in sheep.* British Medical Bulletin, 2003. **66**: p. 171 - 183.

17. van Keulen, L.J.M., Vromans, M.E.W., Dolstra, C.H., Bossers, A., Zijderveld, F.G., *Pathogenesis of bovine spongiform encephalopathy in sheep.* Archives of Virology, 2008. **153**(3): p. 445 - 453.

18. Andreoletti, O., Orge, L., Benestad, S.L., Beringue, V., Litaise, C., Simon, S., Le Dur, A., Laude, H., Simmons, H., Lugan, S., Corbiere, F., Costes, P., Morel, N., Schelcher, F., Lacroux, C. , *Atypical/Nor98 Scrapie Infectivity in Sheep Peripheral Tissues.* PloS Pathogens, 2011. **7**(2): p. 1 - 14.

19. Grassmann, A., Wolf, H., Hofmann, J., Graham, J., Vorberg,I., *Cellular Aspects of Prion Replication in Vitro.* Viruses, 2013. **5**: p. 374-405.

20. Kretzschmar, H., Tatzelt, J., *Prion Disease: A Tale of Folds and Strains.* Brain Pathology, 2013. **23**(3): p. 321 - 332.

21. Vilette, D., *Cell Models of Prion Infection.* Veterinary Research, 2008. **39**(4).

22. Filali, H., Martin-Burriel, I., Harders, F., Varona, L., Lyahyai, J., Zaragoza, P., Pumarola, M., Badiola, J.J., Bossers, A., Bolea, R. , *Gene Expression Profiling and Association with Prion-Related Lesions in the Medulla Oblongata of Symptomatic Natural Scrapie Animals.* PLOS ONE, 2011. **6**(5).

23. Marbiah, M.M., Harvey, A., West, B.T., Louzolo, A., Banerjee, P., Alden, J., Grigoriadis, A., Hummerich, H., Kan, H.M., Cai, Y., Bloom, G.S., Jat, P., Collinge, J., Klohn, P.C. , *Identification of a gene regulatory network associated with prion replication.* The EMBO Journal, 2014. **33**(14): p. 1527-1547.

24. Munoz-Gutierrez, J.F., Pierle, S.A., Schneider, D.A., Baszler, T.V., Stanton, J.B., *Transcriptomic Determinants of Scrapie Prion Propagation in Cultured Ovine Microglia.* PLoS One, 2016. **11**(1): p. 1-20.

25. Collinge, J., Whitfield, J., McKintosh, E., Beck, J., Mead, M., Thomas, D.J., Alpers, M.P., *Kuru in the 21st century- an acquired human prion disease with very long incubation periods.* Lancet, 2006. **367**(9528): p. 2068 - 2074.

26. Oie. *OIE-Listed diseases, infections and infestations in force in 2019*. 2019; Available from: http://www.oie.int/animal-health-in-the-world/oie-listed-diseases-2019/.

27. USDA. *Scrapie*. 2017; Available from: https://www.aphis.usda.gov/aphis/ourfocus/animalhealth/nvap/NVAP-Reference-Guide/Control-and-Eradication/Scrapie.

28. Mitchell, G.B., O'Rourke, K.I., Harrington, N.P., Soutyrine, A., Simmons, M.M., Dudas, S., Zhuang, D., Laude, H., Balachandran, A., *Identification of atypical scrapie in Canadian sheep.* Journal of Veterinary Diagnostic Investigation, 2010. **22**(3): p. 408-411.

29. Cook, R.W., Bingham, J., Besier, A.S., Bayley, C. L., Hawes, M., Shearer, P.L., Yamada, M., Bergfield, J., Williams, D.T., Middleton, D.J., *Atypical scrapie in Australia.* Australian Veterinary Journal, 2016. **94**(12): p. 452 - 455.

30. Babelhadj, B., DiBari, M.A., Pirisinu, L., Chiappini, B., Gaouar, S.B.S., Riccardi, G., Marcon, S., Agrimi, U., Nonno, R., Vaccari, G., *Prion disease in Dromedary Camels, Algeria.* Emerging Infectious Diseases, 2018. **24**(6): p. 1029 - 1035.

31. Schneider, K., Fangerau, H., Michaelson, B., Raab, W.H.M., *The early history of the transmissible spongiform encephalopathies exemplified by scrapie.* Brain Research Bullentin, 2008. **77**(6): p. 343-355.

32. Prusiner, S.B., *Novel Proteinaceous Infectious Particles Cause Scrapie.* Science, 1982. **216**(4542): p. 136-144.

33. Griffith, J.S., *Self replication and scrapie.* Nature, 1967. **215**(5105): p. 1043-1044.

34. Caughey, B.W., Dong A., Bhat, K.S., Ernst, D., Hayes, S.F. and Caughey, W.S., *Secondary structure analysis of the scrapie-associated protein PrP 27–30in water by infrared spectroscopy.* Biochemistry, 1991. **30**: p. 7672 - 7680.

35. Pan, K.M., Baldwin, M., Nguyen, J., Gasset, M., Serban, A., Groth. D., Mehlhorm, I., Huang, Z., Fletterick, R.J., Cohen, F.E., *Conversion of alpha-helices into beta-sheets features in the formation of the scrapie prion proteins.* Proc Natl Acad Sci USA, 1993. **90**(23): p. 10962 - 10966.

36. Zhou, Z., Xiao, G., *Conformational conversion of prion protein in prion diseases.* Acta Biochim Biophys Sin, 2013. **45**(6): p. 465 - 476.

37. Legname, G., Baskakov, I.V., Nguyen, H.O., Riesner, D., Cohen, F.E., DeArmond, S.J., Prusiner, S.B., *Synthetic mammalia prions.* Science, 2004. **305**(5684): p. 673 - 676.

38. Castilla, J., Saa, P., Hetz, C., Soto, C. , *In vitro generation of infectious scrapie prions.* Cell, 2005. **121**(2): p. 195 - 206.

39. Telling, G.C., *Transgenic mouse models of prion diseases.* Methods in Molecular Biology, 2008. **459**: p. 249 - 263.

40. Thackray, A.M., Hopkins, L., Spiropoulos, J., Bujdoso, R., *Molecular and Transmission Characteristics of Primary-Passaged Ovine Scrapie Isolates in Conventional and Ovine PrP Transgenic Mice.* Journal of Virology, 2008. **82**(22): p. 11197-11207.

41. Rheede, T.V., Smolenaars, M.M.W., Madsen, O., de Jong, W.W., *Molecular Evolution of the Mammalian Prion Protein.* Molecular Biology and Evolution, 2002. **20**(1): p. 111-121.

42. Goldmann, W., Hunter, N., Foster, J.D., Salbaum, J. M., Beyreuther, K., Hope, J., *Two alleles of a neural protein gene linked to scrapie in sheep.* Proceedings of the National Academy of Sciences of the United States of America, 1990. **87**: p. 2476 - 2480.

43. Brown, D.R., Schmidt, B., Kretzschmar, H.A., *Role of microglia and host prion protein in neurotoxicity of a prion protein fragment.* Nature, 1996. **380**: p. 345 - 347.

44. Moser, M., Colello, R.J., Pott, U., Oesch, B. , *Developmental expression of the prion protein in glial cells.* Neuron, 1995. **14**: p. 509 - 517.

45. Linden, R., Martins, V.R., Prado, M. A., Cammarota, M., Izquierdo, I., Brentani, R.R., *Physiology of the prion protein.* Physiological Reviews, 2008. **88**: p. 673 - 728.

46. Tranulis, M.A., *Influence of the prion protein gene, Prnp, on scrapie susceptibility in sheep.* APMIS, 2002. **110**: p. 33 - 43.

47. Hunter, N., Foster, J.D., Goldmann, W., Stear, M.J., Hope, J., Bostock, C, *Natural scrapie in a closed flock of Cheviot sheep occurs only in specific PrP genotypes.* Archives of Virology, 1996. **141**(5): p. 809 - 824.

48. Clouscard, C., Beaudry, P., Elsen, J.M., Milan, D., Dussaucy, M., Bounneau, C., Schelcher, F., Chatelain, J., Launay, J.M., Laplanche, J.L., *Different allelic effects of the codons 136 and 171 of the prion protein gene in sheep with natural scrapie.* Journal of General Virology, 1995. **76**: p. 2097 - 2101.

49. Wulf, M.A., Senatore, A., Aguzzi, A., *The biological function of the cellular prion protein: an update.* BMC Biology, 2017. **15**(34): p. 13.

50. Gauczynski, S., Peyrin, J.M., Haik, S., Leucht, C., Hundt, C., Rieger, R., Krasemann, S., Deslys, J.P., Dormont, D., Lasmezas, C.J., Weiss, S. , *The 37-kDa/67-kDa laminin receptor acts as the cell-surface receptor for the cellular protein.* EMBO 2001. **20**(21): p. 5863 - 5875.

51. Gauczynski, S., Nikles, D., El-Gogo, S., Papy-Garcia, D., Rey, C., Alban, S., Barritault, D., Lasmezas, C.I., Weiss, S., *The 37-kDa/67-kDa laminin receptor acts as a receptor for infectious prions and is inhibited by polysulfated glycanes.* Journal of Infectious Diseases, 2006. **194**(5): p. 702 - 709.

52. Arsac, J.N., Baron, T., *Distinct Transmissibility Features of TSE Sources Derived from Ruminant Prion Disease by the Oral Route in a Transgenic Mouse Model (TgOvPrP4) Overexpression the Ovine Prion Protein.* PLOS One, 2014. **9**(5): p. 1-8.

53. Beekes, M., McBride, P.A., *Early accumulation of pathological PrP in the enteric nervous system and gut-associated lymphoid tissue of hamsters orally infected with scrapie.* Neuroscience Letter, 2000. **278**(3): p. 181- 184.

54. Hu, P.P., Morales, R., Duran-Aniotz, C., Moreno-Gonzalez, I., Khan, U., Soto, C., *Role of Prion Replication in the Strain-dependent BrainRegional Distribution of Prions.* THE JOURNAL OF BIOLOGICAL CHEMISTRY, 2016. **291**(24): p. 12880-12887.

55. Solassol, J., Crozet, C., Lehmann, S., *Prion propagation in cultured cells.* British Medical Bulletin, 2003. **66**: p. 87 - 97

56. Munoz-Gutierrez, J.F., Schneider, D.A., Baszler, T.V., Greenlee, J.J., Nicholson, E.M., Stanton, J.B., *hTERT-immortalized ovine microglia propagate natural scrapie isolates.* Virus Research, 2015. **198**: p. 35-43.

57. Stanton, J.B., Knowles, D.P., O'Rourke, K.I., Herrmann-Hoesing, L.M., Mathison, B.A., Baszler, T.V., *Small Ruminant Lentivirus Enhances PrPSc Accumulation in Cultured Sheep Microglial Cells.* Journal of Virology, 2008. **82**(20): p. 9839 - 9847.

58. Kettenmann, H., Hanisch, U.K., Noda, M., Verkhratsky, A., *Physiology of Microglia.* Physiological Reviews, 2011. **91**: p. 461-553.

59. Aguzzi, A., Zhu, C., *Microglia in prion disease.* The Journal of Clinical Investigation, 2017. **127**(9): p. 3230 - 3239.

60. Dinkel, K.D., Schneider, D.A., Munoz-Gutierrez, J.F., McElliott, V.R., Stanton, J.B., *Correlation of cellular factors and differential scrapie prion permissiveness in ovine microglia.* Virus Research, 2017. **240**: p. 69 - 80.

61. Muñoz-Gutiérrez, J.F., Schneider, D.A., Baszler, T.V., Greenlee, J.J., Nicholson, E.M., Stanton, J.B. , *hTERT-immortalized ovine microglia propagate natural scrapie isolates.* Virus Research, 2015. **198**: p. 35 - 43.

62. Dinkel, K.D., Stanton, J.B., Boykin, D.W., Stephens, C.E., Madsen-Bouterse, S.A., Schneider, D.A., , *Antiprion Activity of DB772 and Related Monothiophene- and FuranBased Analogs in a Persistently Infected Ovine Microglia Culture System.* Antimicrobial Agents and Chemotherapy, 2016. **60**(9): p. 5467 - 5482.

63. Ye, J., Coulouris, G., Zaretskaya, I., Cutcutache, I., Rozen, S., Madden, T., *Primer-BLAST: A tool to design target-specific primers for polymerase chain reaction.* BMC Bioinformatics, 2012. **13**(134).

64. Stanton, J.B., Schneider, D.A., Dinkel, K.D., Balmer, B.F., Baszler, T.V., Mathison, B.A., Boykin, D.W., Kumar, A. , *Discovery of a Novel, Monocationic, Small-Molecule Inhibitor of Scrapie Prion Accumulation in Cultured Sheep Microglia and Rov Cells.* PLOS One, 2012. **7**(11): p. 1 - 11.

65. Fredslund, J., Schauser, L., Madsen, L.H., Sandal, N., Stougaard, J., *PriFi: using a multiple alignment of related sequences to find primers for amplification of homologs.* Nucleic Acids Research, 2005. **33**: p. W516-W520.

66. Vandesompele, J., De Preter, K., Pattyn, F., Poppe, B., Van Roy, N., De Paepe, A., Speleman, F., *Accurate normalization of real-time quantitative RT-PCR data by geometric averaging of multiple internal control genes.* Genome Biology, 2002. **3**(7): p. 1 - 12.

67. Kozera, B., Rapacz, M., *Reference genes in real-time PCR.* Journal of Applied Genetics, 2013. **54**: p. 391-406.

68. Kuchipudi, S.V., Tellabati, M., Nelli, R.K., White, G.A., Perez, B.B., Sebastian, S., Slomka, M.J., Brookes, S.M., Brown, I.H., Dunham, S.P., Chang, K-C, *18S rRNA is a reliable normalisation gene for real time PCR based on influenza virus infected cells.* Virology Journal, 2012. **9**(230): p. 1 - 7.

69. Zollinger, A.J., Smith, M.L., *Fibronectin, the extracellular gene.* Matrix Biology, 2016. **60 - 61**: p. 27 - 37.

70. Khan, Z., Khan, A.A., Yadav, H., Prasad, G.B.K.S., Bisen, P.S., *Survivin, a molecular target for therapeutic interventions in squamous cell carcinoma.* Cellular and Molecular Biology Letters, 2017. **22**(8): p. 1 - 32.

71. Lloyd-Burton, S.M., York, E.M., Anwar, M.A., Vincent, A.J., Roskams, A.J., *SPARC Regulates Microgliosis and Functional Recovery following Cortical Ischemia.* The Journal of Neuroscience, 2013. **33**(10): p. 4468 - 4481.

72. Bradshaw, A.D., *The role of SPARC in extracellular matrix assembly.* Journal of Cell Communication and Signaling, 2009. **3**: p. 239 - 246.

73. Booth, S., Bowman, C., Bamgartner, R., Sorensen, G., Robertson, C., Coulthart, M., Phillipson, C., Somorjai, R.L., *Identification of central nervous system genes involved in the host response to the scrapie agent during preclinical and clinical infection.* Journal of General Virology, 2004. **85**: p. 3459 - 3471.

74. Mroczko, B., Groblewska, M., Barcikowska, M. , *The Role of Matrix Metalloproteinases and Tissue Inhibitors of Metalloproteinases in the Pathophysiology of Neurodegeneration: A Literature Study.* Journal of Alzheimer's Disease, 2013. **37**(2): p. 273-283.

75. Nagase, H., Woesner, J.F., , *Matrix Metalloproteinases.* Journal of Biological Chemistry, 1999. **274**(31): p. 21491 - 21494.

76. Parks, W.C., Wilson, C.L. Lopez-Boado, Y.S. , *Matrix Metalloproteinases As Modulators of Inflammation and Innate Immunity.* Nature Reviews in Immunology, 2004. **4**: p. 617 - 629.

77. Rempe, R.G., Hartz, A.M.S., Bauer, B., *Matrix metalloproteinases in the brain and blood-brain-barrier: Versatile breakers and makers.* Journal of Cerebral Blood Flow & Metabolism, 2016. **36**(9): p. 1481 - 1507.

78. Lo, E., Wang, X., Cuzner, M., *Extracellular proteolysis in brain injury and inflammation: role of plasminogen activators and matrix metalloproteinases.* Journal of Neuroscience Research, 2002. **69**(1): p. 1 - 9.

79. Loffek, S., Schilling, O., Franzke, C.W., *Biological role of matrix metalloteinases: a critical balance.* European Respiratory Journal, 2011. **38**: p. 191 - 208.

80. Deryugina, E.I., Ratnikov, B., Monosov, E., Postnova, T.I., DiScipio, R., Smith, J.W., Strongin, A.Y., *MT1-MMP initiates activation of pro-MMP-2 and integrin alphavbeta3 promotes maturation of MMP-2 in breast carcinoma cells.* Experimental Cell Research, 2001. **263**: p. 203 - 229.

81. Nguyen, M., Arkell, J., Jackson, C.J., *Activated protein C directly activates human endothelial gelatinase A.* Journal of Biological Chemistry, 2000. **275**(13): p. 9095 - 9098.

82. Dean, R.A., Overall, C.M., *Proteomics Discovery of Metalloproteinase Substrates in the Cellular Context by iTRAQ™ Labeling Reveals a Diverse MMP-2 Substrate Degradome.* Molecular and Cellular Proteomics, 2007. **6**(4): p. 611 - 623.

83. Klein, T., Bischoff, R., *Physiology and pathophysiology of matrix metalloproteases.* Amino acids, 2011. **41**: p. 271 - 290.

84. Chakrabarti, S., Patel, K.D., *Matrix metalloproteinase-2 (MMP-2) and MMP-9 in pulmonary pathology.* Experimental Lung Research, 2005. **31**(6): p. 599 - 621.

85. Terni, B., Ferrer, I., *Abnormal Expression and Distribution of MMP2 at Initial Stages of Alzheimer's Disease-Related Pathology.* Journal of Alzheimer's Disease, 2015. **46**: p. 461 - 469.

86. Lorenzl, S., Albers, D.S., Narr, S., Chirichigno, J., Beal, M.F., *Expression of MMP-2, MMP-9 and MMP-1 and their endogenous counterregulators TIMP-1 and TIMP-2 in postmortem brain tissue of Parkinson's disease.* Experimental Neurology, 2002. **178**(1): p. 13 - 20

87. Schindelin, J., Arganda-Carreras, I., Frise, E., Kaynig, V., Longair, M., Pietzsch, T., Preibisch, S., Rueden, C., Saalfeld, S., Schmid, B., Tinevez, J.Y., White, D.J., Hartenstein, V., Eliceiri, K., Tomancak, P. Cardona, A. , *Fiji: an ope-source platform for biological-image analysis.* Nature methods, 2012. **9**(7): p. 676 - 682.

88. Schneider, C.A., Rasband, W. S., Eliceiri, K. W., *NIH Image to ImageJ: 25 years of image analysis".* Nature methods, 2012. **9**(7): p. 671 - 675.

89. McIntyre, K.M., del Rio Vilas, V.J., Gubbins, S., *No temporal trends in the prevalence of atypical scrapie in British sheep, 2002 - 2006.* BMC Veterinary Research, 2008. **4**(13): p. 1 - 8.

90. Saunders, G.C., Cawthraw, S. Mountjoy, S.J., Hope, J., Windi, O., *PrP genotypes of atypical scrapie cases in Great Britain.* Journal of General Virology, 2006. **87**(Pt 11): p. 3141 - 3149.

91. Moore, S.J., Simmons, M., Chaplin, M., Spiropoulos, J., *Neuroanatomical distribution of abnormal prion protein in naturally occurring atypical scrapie cases in Great Britain.* Acta Neuropathologica, 2008. **116**: p. 547-559.

92. Imamura, M., Miyazawa, K., Iwamaru, Y., Matsuura, Y., Yokoyama, T., Okada, H., *Identification of the first case of atypical scrapie in Japan.* Journal of Veterinary Medical Science, 2016. **78**(12): p. 1915 - 1919.

93. De Bosschere, H., Roels, S., Benestad, S.L., Vanopdenbosch, E. , *Scrapie case similar to Nor98 diagnosed in Belgium via active surveillance.* Veterinary Record, 2004. **155**: p. 707 - 708.

94. Bruce, M.E., Nonno, R., Foster, J., Goldmann, W., Di Bari, M., Esposito, E., Benestad, S.L., Hunter, N., Agrimi, U., *Nor98-like sheep scrapie in the United Kingdom in 1989.* The Veterinary Record, 2007. **160**(19): p. 665 - 666.

95. Buschmann, A., Biacabe, A.G., Ziegler, U., Bencsik, A., Madec, J.Y., Erhardt, G., Luhken, G., Baron, T., Groschup, M.H., *Atypical scrapie cases in Germany and France are identified by discrepant reaction patterns in BSE rapid tests.* Journal of Virological Methods, 2004. **117**(1): p. 27-36.

96. Cancellotti, E., Mahal, S.P., Somerville, R. , Diack, A., Brown, D., Piccardo, P., Weissmann, C., Manson, J.C., *Post-translational changes to PrP alter transmissible spongiform encephalopathy strain properties.* The EMBO Journal, 2013. **32**(5): p. 756-769.

97. Fraser, H., Dickinson, A.G., *The sequential development of the brain lesions of scrapie in three strains of mice.* Journal of Comparative Pathology, 1968. **78**: p. 301-311.

98. Simmons, M.M., Moore, S. J., Konold, T., Thurston, L., Terry, L.A., Thorne, L., Lockey, R., Vickery, C., Hawkins, S.A.C., Chaplin, M.J., Spiropoulos, J. , *Experimental Oral Transmission of Atypical Scrapie to Sheep.* Emerging Infectious Diseases, 2011. **17**(5): p. 848 - 854.

99. Ryder, S.J., Spencer, Y.I., Bellerby, P.J., March, S.A., , *Immunohistochemical detection of PrP in the medulla oblongata of sheep: the spectrum of staining in normal and scrapie-affected sheep.* Veterinary Record, 2001. **148**: p. 7 - 13.

100. Gonzalez, L.M., S., Begara-McGorum, I., Hunter, N., Houston, F., Simmons, M., Jeffrey, M. , *Effects of agent strain and host genotype on PrP accumulation in the brain of sheep naturally and experimentally affected with scrapie.* Journal of Comparative Pathology, 2002. **126**(1): p. 17-29.

101. Spiropoulos, J., Casalone, C., Caramelli, M., Simmons, M.M., *Immunohistochemistry for PrPSc in natural scrapie reveals patterns which are associated with the PrP genotype.* Neuropathology and Applied Neurobiology, 2007. **33**: p. 398-409.

102. Silva, C.J., Erickson-Beltran, M.L., Martin-Burriel, I., Badiola, J.J., Requena, J.R., Bolea, R., *Determinaing the Relative Susceptibility of Four Prion Protein Genotypes to Atypical Scrapie.* Analytical Chemistry, 2018. **90**: p. 1255-1262.

103. Gordon, W.S., *Advances in Veterinary Research.* Veterinary Record, 1946. **58**(47): p. 516-525.

104. Westergard, L., Christensen, H.M., Harris, D.A., *The cellular prion protein (PrPC): Its physiological function and role in disease.* Biochimica et Biophysica Acta, 2007. **1772**: p. 629-644.

105. Roucou, X., LeBlanc, A.C. , *Cellular prion protein neuroprotective function: implications in prion diseases.* Journal of Molecular Medicine, 2005. **83**(1): p. 3-11.

106. Milhavet, O., Lehmann, S., *Review: Oxidative stress and the prion protein in transmissible spongiform encephalopathies.* Brain Research Reviews, 2002. **38**(3): p. 328-339.

107. Tsui-Pierchala, B.A., Encinas, M., Milbrandt, J., Johnson, E.M., *Lipid rafts in neuronal signaling and function.* Trends in Neurosciences, 2002. **25**(8): p. 412-417.

108. Jeffrey, M., Halliday, W.G., Bell, J., Johnston, A.R., MacLeod, N.K., Ingham, C., Sayers, A.R., Brown, D.A., Fraser, J.R., *Synapse loss associated with abnormal PrP precedes neuronal degeneration in the scrapie-infected murine hippocampus.* Neuropathology and Applied Neurobiology, 2000. **26**(1): p. 41-54.

109. Schmitt-Ulms, G., Legname, G., Baldwin, M.A., Ball, H.L., Bradon, N., Bosque, P.J., Crossin, K.L., Edelman, G.M., DeArmond, S.J., Cohen, F. E., Prusiner, S. B., *Binding of neural cell adhesion molecules (N-CAMs) to the cellular prion protein.* Journal of Molecular Biology, 2001. **314**(5): p. 1209-1225.

110. Kretzschmar, H.A., Prusiner, S.B., Stowring, L.E., DeArmond, S.J. , *Scrapie prion proteins are synthesized in neurons.* American Journal of Pathology, 1986. **122**(1): p. 1-5.

111. Moser, M., Colello, R.J., Pott, U., Oesch, B., *Developmental expression of the prion protein gene in glial cells.* Neuron, 1995. **14**: p. 509-517.

112. Brown, H.R., Goller, N.L., Rudelli, R.D., Merz, G.S., Wolfe, G.C., Wisniewski, H.M., Robakis, N.K., *The mRNA encoding the scrapie agent protein is present in a variety of non-neuronal cells.* Acta Neuropathologica, 1990. **80**: p. 1-6.

113. Ford, M.J., Burton, L.J., Morris, R.J., Hall, S.M., *Selective Expression Of Prion Protein In Peripheral Tissues Of The Adult Mouse.* Neuroscience, 2002. **113**(1): p. 177-192.

114. Riek, R., Hornemann, S., Wider, G., Billeter, M., Glockshuber,R., Wuthrich, K., *NMR structure of the mouse prion protein domain PrP (121-231).* Nature, 1996. **382**(6587): p. 180-182.

115. Jeffrey, M., *Review: Membrane-associated misfolded protein propagation in natural transmissible spongiform encephalopathies (TSEs), synthetic prion diseases and Alzheimer's disease.* Neuropathology and Applied Neurobiology, 2013. **39**(3): p. 196-216.

116. Acquatella-Tran, V.B., Imberdis,T., Perrier, V., *From Prion Diseases to Prion-Like Propagation Mechanisms of Neurodegenerative Diseases.* International Journal of Cell Biology, 2013: p. 1-8.

117. Silveria, J.R., Raymond, G.J., Hughson, A.G., Race, R.E., Sim, V.L., Hayes, S.F., Caughey, B. , *The most infectious prion protein particles.* Nature, 2005. **437**: p. 257 - 261.

118. Paquet, S., Langevin, C., Chapuis, J., Jackson, G.S., Laude, H., Vilette, D. , *Efficient dissemination of prions through preferential transmission to nearby cells.* Journal of General Virology, 2007. **88**: p. 706-713.

119. Rouvinski, A., Karniely, S., Kounin, M., Moussa, S., Goldberg, M.D., Warburg, G., Lyakhovetsky, R., Papy-Garcia, D., Kutzsche, J., Korth, C., Carlson, G.A., Godsave, S.F., Peters, P.J., Luhr, K., Kristensson, K., Taraboulos, *Live imaging of prions reveals nascent PrP^{Sc} in cell-surface, raft-associated amyloid strings and webs.* Journal of Cell Biology, 2014. **204**(3): p. 1 - 19.

120. Hartmann, A., Muth, C., Dabrowski, O., Krasemann, S., Glatzel, M., *Exosomes and the Prion Protein: More than One Truth.* Frontiers in Neuroscience, 2017. **11**(194): p. 1 - 7.

121. Robertson, C., Booth, S.A., Beniac, D.R., Coulthart, M.B., Booth, T.F., McNicol, A., *Cellular prion protein is released on exosomes from activated platelets.* Blood, 2006. **107**: p. 3907 - 3911.

122. Davis, M.E., *Exosomes: What do we love so much about them?* Circulation Research, 2016. **119**(12): p. 1280 - 1281.

123. Fevrier, B., Vilette, D., Archer, F., Loew, D., Faigle, W., Vidal, M., Laude, H., Raposo, G., *Cells release prions in association with exosomes.* Proceedings of the National Academy of Sciences of the United States of America, 2004. **101**(26): p. 9683 - 9688.

124. Jeffrey, M., Martin, S., Gonzalez, L., Ryder, S.J., Bellworthy, S.J., Jackman, R., *Differential Diagnosis of Infections with the Bovine Spongiform Encephalopathy_BSE_and Scrapie Agents in Sheep.* Journal of Comparative Pathology, 2001. **125**(1): p. 271 - 284.

125. Yi, C.W., Xu, W.C., Chen, J., Liang, Y. , *Recent progress in prion and prion-like protein aggregation.* Acta Biochim Biophys Sin, 2013. **45**(6): p. 520 - 526.

126. McNally, K.L., Ward, A.E., Priola, S.A., *Cells expressing anchorless prion protein are resistant to scrapie infection.* Journal of Virology, 2009. **83**(9): p. 4469-4475.

127. Klingeborn, M., Race, B., Meade-White, K.D., Rosenke, R., Striebel, J.F., Chesebro, B., *Crucial role for prion protein membrane anchoring in the neuroinvasion and neural spread of prion infection.* Journal of Virology, 2011. **85**(4): p. 1484-1494.

128. Kocisko, D.A., Come, J.H., Priola, S.A., Chesebro, B., Raymond, G.J., Lansbury, P.T., Caughey, B., *Cell-free formation of protease-resistant prion protein.* Nature, 1994. **370**(6489): p. 471 - 474.

129. Chesebro, B., Trifilo, M., Race, R., Meade-White, K., Teng, C., LaCasse, R., Raymond, L., Favara, C., Baron, G., Priola, S., Caughey, B., Masliah, E., Oldstone, M., *Anchorless Prion Protein Results in Infectious Amyloid Disease Without Clinical Scrapie.* Science, 2005. **308**(5727): p. 1435 - 1439.

130. Mitra, N., Sinha, S., Ramya, T.N.C., Surolia, A., *N-linked oligosaccharides as outfitters for glycoprotein folding, form and function.* Trends in Biochemical Science, 2006. **31**(3): p. 156-163.

131. Nalivaeva, N.N., Turner, A.J., *Post-translational modification of proteins: acetylcholinesterase as a model.* Proteomics, 2001. **1**(6): p. 735-747.

132. Korth, C., Kaneko, K., Prusiner, S.B., *Expression of unglycosylated mutated prion protein facilitates PrPSc formation in neuroblastoma cells infected with different prion strains.* Journal of General Virology, 2000. **81**: p. 2555-2563.

133. Goldmann, W., *PrP genetics in ruminant transmissible spongiform encephalopathies.* Veterinary Research, 2008. **39**(4): p. 14.

134. Gonzalez, L., Pitrarch, J.L., Martin, S., Thurston, L., Simmons, H., Acin, C., Jeffrey, M., *Influence of Polymorphisms in the Prion Protein Gene on the Pathogenesis and Neuropathological Phenotype of Sheep Scrapie after Oral Infection.* Journal of Comparative Pathology, 2014. **150**: p. 57-70.

135. Groschup, M.H., Lacroux, C., Buschmann, A., Luhken, G., Mathey, J., Eiden, M., Lugan, S., Hoffmann, C., Espinosa, J.C., Baron, T., Torres, J.M., Erhardt, G., Andreoletti, O., *Classic scrapie in sheep with the ARR/ARR prion genotype in Germany and France.* Emerging Infectious Diseases, 2007. **13**(8): p. 1201-1207.

136. Cassmann, E.D., Moore, S.J., Smith, J.D., Greenlee, J.J., *Sheep With the Homozygous Lysine-171 Prion Protein Genotype Are Resistant to Classical Scrapie After Experimental Oronasal Inoculation.* Veterinary Pathology, 2019. **56**(3): p. 409 - 417.

137. Mabbott, N.A., MacPherson, G.G. , *Prions and their lethal journey to the brain.* Nature Reviews in Microbiology, 2006. **4**: p. 201-211.

138. Van Keulen, L.J.M., Vromans, M.E.W., Van Zijderveld, F.G., *Early and late pathogenesis of natural scrapie infection in sheep.* APMIS, 2002. **110**: p. 23-32.

139. Jeffrey, M., Gonzalez, L., *Classical sheep transmissible spongiform encephalopathies: pathogenesis, pathological phenotypes and clinical disease.* Neuropathology and Applied Neurobiology, 2007. **33**: p. 373-394.

140. Beekes, M., McBride, P.A., *Early accumulation of pathological PrP in the enteric nervous system and gut-associated lymphoid tissue of hamsters orally infected with scrapie.* Neuroscience Letters, 2000. **278**(3): p. 181-184.

141. Maignien, T., Lasmezas, C.I., Beringue, V., Dormont, D., Deslys, J.P., *Pathogenesis of the oral route of infection of mice with scrapie and bovine spongiform encephalopathy agents.* Journal of General Virology, 1999. **80**: p. 3035-3042.

142. Marruchella, G., Ligios, C., Di Guardo, G. , *Age, scrapie status, PrP genotype and follicular dendritic cells in ovine ileal Peyer's patches.* Research in Veterinary Science, 2012. **93**(2): p. 853-856.

143. Huang, F.P., Farquhar, C. F., Mabbott, N.A., Bruce, M.E., MacPherson, G.G., *Migrating intestinal dendritic cells transport PrPSc from the gut.* Journal of General Virology, 2002. **83**: p. 267-271.

144. Beekes, M., McBride, P.A., Baldauf, E., *Cerebral targeting indicates vagal spread of the infection in hamsters fed with scrapie.* Journal of General Virology, 1998. **79**(3): p. 601-607.

145. Saa, P., Harris, D.A., Cervenakova, L. , *Mechanisms of prion-induced neurodegeneration.* Expert Reviews in Molecular Medicine, 2016. **18**(5): p. 1-18.

146. Garza, M.C., Monzon, M., Marin, B., Badiola, J.J., Monleon, E. , *Distribution of Peripheral PrPSc in Sheep with Naturally Acquired Scrapie.* PLOS ONE, 2014. **9**(5): p. 14.

147. Lacroux, C., Corbiere, F., Tabouret, G., Lugan, S., Costes, P., Mathey, J., Delmas, J.M., Weisbecker, J.L., Foucras, G., Cassard, H., Elsen, J.M., Schelcher, F., Andreoletti, O. , *Dynamics and genetics of PrPSc placental accumulation in sheep.* Journal of General Virology, 2007. **88**: p. 1056-1061.

148. Andreoletti, O., Lacroux, C., Chabert, A., Monnereau, L., Tabouret, G., Lantier, F., Berthon, P., Eychenne, F., Lafond-Benestad, S., Elsen, J.M., Schelcher, F. , *PrPSc accumulation in placentas of ewes exposed to natural scrapie: influence of foetal PrP genotype and effect on ewe-to-lamb transmission.* Journal of General Virology, 2002. **83**: p. 2607-2616.

149. Tamguney, G., Richt, J.A., Hamir, A.N., Greenlee, J.J., Miller, M.W., Wolfe, L.L., Sirochman, T.M., Young, A.J., Glidden, D.V., Johnson, N.L., Giles, K., DeArmond, S.J., Prusiner, S.B. , *Salivary prions in sheep and deer.* Prion, 2012. **6**(1): p. 52-61.

150. Lacroux, C., Simon, S., Benestad, S.L., Maillet, S., Mathey, J., Lugan, S., Corbiere, F., Cassard, H., Costes, P., Bergonier, D., Weisbecker, J.L., Moldal, T., Simmons, H., Lantier, F., Feraudet-Tarisse, C., Morel, N., Schelcher, F., Grassi, J. Andreoletti, O., *Prions in Milk from Ewes Incubating Natural Scrapie.* PloS Pathogens, 2008. **4**(12): p. 1 - 11.

151. Haley, N.J., Mathiason, C.K., Carver, S., Zabel, M., Telling, G.C., Hoover, E.A., *Detection of Chronic Wasting Disease Prions in Salivary, Urinary and Intestinal Tissues of Deer: Potential Mechanisms of Prion Shedding and Transmission.* Journal of Virology, 2011. **85**(13): p. 6309 - 6318.

152. Gains, M.J., LeBlanc, A.C., *CANADIAN ASSOCIATION OF NEUROSCIENCES REVIEW: Prion Protein and Prion Diseases: The Good and the Bad.* Canadian Journalof Neurological Science, 2007. **34**(2): p. 126-145.

153. Nentwig, A., Oevermann, A., Heim, D., Botteron, C., Zellweger, K., Drogemuller, C., Zurbriggen, A., Seuberlich, T. , *Diversity in Neuroanatomical Distribution of Abnormal Prion Protein in Atypical Scrapie.* PloS Pathogens, 2007. **3**(6): p. 1 - 9.

154. Jeffrey, M., Goodbrand, I.A., Goodsir, C.M. , *Pathology of the Transmissible Spongiform Encephalopathies with Special Emphasis on Ultrastructure.* Micron, 1995. **26**(3): p. 277-298.

155. Wells, G.A., *Pathology of nonhuman spongiform encephalopathies: variations and their implications for pathogenesis.* Developments in Biological Standardization, 1993. **80**: p. 61-69.

156. Tsaousi, P., Kaldrymidou, E., Sklaviadis, T., Kanata, E., Papaioannou, N., *Natural Scrapie in Sheep: Pathogenesis of Amyloidosis.* Journal of Comparative Pathology, 2012. **146**(1): p. 75.

157. González, L., Martin, S., Jeffrey, M., *Distinct profiles of PrP(d) immunoreactivity in the brain of scrapie- and BSE-infected sheep_implication for differential cell targeting and PrP processing.* Journal of General Virology, 2003. **84**(Pt 5): p. 1339 - 1350.

158. Chianini, F., Cosseddu, G.M., Steele, P., Hamilton, S., Hawthorn, J., Siso, S., Pang, Y., Finlayson, J., Eaton, S. L., Reid, H.W., Dagleish, M. P., Di Bari, M.A.,, Agostina, C.D., Agrimi, U., Terry, L., Nonno, R. , *Correlation between Infectivity and Disease Associated Prion Protein in the Nervous System and Selected Edible Tissues of Naturally Affected Scrapie Sheep.* PLoS, 2015. **10**(3): p. 1-21.

159. Foster, J.D., Wilson, M., Hunter, N. , *Immunolocalisation of the prion protein (PrP) in the brains of sheep with scrapie.* Veterinary Record, 1996. **139**(21): p. 512-515.

160. Ryder, S.J., Spencer, Y.I., Bellerby, P.J., March, S.A., *Immunohistochemical detection of PrP in the medulla oblongata of sheep: the spectrum of staining in normal and scrapie-affected sheep.* Veterinary Record, 2001. **148**(1): p. 7-13.

161. van Keulen, L.J.M., Schreuder, B.E.C., Vromans, M.E.W., Langeveld, J.P.M., Smits, M.A., *Scrapie-associated Prion Protein in the Gastrointestinal Tract of Sheep with Natural Scrapie.* Journal of Comparative Pathology, 1999. **121**(1): p. 55-63.

162. Lacroux, C., Vilette, D., Fernandez-Borges, N., Litaise, C., Lugan, S., Morel, N., Corbiere, F., Simon, S., Simmons, H., Costes, P., Weisbecker, L., Lantier, I., Lantier, F., Schelcher, F., Grassi, J., Castilla, J., Andreoletti, O., *Prionemia and leuco-platelet associated infectivity in sheep TSE models.* Journal of Virology, 2011. **86**(4): p. 2056-2066.

163. Stack, M.J., Chaplin, M.J., Aldrich, A.M., Davis, L.A., *The distribution of scrapie-associated fibrils in neural and non-neural tissues of advanced clinical cases of natural scrapie in sheep.* Research in Veterinary Science, 1998. **64**(2): p. 141-146.

164. Norenburg, M.D., *Astrocyte Responses to CNS Injury.* Journal of Neuropathology and Experimental Neurology, 1994. **53**(3): p. 213-220.

165. Sarasa, R., Junquera, C., Toledano, A., Badiola, J.J., Monzon, M., *Ultrastructural changes in the progress of natural Scrapie regardless fixation protocol.* Histochemistry And Cell Biology 2015. **144**(1): p. 77-85.

166. Gossner, A., Roupaka, S., Foster, J., Hunter, N., Hopkins, J., *Transcriptional profiling of peripheral lymphoid tissue reveals gens and networks linked to SSBP/1 scrapie pathology in sheep.* Veterinary Microbiology, 2011. **153**(3-4): p. 218-228.

167. Lemke, G., *Biology of the TAM Receptors.* Cold Spring Harbor Perspectives in Biology, 2013. **5**: p. 1-17.

168. Lew, E.D., Oh, J., Burrola, P.G., Lax, I., Zagorska, A., Traves, P.G., Schlessinger, J., Lemke, G. , *Differential TAM receptor-ligand-phospholipid interactions delimit differential TAM bioactivities.* eLife, 2014. **3**: p. 1-23.

169. Stitt, T.N., Conn, G., Gore, M., Lai, C., Bruno, J., Radziejewski, C., Mattsson, K., Fisher, J., Gies, D.R., Jones, P.F., Masiakowski, P., Ryan, T.E., Tobkes, N.J., Chen, D.H., DiStefano, P.S., Long, G.L., Basilico,C., Goldfarb, M.P., Lemke, G., Glass, D.J., and G.D. Yancopoulos, *The anticoagulation factor protein S and its relative, Gas6, are ligands for the Tyro 3/Axl family of receptor tyrosine kinases.* Cell, 1995. **80**(4): p. 661-671.

170. Gardai, S.J., McPhillips, K.A., Frasch, S.C., Janssen, W.J., Starefeldt, A., Murphy-Ullrich, J.E., Bratton, D.L., Oldenborg, P.A., Michalak, M., Henson, P.M., *Cell-Surface Calreticulin Initiates Clearance of Viable or Apoptotic Cells through trans-Activation of LRP on the Phagocyte.* Cell, 2005. **123**: p. 321-334.

171. Goruppi, S., Ruaro, E., Varnum, B., Schneider, C., *Requirement of phosphatidylinositol 3-kinase-dependent pathway and Src for Gas6-Axl mitogenic and survival activities in NIH 3T3 fibroblasts.* Molecular and Cellular Biology, 1997. **17**(8): p. 4442 - 4453.

172. Stenhoff, J., Dahlback, B., Hafizi, S. , *Vitamin-K dependent Gas6 activates ERK kinase and stimulates growth of cardic fibroblasts.* Biochemical and Biophysical Research Communications, 2004. **319**(3): p. 871 - 878.

173. Rea, K., Pinciroli, P., Sensi, M., Alciato, F., Bisaro, B., Lozneanu, L., Raspagliesi, F., Centritto, F., Cabodi, S., Defilippi, P., Avanzi, G.C., Canevari, S., Tomassetti, A., *Novel Axl-driven signaling pathway and molecular signature characterize high-grade ovarian cancer patients with poor clinical outcome.* Oncotarget, 2015. **6**(31): p. 30859 - 30875.

174. Fourgeaud, L., Traves, P.G., Tufail, Y., Leal-Bailey, H., Lew, E.D., Burrola, P.G., Callaway, P., Zagorska, A., Rothlin, C.V., Nimmerjahn, A., Lemke, G., *TAM receptors regulate multiple features of microglia physiology.* Nature, 2016. **532**: p. 240-244.

175. Ertmer, A., Glich, S., Yun, S.W., Flechsig, E., Klebl, B., Stein-Gerlach, M., Klein, M.A., Schatzl, H.M., *The Tyrosine Kinase Inhibitor ST1571 Induces Cellular Clearance of PrPSc in Prion-infected Cells.* THE JOURNAL OF BIOLOGICAL CHEMISTRY, 2004. **279**(40): p. 41918 - 41927.

176. Labat-Robert, J., *Cell–Matrix interactions, the role of fibronectin and integrins. A survey.* Pathologie Biologie, 2012. **60**: p. 15-19.

177. Milner, R., Campbell, I. L., *The extracellular matrix and cytokines regulate microglial integrin expression and activation.* Journal of Immunology, 2003. **170**(7): p. 3850 - 3858.

178. Alitalo, K., Hovi, T., Vaheri, A., *Fibronectin is produced by human macrophages.* Journal of Experimental Medicine, 1980. **152**(3): p. 602 - 613.

179. Takahashi, S., Leiss, M., Moser, M., Ohashi, T., Kitao, T., Heckmann, D., Pfeifer, A., Kessler, H., Takagi, J., Erickson, H.P., Fassler, R. , *The RGD motif in fibronectin is essential for development but dispensable for fibril assembly.* The Journal of Cell Biology, 2007. **178**(1): p. 167-178.

180. Mita, A.C., Mita, M.M., Nawrocki, S.T., Giles, F.J., *Survivin: Key Regulator of Mitosis and Apoptosis and Novel Target for Cancer Therapeutics.* Molecular Pathways, 2008. **14**(16): p. 1 - 7.

181. Baratchi, S., Kanwar, R.K., Kanwar, J.R., *Survivin: A target from brain cancer to neurodegenerative disease.* Critical Reviews in Biochemistry and Molecular Biology, 2010. **45**(6): p. 535 - 554.

182. Alteri, D.C., *Survivin-The Inconvenient IAP.* Seminars in Cell & Developmental Biology, 2015. **39**: p. 91 - 96.

183. Boidot, R., Ve´gran, F., Lizard-Nacol, S., *Transcriptional regulation of the survivin gene.* Molecular Biology Reports, 2014. **41**: p. 233 - 240.

184. Jiang, Y., de Bruin, A., Caldas, H., Fangusaro, J., Hayes, J., Conway, E.M., Robinson, M.L., Altura, R.A., *Essential Role for Survivin in Early Brain Development.* The Journal of Neuroscience, 2005. **25**(30): p. 6962 - 6970.

185. Rapraeger, A.C., Ott, V.L., *Molecular interactions of the syndecan core proteins.* Current Opinion in Cell Biology, 1998. **10**(5): p. 620-628.

186. Echtermeyer, F., Harendza, T., Hubrich, S., Lorenz, A., Herzog, C., Mueller, M., Schmitz, M., Grund, A., Larmann, J., Schieffer, J.S.B., Lictinghagen, R., Hilfiker-Kleiner, D., Wollert, K.C., Heineke, J., Theilmeier, G., *Syndecan-4 signalling inhibits apoptosis and controls NFAT activity during myocardial damage and remodeling.* Cardiovascular Research, 2011. **92**(1): p. 123 - 131.

187. Horonchik, L., Tzaban, S., Ben-Zaken, O., Yedidia, Y., Rouvinski, A., Papy-Garcia, D., Barritault, D., Vlodavsky, I., Taraboulos, A., *Heparan Sulfate Is a Cellular Receptor for Purified Infectious Prions.* The Journal of Biological Chemistry, 2005. **280**(17): p. 17062-17067.

188. Brekken, R.A., Sage, E.H., *SPARC, a matricellular protein: at the crossroads of cell-matrix communication.* Matrix Biology, 2001. **19**(8): p. 816-827.

189. Vincent, A.J., Lau, P.W., Roskams, A.J., *SPARC is expressed by macroglia and microglia in the developing and mature nervous system.* Developmental Dynamics, 2008. **237**(5): p. 1449-1462.

190. Ghaemmaghami, S., Phuan, P.W., Perkins, B., Ullman, J., May, B.C.H., Cohen, F.E., Prusiner, S.B. , *Cell division modulates prion accumulation in cultured cells.* Proceedings of the National Academy of Sciences of the United States of America, 2007. **104**(46): p. 17971 - 17976.

191. Shibanuma, M., Mashimo, J., Mita, A., Kuroki, T., Nose, K., *Cloning from a mouse osteoblastic cell line of a set of transforming-growth-factor-β1-regulated genes, one of which seems to encode a follistatin-related polypeptide.* European Journal of Biochemistry, 1993. **217**(1): p. 13-19.

192. Chaly, Y., Fu, Y., Marinov, A., Hostager, B., Yan, W., Campfield, B., Kellum, J.A., Bushnell, D., Wang, Y., Vockley, J., Hirsch, R. , *Follistatin-like protein 1 enhances NLRP3 inflammasome mediated IL-1β secretion from monocytes and macrophages.* European Journal of Immunology, 2014. **44**(5): p. 1467-1479.

193. Liu, S., Shen, H., Xu, M., Liu, O., Zhao, L., Liu, S., Guo, Z., Du, J., *FRP inhibits ox-LDL-induced endothelial cell apoptosis through an Akt-NF- kB-Bcl-2 pathway and inhibits endothelial cell apoptosis in an apoE-knockout mouse model.* American Journal of Physiology Endocrinology and Metabolism, 2010. **299**(3): p. E351-363.

194. Sylva, M., Moorman, A.F.M., van den Hoff, M.J.B., *Follistatin-like 1 in Vertebrate Development.* Birth Defects Research, 2013. **99**(1): p. 61-69.

195. Oshima, Y., Ouchi, N., Sato, K., Izumiya, Y., Pimentel, D.R., Walsh, K., *Follistatin-like 1 is an Akt-regulated cardioprotective factor that is secreted by the heart.* Circulation 2008. **117**(24): p. 3099-3108.

196. Chaly, Y., Blair, H.C., Smith, S.M., Bushnell, D.S., Marinov, A.D., Campfield, B.T., Hirsch, R.. *Follistatin-like protein 1 regulates chondrocyte proliferation and chondrogenic differentiation of mesenchymal stem cells.* Annals of the Rheumatic Diseases, 2014. **74**(7): p. 1467-1473.

197. Trojan, L., Schaaf, A., Steidler, A., Haak, M., Thalmann, G., Knoll,T., Gretz, N., Alken, P., Michel, M.S., *Identification of metastasis-associated genes in prostate cancer by genetic profiling of human prostate cancer cell lines.* Anticancer Research, 2005. **25**(1A): p. 183-191.

198. Visse, R., Nagase, H. , *Matrix Metalloproteinases and Tissue Inhibitors of Metalloproteinases: Structure, Function and Biochemistry.* Circulation Research, 2003. **92**: p. 827-839

199. Sela-Passwell, N., Rosenblum, G., Shoham, T., Sagi, I., *Structural and functional bases for allosteric control of MMP activities: Can it pave the path for selective inhibition.* Biochimica et Biophysica Acta, 2010. **1803**(1): p. 29-38.

200. Lewis, V., Johanssen, V.A., Lothian, A., Roberts, B.R., Crouch, P. J., Collins, S.J. *Elucidating the role of Matrix Metalloproteases in Prion protein proteolysis*. in *PRION*. 2015.